Interactive comment on "Aerosol and dynamic effects on the formation and evolution of pyro-clouds" by D. Chang et al.
MS No.: acp-2014-61

Dear Reviewer,
We would like to thank you for the valuable and constructive comments/suggestions on our manuscript. We have revised the manuscript accordingly and please find our point-to-point responses below (line numbers refer to the new version of manuscript). In addition, the title of the manuscript is revised to be "Regime dependence of aerosol effects on the formation and evolution of pyro-convective clouds".

Reply to Anonymous Referee #1

This paper is a follow-on study on aerosol effects under different heat forcing conditions by conducting 2-D simulations using the Active Tracer High Resolution Atmospheric Model with a two-moment cloud microphysics parameterization. Although the different sensitivity regimes are classified and associated processes are analyzed, the results of the study are not new (some results have been the common senses for scientists in this area) and many previous studies with even more advanced microphysics have indicated similar results. Since most of those previous studies are 2-D, 2-D dynamics is very different from 3-D, and this study has an emphasis on dynamic effect, investigations with 3-D simulations would be something building on past research.
The paper does not provide further explanations for the phenomena they see (see specific comments). The introduction of the paper is poorly written (see details in my specific comments). Most importantly, many process rates heavily depend on the process parameterizations (scheme-dependent), but there is no any discussion about those uncertainties.
The paper is misleading in wording such as fire forcing and biomass burning aerosols.
What I found out eventually is that there is nothing to do that fire and biomass burning aerosols. It is just a heat forcing to produce different intensity of updrafts. See my specific comments for details.
Therefore, the paper needs very significant revisions to reach the point being accepted as a publication.

Response: Thanks for the comments. We have revised the introduction part with an emphasis on clarifying the motivations and new aspects of this work. One motivation is to determine the regime-dependence of aerosol effect. The other problem that we try to solve is the nonlinearity in the aerosol-cloud interactions. In the main text, more discussions concerning the uncertainties of microphysical scheme have been added.

Besides, the results and discussions from the 3-D simulations have been included in the supplementary material. Take cloud droplets for example (Fig. R1), the regime dependence from the 3-D simulations (Fig. R1b) looks similar to the 2-D results (Fig. R1a) though the absolute dependency may vary. This suggests that the use of such regime dependence requires caveats because it may differ for different model dimensionality (2D vs. 3D). In the main text, we have included more discussion concerning these uncertainties: "In this study, we demonstrate the performance of ensemble simulations in determining the regime dependence of aerosol effects. The use of such regime dependence requires caveats because it may differ for different cloud types, aerosol properties, meteorological conditions and model configurations (e.g., microphysical schemes, dynamic schemes, dimensionality, etc.; the 3-D results are in the supplementary material)". Please see Lines 739-743.

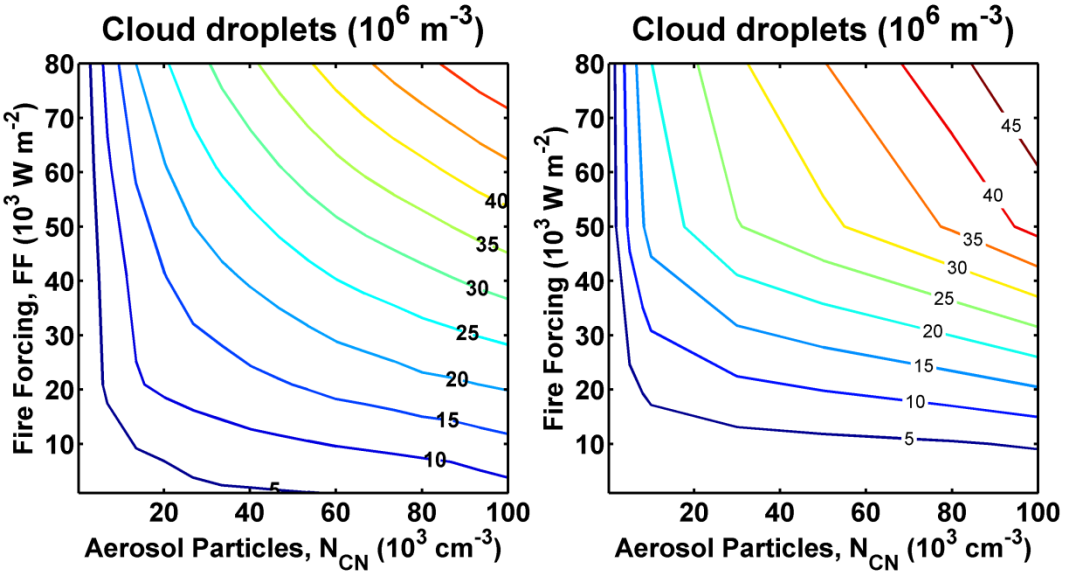

(a) (b)

Figure R1. Number concentration of cloud droplets calculated as a function of aerosol number concentration (N_{CN}) and updraft velocity (represented by *FF*) from 2-D (a) and 3-D (b) simulations.

The wording "fire forcing" was adopted from previous application of ATHAM model (Luderer, 2007) for the same fire event. The wording "bio-mass burning aerosols" is used because the CCN activation properties in our model simulation are taken from that of biomass burning aerosols.

Specific comments

1. Introduction 1. First paragraph of introduction needs to be cleared up a lot. First, aerosol impacts on precipitation are very different for different cloud types such as shallow warm clouds and deep convective clouds. Therefore, not to be more confusing, please discuss them by separating cloud types.

Response: Thanks for the suggestion. We discuss the aerosol effects on the precipitation formed in different cloud types separately, mostly stratiform and convective clouds. The text is "Precipitation from stratiform clouds can be inhibited by elevated aerosol concentration (Zhang et al., 2006), while precipitation from convective clouds can be either suppressed or enhanced (Ackerman et al., 2003; Andreae et al., 2004; Altaratz et al., 2008; Lee et al., 2008; Teller and Levin, 2008; Fan et al., 2013; Camponogara et al., 2014)." Please see Lines 51-54 in the new manuscript.

2. P7779, Line 18-21: Li et al. 2008 detailed the non-monotonic behavior. Line 21-25: Qian et al. 2009 was not such study. Khain 2009 and Fan et al. 2009 are typical such studies.

Response: The sentence in Line 18-19 in old manuscript is revised to be "In addition, changing aerosol concentrations have also been found to exert non-monotonic influences (either positive or negative) on a wide range of cloud properties". Please see 54-56 in revised manuscript.

The work of *Khain (2009) and Fan et al. (2009)* indicated that the environmental conditions (e.g., relative humidity, wind shear) could regulate the aerosol effect on the cloud and precipitation. Here we have deleted the citation of *Qian et al. (2009)* paper, and add the citation of *Khain (2009) and Fan et al. (2009)* paper. Please see the revised sentence in Lines 59-65 in the new manuscript: "One explanation for these seemingly contradictory results is that aerosol effects are regime-dependent, which means that it can vary under different meteorological conditions (updraft velocity, relative humidity, surface temperature, and wind shear), cloud types, aerosol properties (size distribution and chemical composition) and observational or analysis scales (Levin and Cotton, 2007; Tao et al., 2007; Khain et al., 2008; Rosenfeld et al., 2008; Fan et al., 2009; Khain, 2009; Reutter et al., 2009; McComiskey and Feingold, 2012; Tao et al., 2012)."

3. Recent progresses on aerosol effects on convective clouds are not introduced. For example, a recent review study (Tao et al., Rev Geophys, 2012) on aerosol impacts on convective clouds is not even mentioned. A nice related paper on the relative importance of the thermodynamic and microphysical aerosol effects (Fan et al., PNAS, 2013) is missed too. Anyway, there are so many significant studies on aerosol impacts on convective clouds since 2011 in literature (Morrison, van den Heever, etc) but these progresses are not discussed at all. It is recommended that the authors do a thorough literature study of this topic.

Response: Thanks for the comments. Tao et al. (2012) summarized the aerosol effects on the CCN activation, warm-rain process, mixed-phase clouds, and precipitation in terms of microphysical scale, cloud-resolving scale, and regional scale, which are retrieved from the theoretical analysis, observations, and numerical modeling. The underlying mechanisms and the comparison between the results from different studies was also presented and analyzed. Fan et al. (2013) carried out monthly 3-D simulations over three different regions and found the microphysical effect controlled by aerosols is the major factor that determines the properties of deep convective clouds, rather than the updraft-related dy-

namics. The introduction has been reformulated with these suggested papers which will be included in the revised manuscript.

4. The third paragraph of introduction: I do not see how your study is connected with biomass burning aerosols, only through the heat you added? Are the aerosol properties used in the study taken from biomass burning aerosols? If not, this is just a general test, not for biomass burning aerosols.

Response: We connect our study with biomass burning aerosols through the setting of aerosol properties. The properties of aerosol particles (used in the look-up table for cloud nucleation process) are for soot particles. In the revised manuscript, we emphasize the connection between our simulations and biomass burning aerosols in Sect. 2.2. The corresponding text is "As mentioned above, we used the lookup table of Reutter et al. (2009) for the CCN activation. This table is determined for fresh biomass burning aerosols with a hygroscopicity parameter κ of 0.2 and a log-normal size distribution (a geometric mean diameter of 120 nm and a geometric standard deviation of 1.5, Reutter et al. 2009)." Please see Lines 157-160.

5. The motivation based on Reutter et al 2009 (as stated in the first sentence of the abstract) is missing from the introduction.

Response: In the third paragraph of the introduction section, we extend the motivation stated in abstract in terms of the fact that aerosol effect on convective clouds is regime-dependent based on the research from Reutter et al. (2009) and some other previous studies. The corresponding text can be found in Lines 59-70: "One explanation for these seemingly contradictory results is that aerosol effects are regime-dependent, which means that it can vary under different meteorological conditions (updraft velocity, relative humidity, surface temperature, and wind shear), cloud types, aerosol properties (size distribution and chemical composition) and observational or analysis scales (Levin and Cotton, 2007; Tao et al., 2007; Khain et al., 2008; Rosenfeld et al., 2008; Fan et al., 2009; Khain, 2009; Reutter et al., 2009; McComiskey and Feingold,

2012; Tao et al., 2012). It is thus important to investigate the regime-dependence of aerosol-cloud interactions and to improve the representation of cloud regimes in models (Stevens and Feingold, 2009). If we were able to distinguish under which conditions cloud formation is updraft-limited (aerosol-insensitive) as discussed in Reutter et al. (2009), it would have the advantage that in future work one could for many purposes neglect aerosol effects on clouds in areas that are usually updraft limited."

6. Section 2.2: It is very confusing by saying fire forcing. I was misled by the wording and thought that a real fire situation is set up such as T, RH, and aerosol emissions from fires. Until I finished the whole section, I realized that it is not about fire forcing at all. It is just a heat forcing to produce different intensity of updrafts (if for fire, at least aerosol emissions from the heating plume should be assumed, not the uniform aerosols over the entire domain). Based on the general aerosol type and a simple heating setup, please remove all those fire forcing or biomass burning aerosols.

Response: Thanks for the comments. We adopted the terminology "fire forcing" from the paper of Luderer (2007) for the same fire event, which stated that the "fire forcing" results in the vertical development, and favors for the formation of pyro-convective clouds. Within our simulations, the variation in updraft velocities is through changing the input fire forcing.

We admit that we did not consider the spatial and temporal distributions of atmospheric aerosols during the simulation. Instead of this, the concentration of ambient aerosols is set to be homogeneous over the modeling domain. We admit the variability of aerosols during the simulation is ignored and may leads to a bias compared to a real fire (Wang et al., 2013). However, this study aims to estimate the sensitivity of clouds and precipitation to the orders-of-magnitude change in the aerosol concentrations, and the similar treatment of aerosols has been used in previous studies (Seifert et al., 2012; Reutter et al., 2013). We add this discussion about the bias in the revised manuscript; please see lines 152-156. This work follows the old terminology (fire forcing) and treatment of aerosols from previous research paper. For the future research,

we will try to improve the representation of the aerosol particles and take into account the full complexity of all chemistry-aerosol-cloud interactions.

Section 2.3: The process analysis used here is not something new or unique. Modeling studies like this do those analyses all the time. I do not see why a section is needed to introduce the analysis. Simply, you only need 1-2 sentences to introduce the table A1 for the quantities you look at.

Response: Thanks for the comment. Within the ATHAM model, process analysis is a newly-developed module, and here we tried to state the development on the existing model scheme. Different from the simple process rate calculations under four extreme conditions in the previous version of this paper, in the revised manuscript, we figure out how each microphysical process contribute to each hydrometeor over a wide range of aerosol concentrations and fire forcing, just as shown in Fig. R2. What is the percentage of the contribution of each process and how do they response to the changing updrafts and aerosols in the atmosphere? This is the fundamental questions with which the newly-developed PA module tries to deal. In Sect. 2.3, we intended to make clear what we have changed inside the model and what we want to get from it. So far as we know, there was no similar form of process analysis of cloud microphysics in literature.

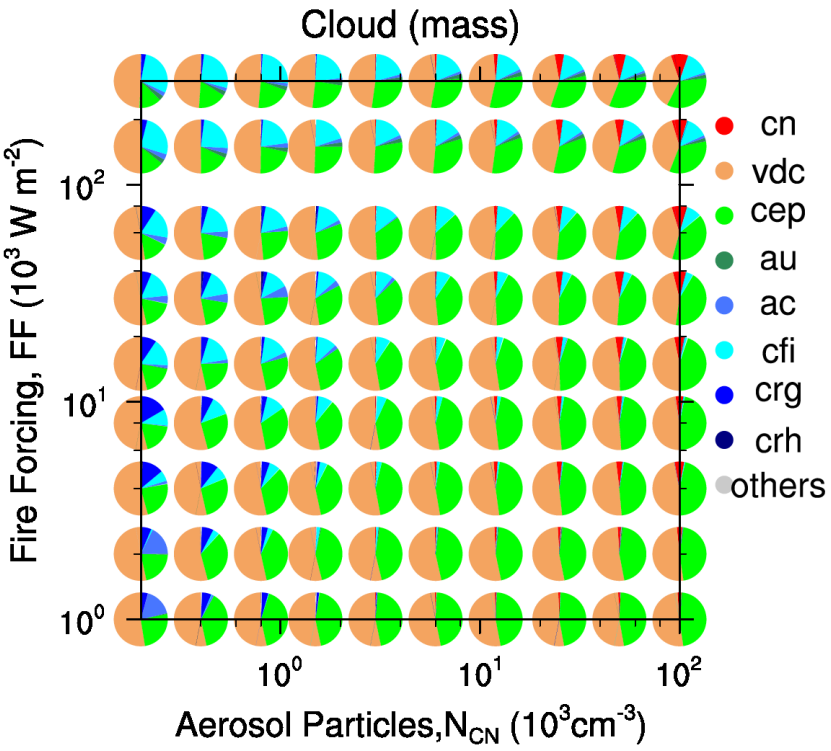

Figure R2. The pie charts summarize the relative percentage of the microphysical processes involving cloud droplets as a function of N_{CN} and fire forcing. Colors within each pie chart reflect the contribution of processes under the specific condition. Warm colors denote the source, while cold colors denote the sink. The acronyms indicate cn: cloud nucleation; vdc: condensational growth of cloud droplets; cep: evaporation of cloud droplets; au: autoconversion; ac: accretion; cfi: freezing of cloud droplets to form ice crystals, including homogeneous and heterogeneous nucleation; crg/h: riming of cloud droplets to form graupel/hail.

Section 3.2 Please use the temperature instead of Wm-2 to be more straightforward to general readers about the heating that you imposed in the experiments throughout the paper.

Response: Thanks for the suggestion. We plotted the relationship between fire forcing and the corresponding maximum temperature at cloud base under different aerosol conditions, and found the aerosol impact on the temperature is negligible. Take N_{CN}=5,000 cm^{-3} for example, the correlation of fire forcing and temperature is shown in Fig. R3. The shaded area indicates the variability of

estimation over each simulation period. According to the figure, the temperature at cloud base varies monotonically from 7.6 to 16.4 ℃ as fire forcing increases from 1 × 10^3 to 3 × 10^5 W m^{-2}. We add this discussion in Sect. 3.1. Please see Lines 221-230.

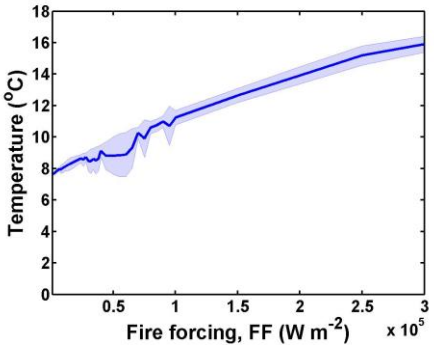

Figure R3. The correlation of fire forcing and the corresponding maximum temperature at cloud base. The shaded area indicates the variability of estimation (±½σ) over each simulation period.

In Sect. 3.2.1, we add the temperature as the secondary vertical axis in the contour plot for reference, as displayed in Fig. R4 (Fig. 7b in the revised manuscript).

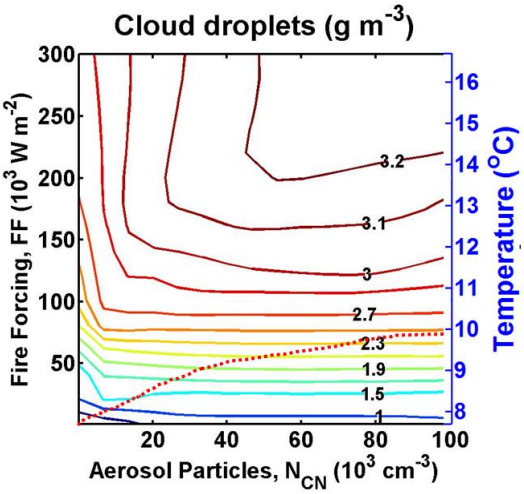

Figure R4. Mass concentration of cloud droplets calculated as a function of aerosol number concentration (N_{CN}) and updraft velocity (represented by *FF*). Red dashed lines indicate the borders between different regimes defined by *RS* (N_{CN})/*RS*(*FF*)=4 or 1/4, respectively.

Section 3.2.1 Need to explain the reasons for aerosol-limited, updraft-limited and the transitional regime.

Response: For the three-regime structure of number concentration of cloud droplets in Sect. 3.2.1, we discussed the reasons in detail in Sect. 3.3.1. Please see Lines 426-450.

Section 3.2.2 The sensitivity of raindrop really depends on autoconversion parameterization, snow/graupel/hail productions and melting processes. All those parameterizations have very large uncertainties, especially with bulk microphysical parameterizations.
For example, most of the autoconversion schemes were developed or evaluated for stratocumuls clouds. They may not be appropriate for convective clouds. All I want to say is that the authors have to be aware of all these uncertainties and discuss them accordingly.

Response: Thanks for the suggestions. We explained the response of raindrops to aerosols/fire forcing (Sect. 3.2.2) in Sect. 3.3.2. Concerning the uncertainties of individual microphysical processes, we share the same concern as the referee. In our study, we have quantitatively shown the importance of different microphysical processes in regulating the number and mass flow of clouds. Currently, more efforts have been spent on improving the description of CCN/IN activation. However, the overall uncertainties will not be reduced if understanding the other microphysical processes is not improved as well.

Evaluating the uncertainties of all microphysical processes, however, will become a comprehensive review going beyond the purpose of the present study. In Sect. 3.3.2 of the revised manuscript, we add more discussion about the uncertainties concerning the main microphysical processes relevant to raindrops. The text is "The sensitivity of raindrops to aerosols depends on autoconversion parameterization, and the melting processes, etc. All those parameterizations have very large uncertainties, especially with bulk microphysical parameterizations. For example, most of the autoconversion schemes were developed or evaluated for stratocumulus clouds, which may not be appropriate for convective clouds. Based on the simulations during the convective phase of squall-line development, van Lier-Walqui et al. (2012) presented the uncer-

tainty in the microphysical parameterization by the posterior probability density functions (PDFs) of parameters, observations, and microphysical processes. With the purpose to improve the representation of microphysics, it is of significance to quantify the parameterization uncertainty by using observation data to constrain parameterization." Please see Lines 547-556.

P7789, first paragraph, it is very vague by using buffering effect to explain the less sensitivity. Please stick on processes.

Response: Yes, by adding a sentence in lines 329-330 "Detailed analysis of the microphysical buffering processes will be presented in Sect. 3.3.2.", we will direct the readers to the process analysis. The text for the process analysis in Sect. 3.3.2 is "The PA clearly demonstrates that aerosols could significantly alter the microphysical pathways and their intensities. Although the variation in individual microphysical process is remarkable, the net result of all processes is not obvious and even insusceptible to aerosol perturbations. This is especially obvious when we consider the aerosol effect on rain water: it is observed that as aerosols is enhanced by a factor of 500, the intensities of the source processes only decrease by a factor of 10; however, there is only a two-fold change in the net rain water content. This implies that the microphysical scheme itself is a self-regulatory system, which can produce equilibrium and buffers the effect of aerosol disturbance (negative feedback)." Please see lines 538-546.

Section 3.2.3 Again for frozen water content and particle numbers, ice nucleation parameterizations and drop freezing parameterizations impact them dramatically. Please connect them with the parameterizations of these processes in your model and discuss the uncertainties.

Response: Thanks for the suggestions. We explained the response of frozen particles to aerosols/fire forcing (Sect. 3.2.3) in Sect. 3.3.3. In Sect. 3.3.3, we analyze the change trend of frozen particles in terms of microphysical processes, and try to find the dominant factors that regulate the process rate. As explained before,

reviewing the uncertainties of all microphysical processes is beyond the current work. In Sect. 3.3.3 of the revised manuscript, we add more discussion about the possible uncertainties of these processes based on previous research. The text is "As shown aforementioned, drop freezing parameterizations and ice nucleation parameterizations influence frozen water content dramatically, which involve large uncertainties. Ice microphysics is significantly more complicated due to the wide variety of ice particle characteristics. On one hand, the intensities of these processes differ greatly among different microphysical schemes. Eidhammer et al. (2009) have compared three different ice nucleation parameterizations, and found that different assumptions could result in similar qualitative conclusions although with distinct absolute values. The parameterization with observational constraints agrees well with the measurements. On the other hand, van Lier-Walqui et al. (2012) suggested the processes contributing to frozen particles are dependent on both particle size distribution and density parameters. Parameterization improvement based on observations could help to reduce the uncertainties." Please see Lines 597-607.

Section 3.2.4 Need to provide the reasons to explain the enhanced and suppressed rain rate regimes.

Response: We run more simulations and conduct more analysis to solve this question. By doing process analysis (PA), the most of rainfall is from melting of frozen particles. As shown in Fig. R5, the green diamond points is averaged rain rate under different aerosol concentrations. The columns represent the integrated melting rate from individual frozen particles. We found the rain rate is well correlated with the melting rate (as shown in Fig. R5). For $N_{CN} > 1{,}000$ cm^{-3}, increasing N_{CN} results in more small frozen particles (i.e., snow) with low fall velocities. These small frozen particles cannot fall into the warm areas and melt efficiently, resulting in a reduced melting rate. For $N_{CN} < 1{,}000$ cm^{-3}, the ratio between large and small frozen particles is not sensitive to N_{CN} anymore and the vertical distribution of frozen particles become important. Increasing N_{CN} leads to earlier formation of frozen particles at low altitude, which evapo-

rate less and result in more rainfall. We add this explanation in the main text. Please see lines 400-407.

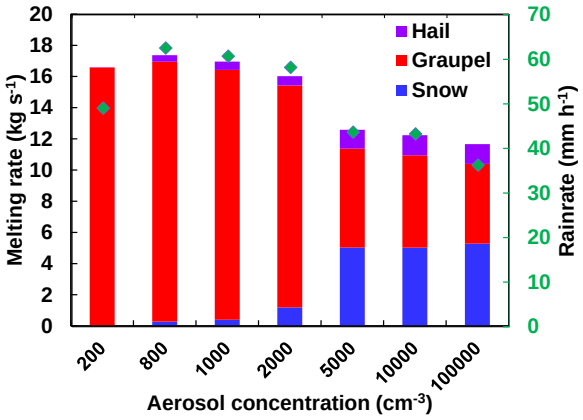

Figure R5. The correlation of rain rate and the melting rate of the frozen particles. The green diamond points are the averaged rain rate under different aerosol concentrations (FF = 10^5 W m^{-2}). The columns represent the integrated melting rate from individual frozen particles.

Section 3.3 I would not trust too much on those process rates since they really depend on the parameterizations of processes. I saw very different process rates between bulk and bin microphysical parameterizations and even between two 2-moment bulk schemes. Many of those sensitivities are scheme-dependent. Please discuss it.

Response: Yes, we agree with the referee. In Sect. 3.3, we add more discussion to emphasize the bias which could be caused by using different microphysical schemes. The text is "We are aware that the exact process rates may vary depending on the microphysical schemes used in the simulation (Muhlbauer et al., 2010). Therefore, we stress that the process analysis here is based on the Seifert microphysical scheme (Seifert and Beheng, 2006). In the future, further observations from laboratory and field measurements are needed to improve the understanding of aerosol-cloud interactions and to better constrain microphysical parametrizations." "In this study, we demonstrate the performance of ensemble simulations in determining the regime dependence of aerosol effects. The use of such regime dependence requires caveats because it

may differ for different cloud types, aerosol properties, meteorological conditions and model configurations (e.g., microphysical schemes, dynamic schemes, dimensionality, etc.; the 3-D results are in the supplementary material)". Please see Lines 489-494, and 739-743 respectively.

P7798, Line 5-10: cloud radiative forcing and cloud lifetime effects are not examined in this study, what do the conclusions come from? A recent study over long time scale (Fan et al., 2013) suggested significant aerosol effects on deep convective cloud morphology and lifetime.

Response: Since we did not directly calculate the forcing, here we just delete the comments on the radiative forcing and cloud lifetime. We also cite Fan et al. (2013) in this part. The text is "For this case study of pyro-convective clouds, then, we conclude that aerosol effects on cloud droplet number concentrations and cloud droplet size are likely more important than effects on precipitation, since precipitation is far less sensitive to aerosol number concentrations than to updraft velocity. This is in agreement with other studies (e.g., Seifert et al., 2012). A recent long-term convective cloud investigation found that microphysical effects driven by aerosol particles dominate the properties and morphology of deep convective clouds, rather than updraft-related dynamics (Fan et al., 2013). Therefore, it must still be determined whether this conclusion applies to other cloud types and over longer time scales." Please see lines 730-738.

Minor comments: 1. p7783 Line 16, how do you get 85 km with 110 grids of 500 meter spacing?

Response: The simulation grids are stretched, not evenly divided. Only the horizontal grid at the center of the modeling domain is equal to 500 m, and towards to the lateral boundaries the grid size becomes bigger according to the width of zoom (which was set in the input file).

2. Please use correct terminology: cloud freezing should be "drop freezing", deposition-al growth of droplets should be "condensational growth of droplets".

Response: Accepted. We have corrected these terms through the text.

References

Ackerman, A. S., Toon, O. B., Stevens, D. E., and Coakley, J. A.: Enhancement of cloud cover and suppression of nocturnal drizzle in stratocumulus polluted by haze, Geophys Res Lett, 30, 1381, doi: 10.1029/2002gl016634, 2003.

Altaratz, O., Koren, I., Reisin, T., Kostinski, A., Feingold, G., Levin, Z., and Yin, Y.: Aerosols' influence on the interplay between condensation, evaporation and rain in warm cumulus cloud, Atmospheric Chemistry and Physics, 8, 15-24, 2008.

Andreae, M. O., Rosenfeld, D., Artaxo, P., Costa, A. A., Frank, G. P., Longo, K. M., and Silva-Dias, M. A. F.: Smoking Rain Clouds over the Amazon, Science, 303, 1337-1342, 2004.

Camponogara, G., Dias, M. A. F. S., and Carrio, G. G.: Relationship between Amazon biomass burning aerosols and rainfall over the La Plata Basin, Atmospheric Chemistry and Physics, 14, 4397-4407, doi: 10.5194/acp-14-4397-2014, 2014.

Fan, J. W., Yuan, T. L., Comstock, J. M., Ghan, S., Khain, A., Leung, L. R., Li, Z. Q., Martins, V. J., and Ovchinnikov, M.: Dominant role by vertical wind shear in regulating aerosol effects on deep convective clouds, J Geophys Res-Atmos, 114, doi: 10.1029/2009jd012352, 2009.

Fan, J. W., Leung, L. R., Rosenfeld, D., Chen, Q., Li, Z. Q., Zhang, J. Q., and Yan, H. R.: Microphysical effects determine macrophysical response for aerosol impacts on deep convective clouds, P Natl Acad Sci USA, 110, E4581-E4590, doi: 10.1073/pnas.1316830110, 2013.

Khain, A. P., BenMoshe, N., and Pokrovsky, A.: Factors determining the impact of aerosols on surface precipitation from clouds: An attempt at classification, J Atmos Sci, 65, 1721-1748, doi: 10.1175/2007jas2515.1, 2008.

Khain, A. P.: Notes on state-of-the-art investigations of aerosol effects on precipitation: a critical review, Environ Res Lett, 4, doi: 10.1088/1748-9326/4/1/015004, 2009.

Lee, S. S., Donner, L. J., Phillips, V. T. J., and Ming, Y.: The dependence of aerosol effects on clouds and precipitation on cloud-system organization, shear and stability, J Geophys Res-Atmos, 113, doi: 10.1029/2007jd009224, 2008.

Levin, Z., and Cotton, W.: Aerosol Pollution Impact on Precipitation: A Scientific Review, World Meteorol. Organ, Geneva, Switzerland, 2007.

Luderer, G. G.: Modeling of Deep-Convective Vertical Transport of Foreset Fire Smoke into the Upper Troposphere and Lower Stratosphere, Ph.D, Physics Department, Johannes Gutenberg University Mainz, Mainz, 2007.

McComiskey, A., and Feingold, G.: The scale problem in quantifying aerosol indirect effects, Atmospheric Chemistry and Physics, 12, 1031-1049, doi: 10.5194/acp-12-1031-2012, 2012.

Reutter, P., Su, H., Trentmann, J., Simmel, M., Rose, D., Gunthe, S. S., Wernli, H., Andreae, M. O., and Poschl, U.: Aerosol- and updraft-limited regimes of cloud droplet formation: influence of particle number, size and hygroscopicity on the activation of

cloud condensation nuclei (CCN), ATMOSPHERIC CHEMISTRY AND PHYSICS, 9, 7067-7080, 10.5194/acp-9-7067-2009, 2009.

Rosenfeld, D., Lohmann, U., Raga, G. B., O'Dowd, C. D., Kulmala, M., Fuzzi, S., Reissell, A., and Andreae, M. O.: Flood or drought: How do aerosols affect precipitation?, Science, 321, 1309-1313, doi: 10.1126/science.1160606, 2008.

Tao, W. K., Li, X. W., Khain, A., Matsui, T., Lang, S., and Simpson, J.: Role of atmospheric aerosol concentration on deep convective precipitation: Cloud-resolving model simulations, J Geophys Res-Atmos, 112, D24S18, doi: 10.1029/2007jd008728, 2007.

Tao, W. K., Chen, J. P., Li, Z. Q., Wang, C., and Zhang, C. D.: Impact of Aerosols on Convective Clouds and Precipitation, Rev Geophys, 50, doi: 10.1029/2011rg000369, 2012.

Teller, A., and Levin, Z.: Factorial method as a tool for estimating the relative contribution to precipitation of cloud microphysical processes and environmental conditions: Method and application, J Geophys Res-Atmos, 113, doi: 10.1029/2007jd008960, 2008.

van Lier-Walqui, M., Vukicevic, T., and Posselt, D. J.: Quantification of Cloud Microphysical Parameterization Uncertainty Using Radar Reflectivity, Mon Weather Rev, 140, 3442-3466, doi: 10.1175/Mwr-D-11-00216.1, 2012.

Wang, Y., Fan, J. W., Zhang, R. Y., Leung, L. R., and Franklin, C.: Improving bulk microphysics parameterizations in simulations of aerosol effects, J Geophys Res-Atmos, 118, 5361-5379, doi: 10.1002/Jgrd.50432, 2013.

Zhang, L. M., Michelangeli, D. V., and Taylor, P. A.: Influence of aerosol concentration on precipitation formation in low-level, warm stratiform clouds, J Aerosol Sci, 37, 203-217, doi: 10.1016/j.jaerosci.2005.04.002, 2006.

Interactive comment on "Aerosol and dynamic effects on the formation and evolution of pyro-clouds" by D. Chang et al.
MS No.: acp-2014-61

Dear Reviewer,
We would like to thank you for the valuable and constructive comments/suggestions on our manuscript. We have revised the manuscript accordingly and please find our point-to-point responses below (line numbers refer to the new version of manuscript). In addition, the title of the manuscript is revised to be "Regime dependence of aerosol effects on the formation and evolution of pyro-convective clouds".

Reply to Anonymous Referee #2

This manuscript investigates the impacts of cloud condensation nuclei (CCN) and dynamic condition on pyro-clouds using a 2-D Active Tracer High Resolution Atmospheric Model (ATHAM) with a double-moment cloud microphysical scheme. Wide ranges of CCN concentration and convection strength were used to configure the sensitivity simulations with totally over 1000 runs. By carefully assessing the budget and evolution of hydrometeors as well as microphysical processes rates, the paper sorted out the different sensitivity regimes for aerosol and updraft velocity individually, and potentially shed some light on physical mechanism involved in the aerosol-cloud interaction. However, there are several problems that need to be adequately addressed before the paper can be accepted for publication.

1) In the abstract, authors emphasized that aerosols suppress the surface precipitation when aerosol concentration is between 1000 to 3000 cm^{-3}. However, Li et al. (2008, JGR) showed the opposite aerosol effect during the same aerosol range for the cumulus cloud. It indicates that CCN values here are not representative as thresholds to distinguish the aerosol effect.

Response: We thank the reviewer for pointing this out. We agree that the exact threshold value is subject to certain regime and may not be universally applicable to all conditions. It may change due to the differences in the model dimensionality

(2D vs. 3D), spatial dimension (single cloud convection vs. regional cloud evolution), microphysics and etc.

We make clear of this point and include more discussion concerning these uncertainties in the main text: "The threshold to distinguish the aerosol positive and negative effects is derived from the current simulated pyro-convective clouds. The cumulus cloud investigation in Li et al. (2008) also suggested this non-monotonic trend, with the threshold aerosol value around 3000 cm^{-3}. The existence of threshold N_{CN} in both studies implies that similar cloud types may have a similar regime dependence, of which the exact shape may differ due to difference in the meteorological conditions, aerosol properties, etc." "In this study, we demonstrate the performance of ensemble simulations in determining the regime dependence of aerosol effects. The use of such regime dependence requires caveats because it may differ for different cloud types, aerosol properties, meteorological conditions and model configurations (e.g., microphysical schemes, dynamic schemes, dimensionality, etc.; the 3-D results are in the supplementary material)". Please see Lines 389-394, and 739-743 respectively.

2) Fig. 1 doesn't deliver many messages, especially in the introduction part. I would suggest move it to the conclusion part and replace the question mark by the major findings in this study.

Response: Accepted and thanks for the suggestion. This figure helps us review the study progress of aerosol-cloud interaction at different scales and conclude our main research findings. We complete this figure and move it to the conclusion section. Please see Fig. R1, which is Fig. 23 in the revised manuscript.

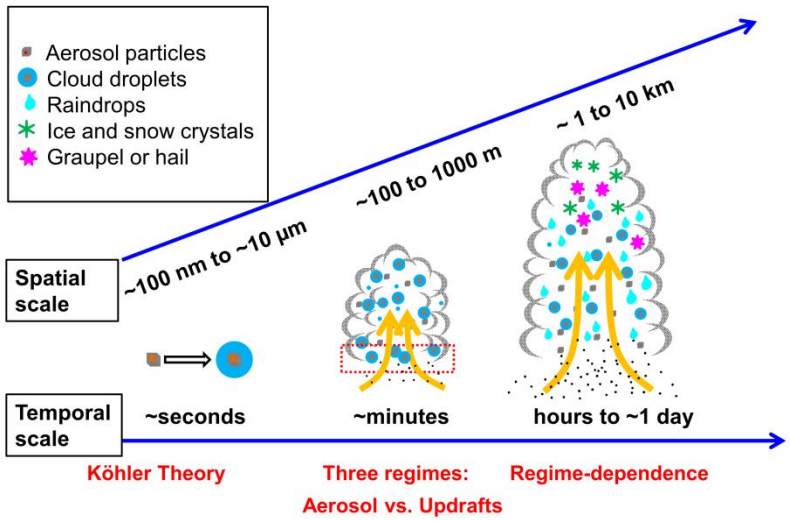

Figure R1. Overview of the research approaches on multi-scale cloud initialization and development.

3) Each simulation was conducted for only three hours. Is three-hour long enough to capture the lifetime of a typical pyro-cloud? From Fig. 12, it is clear that the precipitation was still going on after three hours.

Response: This is a good point. We agree that different time scales may change the regime dependence of aerosol effects (McComiskey and Feingold, 2012). The lifetime of deep convective clouds varies from several hours to days based on previous studies (Lindsey and Fromm, 2008; Hagos et al., 2013). Within our work, when fire forcing is weak, 3 simulation hours could cover the lifetime of most pyro-convective clouds. When fire forcing is very strong, the production of cloud hydrometeors and precipitation keeps in a steady level within 3 simulation hours (HULA, HUHA cases in Figs. 5, 9).

We have tested a longer simulation time (6 simulation hours) to examine the dependence of rain rate on aerosol concentration and fire forcing. As shown in Fig. R2, the results of 6-hour simulation are qualitatively similar to the 3-hour case (Figure 13a in new manuscript), we thus stick to the 3-hour results.

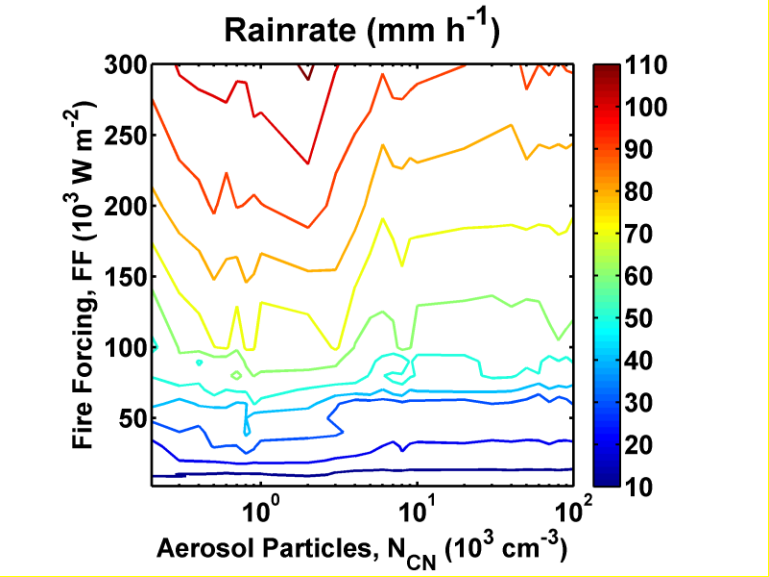

Figure R2. Contour plot of rain rate calculated as a function of aerosol number concentration (N_{CN}) and updraft velocity (represented by *FF*). Data are from the results of 6 simulation hours.

4) The prescribed aerosol budget used in this study could bias aerosol effects. Wang et al. (2013, JGR) has pointed out that prescribed aerosol scheme overestimates the magnitude of aerosol effects, and even changes the sign of aerosol effects with bulk microphysics. Similar discussion is necessary here and an implementation of a prognostic aerosol approach would be more valuable.

Response: Thanks for the comments. We admit that the prescribed aerosol method can lead to bias in the results. One of the main reasons is because our ATHAM model doesn't have an aerosol module. Therefore, we followed some previous studies (Seifert et al., 2012; Reutter et al., 2013) and used the prescribed aerosol distributions as an alternative. We have included more discussion about the uncertainty of prescribed aerosol approach and the importance of prognostic approach. Lines 152-156: "A similar prescribed approach has been used in previous studies (Seifert et al., 2012; Reutter et al., 2013). Some previous studies have pointed out that a prescribed aerosol scheme overestimates the magnitude of CCN concentrations compared to a prognostic aerosol scheme,

because it lacks a representation of the efficient removal of particles by nucleation scavenging (Wang et al., 2013)."

5) Page 7787 line 20, the statement "As N_{CN} or FF increases, their impact becomes weaker" is not accurate. Clearly from Fig. 3b, sensitivities of cloud droplets to FF become larger after $4*10^4$ W m^{-2}.

Response: We have revised the manuscript accordingly as "High sensitivities were found for low conditions of N_{CN} and *FF*. While there are some deviations (which appear to be random numerical noise), in general, as either N_{CN} or *FF* increases, the impact on the cloud droplet number concentration of further changes to either the variable becomes weaker (Figs. 7c and 7d)." Please see lines 280-283.

6) Page 7788 line 4, the statement "when we evaluate the cloud responses to the changes in the ambient aerosol particles for global models or satellite data, we should focus more on the aerosol effect on cloud droplet number concentration, rather than on the liquid water path" is problematic. From Fig. 3c, it is clear that the sensitivities of cloud mass to CCN is quite pronounced under low updraft condition with CCN concentration less than 2000 cm^{-3}. Meanwhile, this is the typical maritime condition for stratocumulus clouds, which are prevalent over the most ocean region. Therefore, the aerosol effect on cloud liquid contend is very important.

Response: We agree and we have removed this statement in the revised manuscript.

7) Section 3.2.2, there is no physical explanation of the complicated response of the raindrop concentration to aerosols and updrafts.

Response: Sorry for the confusion. Within the main text, we put the general results in Sect. 3.2, and present the corresponding detailed physical explanation in Sect. 3.3. The microphysical explanations for raindrops will be found in Sect. 3.3.2.

8) Page 7789 line 19-22, it is reported that "greater concentrations of aerosol result in more snow and less graupel", but actually some other studies suggested that elevated aerosols could increase the graupel/hail in the convective system (Khain et al., 2009, JGR;Wang et al., 2011, ACP). This is attributed to the competing effects of aerosols on the graupel formation. Since graupel is mainly formed by the accretion of supercooled drops by ice or snow, the smaller but more abundant supercooled cloud droplets in the polluted condition could be either favorable or not for graupel formation.

Response: Thank for the comments. In the work of Khain et al. (2009) and Wang et al. (2011), more aerosols are suggested to enhance the collision between graupel particles and small supercooled droplets, and thus the graupel/hail formation. Within our work, we found only under LULA (low updrafts and low aerosol) condition, riming of cloud droplets and raindrops (*crg* and *rrg*) is an important source of graupel (Fig. R3). When aerosol concentration increases, more droplets are prone to form small frozen particles (ice and snow) firstly, and the main source of graupel is from the collection of these small frozen particles. This may explain the difference with Khain et al. (2009) and Wang et al. (2011).

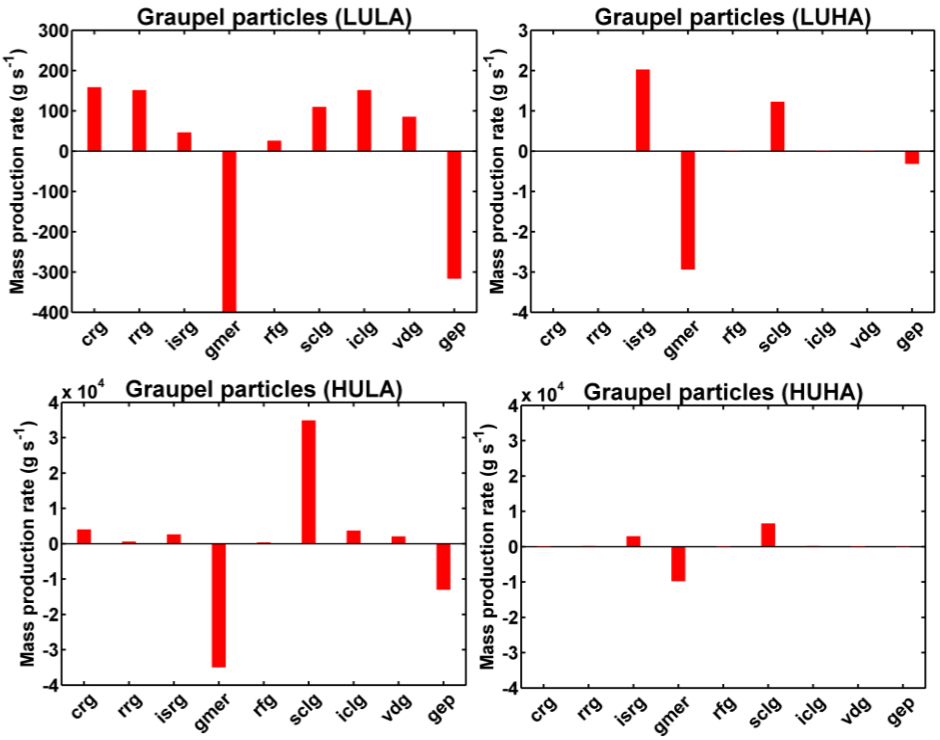

Figure R3. Comparisons of the time-averaged rates of change in graupel concentration resulting from the main processes, which were obtained from the domain-integrated values. Sources are plotted as positive values, and sinks are negative. The acronyms indicate *c/r/i/srg*: riming of cloud droplets/raindrops/ice/snow to form graupel; *gmer*: melting of graupel to form raindrops; *rfg*: freezing of raindrops to form graupel; *i/sclg*: collection of ice/snow to form graupel; *vdg*: condensational growth of graupel by water vapor; *gep*: evaporation of graupel.

In the main text, we have included more discussion to address the diverse aerosol effects on the graupel production. Please see Lines 354-359. The text is "Other research has suggested that elevated aerosols could increase the concentration of large frozen particles (graupel/hail) in the convective system (Khain et al., 2009; Wang et al., 2011), which was attributed to the competing effects of aerosols on the graupel formation. Since graupel is mainly formed by the accretion of supercooled droplets by ice or snow, the smaller but more abundant supercooled drops under polluted conditions could be either favorable or unfavorable for graupel formation."

9) It is nice to see that authors stress the importance of a longer period simulation. Actually, Fan et al. (2013, PNAS) and Wang et al. (2014, Nature Communication) have done some long-term (more than one month) cloud-resolving modeling studies over certain cloud regions. Please discuss accordingly.

Response: Fan et al. (2013) and Wang et al. (2014) suggested that anthropogenic aerosols will increase accumulated rain trend. They also conclude that the most important influence induced by aerosols is the redistribution of precipitation, indicated by the reduced light rain occurrence frequency and increased heavy rain frequency in polluted regions. This could lead to higher risk of droughts and floods in monsoon regions due to more serious pollution. In the revised manuscript, we add the following discussion on lines 416-418: "Simulations for a longer period should be carried out in future studies to investigate the influence of aerosols on precipitation over longer time scales as in Fan et al. (2013) and Wang et al. (2014)."

10) I'm concerned about the way authors calculate the microphysical process rates. Since the rates are averaged over the whole domain, I would expect that the cloud occurrence/fraction over the domain might significantly affect the microphysical rates there. It will be important to report the rates from cloud-only-points as well.

Response: We have been thinking of both ways of calculating process rates. The reason that we finally made the average over the domain is to be consistent with the way we calculated the averaged number/mass concentration. Otherwise, the rate and concentration will not be directly comparable due to the influence of cloud occurrence/fraction.

11) In Fig. 13 and 15, g/h/s/imer should be melting to form raindrops, rather than "multiplication to form ice crystals".

Response: Accepted. We corrected this explanation. Please see Figs. 18 and 20 in the revised manuscript.

12) In Fig. 11 and 13, it shows that autoconvertion rate from cloud droplets to raindrops is higher in the high aerosol scenario (HA) than that in the clean case (LA). Why?

Response: The domain-averaged rate is in fact slightly reduced as N_{CN} increases (LA→HA) under high updraft (HU) condition. The apparent difference may result from different scales used in these figures.

13) Page 7795 line 7, what is the reason behind the phenomena "although snow is the dominant constituent of frozen particle mass (Fig. S4), the deposition of vapor on ice (vdi) rather than on snow is the major pathway for frozen particles"?

Response: After examining the budge of snow, the process of collecting of ice to form snow (processes of *iscs*, and *icls*) is much more efficient than other source processes (Fig. R4), which are internal conversions not counted as either a source or a sink of frozen water content. The ice crystals used for conversion to snow is mostly from the deposition of vapor on ice (*vdi*). Once small ice crystals appear, they can quickly collide to be snow. We add this explanation in the main text, and please see Lines 571-574: "The increase of snow mass is

mostly caused by collecting of ice (*ics*) and ice self-collection (coagulation of ice particles, *iscs*), which are internal conversions not counted as either a source or a sink of frozen water content. The ice crystals used for conversion to snow derive mostly from the *vdi* process".

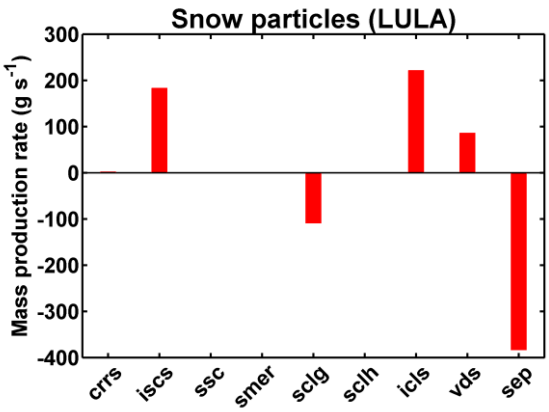

Figure R4. Comparisons of the time-averaged rates of change in snow concentration resulting from the main processes, which were obtained from the domain-integrated values. Sources are plotted as positive values, and sinks are negative. The acronyms indicate crrs: riming of cloud droplets and raindrops to form snow; iscs: selfcollection of ice to form snow; ssc: selfcollection of snow; smer: melting of snow to form raindrops; sclg/h: collection of snow to form graupel/hail; icls: collection of ice to form snow; vds: condensational growth of snow by water vapor; sep: evaporation of snow.

References

Fan, J. W., Leung, L. R., Rosenfeld, D., Chen, Q., Li, Z. Q., Zhang, J. Q., and Yan, H. R.: Microphysical effects determine macrophysical response for aerosol impacts on deep convective clouds, P Natl Acad Sci USA, 110, E4581-E4590, doi: 10.1073/pnas.1316830110, 2013.

Hagos, S., Feng, Z., McFarlane, S., and Leung, L. R.: Environment and the Lifetime of Tropical Deep Convection in a Cloud-Permitting Regional Model Simulation, J Atmos Sci, 70, 2409-2425, doi: 10.1175/Jas-D-12-0260.1, 2013.

Khain, A. P., Leung, L. R., Lynn, B., and Ghan, S.: Effects of aerosols on the dynamics and microphysics of squall lines simulated by spectral bin and bulk parameterization schemes, J Geophys Res-Atmos, 114, doi: 10.1029/2009jd011902, 2009.

Li, G. H., Wang, Y., and Zhang, R. Y.: Implementation of a two-moment bulk microphysics scheme to the WRF model to investigate aerosol-cloud interaction, J Geophys Res-Atmos, 113, doi: 10.1029/2007jd009361, 2008.

Lindsey, D. T., and Fromm, M.: Evidence of the cloud lifetime effect from wildfire-induced thunderstorms, Geophys Res Lett, 35, doi: 10.1029/2008gl035680, 2008.

McComiskey, A., and Feingold, G.: The scale problem in quantifying aerosol indirect effects, Atmospheric Chemistry and Physics, 12, 1031-1049, doi: 10.5194/acp-12-1031-2012, 2012.

Reutter, P., Trentmann, J., Seifert, A., Neis, P., Su, H., Herzog, M., Wernli, H., Andreae, M. O., and Poschl, U.: 3-D model simulations of dynamical and microphysical interactions in pyro-convective clouds under idealized conditions, Atmos Chem Phys Disscuss, 13, 19527-19557, doi:10.5194/acpd-13-19527-2013, 2013.

Seifert, A., Kohler, C., and Beheng, K. D.: Aerosol-cloud-precipitation effects over Germany as simulated by a convective-scale numerical weather prediction model, Atmospheric Chemistry and Physics, 12, 709-725, doi: 10.5194/acp-12-709-2012, 2012.

Wang, M., Ghan, S., Ovchinnikov, M., Liu, X., Easter, R., Kassianov, E., Qian, Y., and Morrison, H.: Aerosol indirect effects in a multi-scale aerosol-climate model PNNL-

MMF, Atmospheric Chemistry and Physics, 11, 5431-5455, doi: 10.5194/acp-11-5431-2011, 2011.

Wang, Y., Fan, J. W., Zhang, R. Y., Leung, L. R., and Franklin, C.: Improving bulk microphysics parameterizations in simulations of aerosol effects, J Geophys Res-Atmos, 118, 5361-5379, doi: 10.1002/Jgrd.50432, 2013.

Wang, Y., Zhang, R. Y., and Saravanan, R.: Asian pollution climatically modulates mid-latitude cyclones following hierarchical modelling and observational analysis, Nat Commun, 5, doi: 10.1038/Ncomms4098, 2014.

Interactive comment on "Aerosol and dynamic effects on the formation and evolution of pyro-clouds" by D. Chang et al.
MS No.: acp-2014-61

Dear Reviewer,
We would like to thank you for the valuable and constructive comments/suggestions on our manuscript. We have revised the manuscript accordingly and please find our point-to-point responses below (line numbers refer to the new version of manuscript). In addition, the title of the manuscript is revised to be "Regime dependence of aerosol effects on the formation and evolution of pyro-convective clouds".

Anonymous Referee #3

This paper reports on results of 1000s of 2D aerosol-cloud model simulations to study the impact of aerosols on a pyro-convective cloud under various aerosol and dynamical conditions. The quality of the work is very good because it provides a parameter space explaining where to expect clouds to be sensitive to aerosol effects and what conditions are not conducive to aerosol effects. The first half of the paper is well written. It was a pleasure to read. However, the discussion of the results became quite confusing. There were not good interpretations of the results. The study is limited to the 2D framework, and may be even more limited to certain environmental conditions (T, RH, and wind profiles). The limitations of the present study and the interpretation of results must be discussed more fully before publishing the paper.

Response: We appreciate the comments very much. Within this work, we aim to investigate the sensitivity of the pyro-convective clouds to a wide range of aerosol concentrations under different updraft conditions. We have revised and extended the discussion of the results. Especially, a new approach has been adopted in which the spatial and time-resolved contribution of individual processes has been visualized for the interpretation of the results. With similar approach, we are also able to show the integrated process rates for all the stud-

ied cases, not only the four individual cases. Please see Figs. 16, 18 and 20 for the process analysis of cloud droplets, raindrops and frozen water content respectively, and the corresponding text is in Sect. 3.3. The relative importance of each microphysical process is evaluated and discussed in Sect. 3.3.4. The ATHAM model consists of several tens of microphysical processes. By identifying the contribution from individual processes, PA may also provide an opportunity for the simplification of microphysical schemes. For example, out of 24 microphysical processes that are directly related to the budget of liquid droplets, over 90% of the mass and number changes are contributed by only 10 processes.

We agree with the referee about the limitations and have emphasized that caveats are required in the interpretation of our results. Besides, we have performed complimentary 3-D simulations to illustrate such potential problem as in the supplementary material.

Major comments:

While it makes sense to do 2D simulations in order to conduct 1000s of simulations, the ability of the 2D simulations should be evaluated with a comparison of results to a 3D simulation. This has been common practice in many past cloud modeling studies.

Response: We agree. In the revised manuscript, we run a series of complimentary 3-D simulations (~100 cases), and the discussion concerning the 3-D results (cloud droplets, raindrops, frozen water content, and precipitation) have been included in the supplementary material. Take cloud droplets for example, the regime dependence from the 3-D simulations (Fig. R1b) looks similar to the 2-D results (Fig. R1a) though the absolute dependency may vary. This implies that the use of such regime dependence requires caveats because it may differ for different model dimensionality (2D vs. 3D). In the main text, we have included more discussion concerning these uncertainties: "In this study, we demonstrate the performance of ensemble simulations in determining the regime de-

pendence of aerosol effects. The use of such regime dependence requires caveats because it may differ for different cloud types, aerosol properties, meteorological conditions and model configurations (e.g., microphysical schemes, dynamic schemes, dimensionality, etc.; the 3-D results are in the supplementary material)". Please see Lines 739-743.

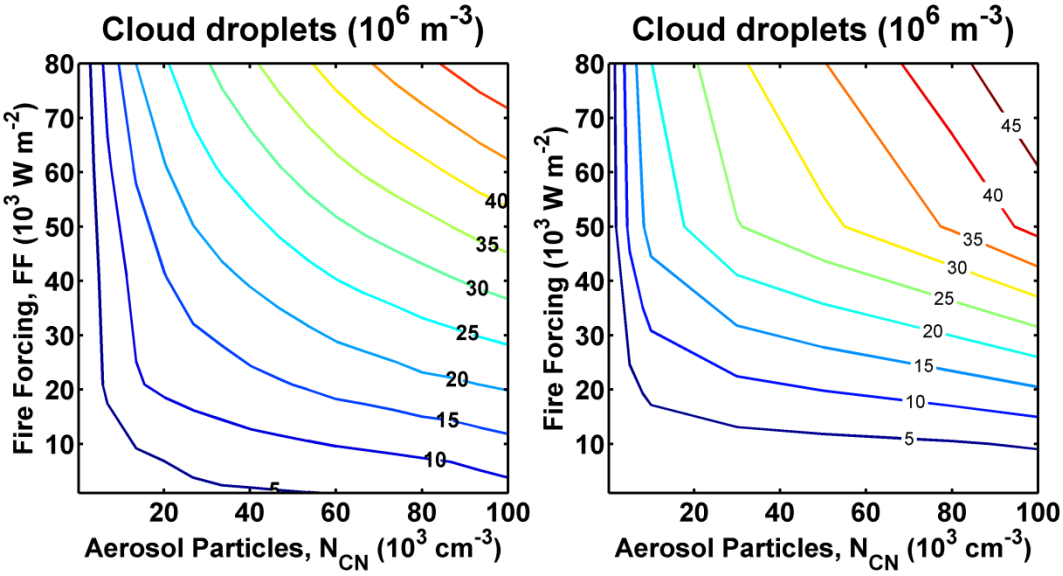

(a) (b)

Figure R1. Number concentration of cloud droplets calculated as a function of aerosol number concentration (N_{CN}) and updraft velocity (represented by *FF*) from 2-D (a) and 3-D (b) simulations.

I recommend including all the supplementary material in the main manuscript. I found the supplementary figures relevant to the discussion and quite interesting. I also recommend removing the normalized number and mass concentrations (Fig 2c-f, Fig 4c-f, Fig 6c-f, and Fig 8b-c) and replacing them with the relative sensitivity plots in Figures 3, 5, 7, and 9. Better yet, would be to just remove the former and keep the relative sensitivity plots in separate figures.

Response: Accepted. We have moved all the tables and figures in the supplementary to the main text, and replaced the figures for the normalized concentrations of

each hydrometeor with the relative sensitivity plots. Please see Figs. 7, 9, 12 and 13 in the revised manuscript.

I believe the intended audience is the aerosol-cloud community, and not necessarily the pyro-cumulus community. The cloud community is much more concerned about updraft speeds than the forcing of the convective updrafts. Thus, I strongly recommend that the approximate updraft strength (maximum vertical velocity is a good measure) be given along with the fire forcing values as another axis in the plots. The readers would then be able to put this paper's results in context of their knowledge of convective storms.

Response: Accepted. The relationship between fire forcing and the corresponding updraft velocities is given in Sect. 2.2, which is logarithmic. Thus we add the maximum vertical velocity along with the fire forcing as the second y axis in the contour plot for the number concentration of cloud droplets (Fig. R2, which is Fig. 7a in the new manuscript).

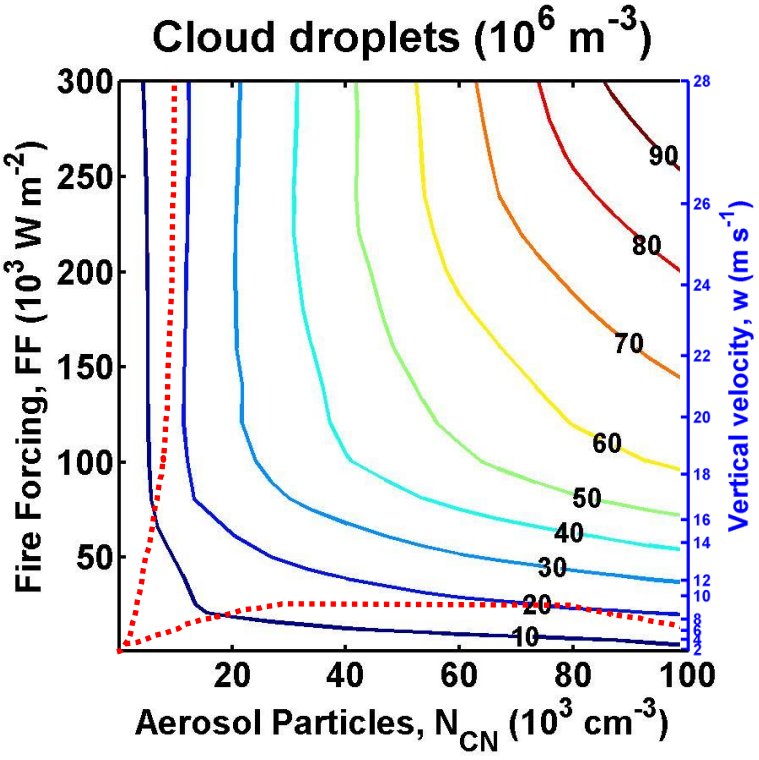

Figure R2. Number concentration of cloud droplets calculated as a function of aerosol number concentration (N_{CN}) and updraft velocity (represented by *FF*).

The results presented in sections 3.2 and 3.3 are quite complicated. I would recommend introducing the results in a simpler manner before Figure 2 is discussed. My suggestion would be to show an instantaneous cross-section of the cloud for the LULA, LUHA, HULA, and HUHA cases. The cloud could be color coded by droplet number concentration or cloud mass concentration (or cloud and rain mass concentration). This type of figure would allow the reader to see a figure of something they are familiar with, and allow the authors to introduce the more complicated subsequent figures (Figures 2-9).

Response: Accepted. In Sect. 3.2 of the revised manuscript, we put the time evolution of horizontally-averaged concentration of each hydrometeor for four extreme cases in the beginning of the result part. After briefly introducing the temporal and spatial distribution of each hydrometeor, their dependence on the aerosol and fire forcing would be presented. For the temporal and spatial distribution of cloud droplets, please see Lines 244-250:"Figure 6 shows the temporal evolution of horizontally-averaged mass concentration of cloud droplets (M_{CD}) under the four pairs of FF and N_{CN} conditions. Under weak fire forcing conditions (LU), the formation of cloud droplets usually occurs from 20 min, and concentrates at an altitude of 4-7 km. The duration of cloud droplets usually last for a short period (40~60 min). Under strong fire forcing conditions (HU), the cloud droplets form earlier (around 5 min), and most cloud droplets are located at a height of 5-9 km. Besides, the cloud droplets reach steady state because of the cycling of cloud formation."

For raindrops, please see Lines 303-307:"Figure 8 exhibits the temporal evolution of the horizontally-integrated mass concentration of raindrops under four different conditions. Compared with cloud droplets (Fig. 6), the occurrence of raindrops is much later, especially when N_{CN} and fire forcing are in a high level. Only for LULA case, numerous raindrops can be found in a high altitude (5-7 km), while for other cases, most of raindrops are located below 5 km (~0 ℃)."

For frozen particles, please see Lines 334-340: "The time evolution of frozen water content in Fig. 10 suggests that the formation of frozen water content

usually occurs in a high level (5-9 km for LU case, and 7-13 km for HU case), and the height of base layer and top layer decreases as time goes by. Under LU condition, the appearance of frozen water content is around 35 min, and lasts for ~120 min, with the peak concentration around 50~70 min. Under HU condition, the frozen particles form around 10 min, and keep in a steady state."

The main reason the results become difficult to understand is because a lot of jargon is used, and the authors mostly describe what is shown in the figure, but don't do a very good job of interpreting what the figure says. For example, instead of saying "FF exhibits positive effects on raindrop formation", it could be written like, "as the fire forcing (or updrafts) increases in magnitude, the amount of rain increases (Figure 4b), but the size of rain drops vary because of the complex behavior of the response of the rain drop number with fire forcing (Figure 4a)". The other reason the results are difficult to comprehend is that the text jumps from one figure to another in a single sentence. Some of this jumping would be reduced by putting the relative sensitivity plots in the same figure as the contour plots (as a function of aerosol number concentration and fire forcing).

Response: Thanks for the constructive suggestions. In the revised manuscript, we optimized the formulation and reduce the use of jargon. To make the transition of discussion smoother and easier to comprehend, we move the relative sensitivity plots in the same figure as the contour plots. For raindrops, we have modified the text, and please see lines 315-325. "As *FF* increases in magnitude, the amount of rain produced (M_{RD}) increases (Fig. 9b), but the size of raindrops varies because of the complex behavior of the response of the rain drop number (N_{RD}) to *FF* (Fig. 9a). The aerosol effect is non-monotonic: M_{RD} increases with aerosols in the lower range of N_{CN} values (<~1000 cm^{-3}), but further increases in N_{CN} result in a decrease in M_{RD}. Combining with the relative sensitivities (Figs. 9e, and 9f), the influence of *FF* is much more significant than that of N_{CN} in most cases. For example, the upper left corner (an aerosol-limited regime for N_{CD}) becomes a transitional regime for M_{RD} with *RS* (*FF*) of 0.1 and *RS* (N_{CN}) of -0.06 (Fig. 9). High sensitivities of M_{RD} to N_{CN} are found at low N_{CN} conditions, but the sensitivity decreases as N_{CN} increases

(Fig. 9e). The N_{CN} plays the most negative role in M_{RD} under intermediate N_{CN} conditions (N_{CN} of several 1000 cm^{-3})." For frozen particles, instead of "The FF and N_{CN} show positive effects for both the number and mass concentrations of the", it is written to be "With the enhancement in FF and N_{CN}, both the number and mass concentrations of the frozen water particles (N_{FP} and M_{FP}, respectively) increase". Please see Lines 365-366. For other hydrometeors, the language description in the discussion part is also modified to avoid the use of jargon.

Specific comments:

1. p. 7784, line12. Are the aerosols distributed uniformly in the vertical direction too? What are the initial horizontal winds? Do initial horizontal winds vary with height? That is, is there any vertical wind shear? (Fan et al., 2009 show how aerosol-cloud-precipitation results vary with vertical wind shear)

Response: (1) The concentration of ambient aerosols is set to be homogeneous over the modeling domain, without considering the spatial and temporal distributions of atmospheric aerosols during the simulations, which is similar to some previous studies (Seifert et al., 2012; Reutter et al., 2013). We admit the variability of aerosols during the simulation is ignored and may leads to a bias compared to a real fire (Wang et al., 2013). We add this discussion about the bias in the revised manuscript; please see lines 152-156. For the future research, we will try to improve the representation of the aerosol particles and take into account the full complexity of all chemistry-aerosol-cloud interactions.

(2) Within our 2-D simulations, the initial horizontal wind was set to be zero, and therefore there is no vertical wind shear. We admit further work is still needed to investigate the wind shear impact on the convection strength as suggested in Fan et al. (2009), which is for now beyond the scope of this manuscript. Therefore, we add some brief discussion in Sect 3.1 of the main text, which is "Finally, we note that the horizontal wind shear can also affect the convection strength (Fan et al., 2009), which could be investigated in detail in future studies." Please see Lines 231-232.

2. p. 7785, line 20. As it is spring convection season here in the United States, it is important to note that severe convection has updrafts much greater than 20 m/s. Severe convection also transports much more mass to the upper troposphere and delivers more precipitation to the surface than the smaller storms found over the U.S. Thus, I recommend saying that the updrafts simulated represent those found in air mass thunderstorms or trade wind cumulus.

Response: Accepted. We revised this sentence to be "In pyro-convective clouds, the updraft velocities range from ca. 0.25 to 20 m s^{-1} (Reutter et al., 2009), which represent the range found in trade wind cumulus to thunderstorms (Pruppacher and Klett, 1997)." Please see lines 206-209.

3. p. 7787, lines 3-24. I was confused as to why Figure 2 was introduced here, but not explicitly discussed before Figure 3 was discussed on line 20. Here is an example of why I think Figure 3 should replace Figure 2c-f.

Response: In the revised manuscript, we have changed the figure arrangement. Please see Figs. 7, 9, 12 and 13 in the revised manuscript.

4. p. 7787, lines 21-24. Can you show how the cloud system buffering effect is affecting the droplet number concentration? I thought this study was modeling a single convective storm (p. 7782, line 4) and therefore do not see a cloud system effect for this study. A better explanation is needed.

Response: It is true that this work focused on the aerosol effect on the isolated pyro-convective clouds. We have modified the text to be: "The reduced sensitivity of cloud droplets to aerosols can be explained by the buffering effect of the cloud microphysics, so that the response of the cloud system to aerosols is much smaller than would have been expected." Please see Lines 283-286. The explanation can be "Under weak updrafts, the N_{CD}/N_{CN} ratio is sensitive to ambient supersaturations. In this case, a larger supersaturation induced by stronger updrafts can effectively change the N_{CD}/N_{CN} ratio and thus N_{CD} is sensitive to the updraft velocity. On the other hand, the stronger dependence of N_{CD}/N_{CN} on the supersaturation also changes the role of aerosols. As more

aerosols reduce supersaturation, increasing N_{CN} tends to reduce the activated fraction, N_{CD}/N_{CN}. Taking N_{CN} = 60,000 cm^{-3} (*FF* = 2,000 W m^{-2}), for example, a 10% increase in N_{CN} causes a 4% decrease in N_{CD}/N_{CN}, whereas a 10% decrease in N_{CN} leads to an 8% increase in N_{CD}/N_{CN}. The impact of changing N_{CN} on the N_{CD}/N_{CN} ratio counteracts partly or mostly the positive effect of N_{CN} on cloud droplet formation. " Please see Sect. 3.3.1 (Lines 442-450).

5. p. 7789. Perhaps it is because I am used to U.S. convective storms where hail is common, but why is there no hail in 3 of the 4 cases shown in Figure S4? Hail is only in the LULA case, which does not make sense since hail is associated with high updrafts. I am concerned about the worthiness of these results.

Response: Actually the absolute concentration of hail generally increases with the enhancement in the fire forcing, as displayed in Fig. R3, although there is some deviations. But compared to other hydrometeors, its contribution is not important. Thus from Fig. 11 in revised manuscript, it seems the relative percentage of hail is very low. We add some discussion in the main text, which are "It is worth noting that stronger *FF* leads to increasing absolute concentration of hail. But compared to other hydrometeors, its contribution is not important and the relative percentage is very low." Please see Lines 361-363.

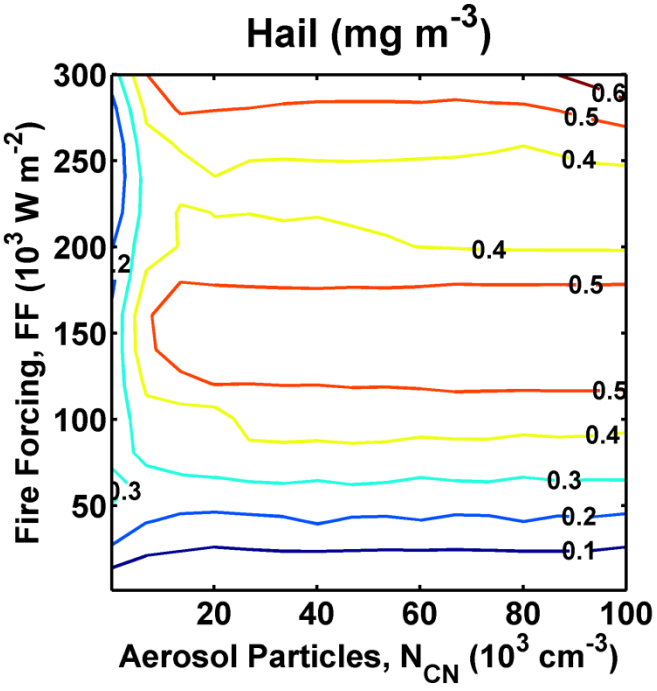

Figure R3. Mass concentration of hail calculated as a function of aerosol number concentration (N_{CN}) and updraft velocity (represented by FF).

6. p. 7789. I am also surprised that the primary loss of cloud water to any of the ice hydrometeors is through cloud drop freezing. Does this mean that cloud drops do not transfer to the ice hydrometeors until they are at temperatures < -40 C? In my past work (albeit, with microphysics not quite as sophisticated as that presented here), the most common way for cloud drops to freeze was through the riming process, especially snow accreting cloud drops, or graupel accreting cloud drops.

Response: The cloud drop freezing is a primary loss of cloud water concerning the budget of ice particle number. For the mass budget from cloud water to ice hydrometeors, the major path way is the Wegener-Bergeron-Findeisen (WBF) process. The evaporation of small cloud droplets (*cep*) provides more water vapor, leading to a higher supersaturation with respect to ice and enhanced growth of ice embryos by vapor deposition (*vdi*). At the same time, the consumption of water vapor could reduce the water saturation, thereby further boosting the evaporation of cloud droplets. The other freezing processes (e.g., riming of

cloud droplets to snow, graupel and hail) also take place, but their contribution is relatively small within our ATHAM modeling results. The contribution of cloud freezing to the mass budget become comparable to WBF process only at extremely high updraft (FF>10^5 W m^{-2}).

7. p. 7790, lines 8-14. Why does the rain rate (Figure 8a) behave so differently from rain mass concentration (Figure 4b)?

Response: In the old version of manuscript, the contour plots for raindrops are smoothed, while the rainfall contour plot is not smoothed. In the revised version, we replot the contour plots for raindrops based on the original data, and found the isolines of the rain water content (Fig. R4, which is Fig. 9b in revised manuscript) behave similar with the rain rate (Fig. 13a in the revised manuscript).

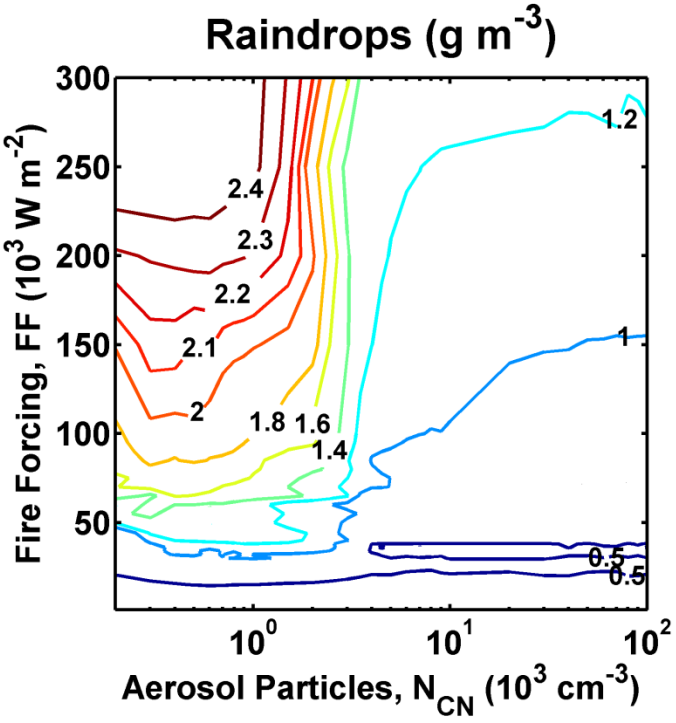

Figure R4. Mass concentration raindrops calculated as a function of aerosol number concentration (N_{CN}) and updraft velocity (represented by FF).

8. p. 7790, lines 19-20, Could the authors please clarify where these precipitation-enhanced and suppressed regimes are on the figure?

Response: We make clear of the definition of the regimes for precipitation, which can be found in Lines 384-387: "In the precipitation-invigorated regime (N_{CN} < ~1000 cm^{-3}), an increase in N_{CN} leads to the increase in the precipitation rate, and reduction in *RS* (N_{CN}) (Fig. 13b). In the precipitation-inhibited regime (N_{CN} > ~1000 cm^{-3}), aerosols start to reduce the precipitation, which is reflected in a negative *RS*(N_{CN})." Besides, these two regimes are also marked in the figure (Fig. R5, which is Fig. 13a in the revised manuscript).

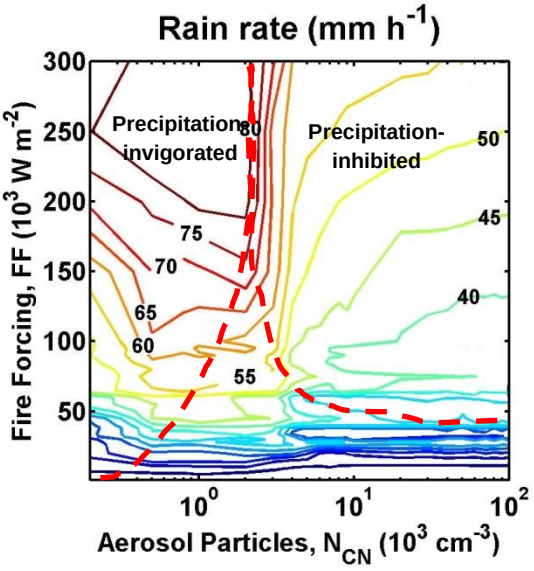

Figure R5. Contour plot of rain rate calculated as a function of aerosol number concentration (N_{CN}) and updraft velocity (represented by *FF*).

9. p. 7792, lines 4-8. At what updraft speeds does the change in updraft speed not significantly influence the N_{CD} to N_{CN} ratio?

Response: Within our model, the cloud nucleation (CCN activation) process is based on the lookup table derived from parcel model simulations for pyro-convective clouds (Reutter et al., 2009). It is observed that for pyro-convective clouds

with high aerosol concentration (>10^4 cm^{-3}), when the updraft velocity is above 15 m s^{-1}, the N_{CD} to N_{CN} ratio is 0.9 (Reutter et al., 2009), and the further increase in fire forcing does not largely change N_{CD} to N_{CN} ratio. We also include this threshold value in the main text. Please see line 438-439.

10. Section 3.3, While these results are interesting and useful, I was wondering if there is anything interesting in the time evolution of these microphysics processes. Are the relative contributions of the different processes shown in the figures hold true at different times in the simulation?

Response: Thanks for the stimulating suggestions. We plotted the contribution of the microphysical processes in each modeling grid under different simulation period. Here we take raindrops under HUHA condition (w = 27 m s^{-1}; N_{CN}=100,000 cm^{-3}) for example (Fig. R6). Each plot shows the vertical cross sections of the averaged change rate of main processes contributing to raindrops over 30 simulation minutes. Colors within each pie chart reflect the percentage of processes in each grid. As mentioned in the main text, the warm rain process is quite unimportant under strong *FF* condition. However, it is observed from Fig. R6 that the warm rain process is the leading source of raindrops at the beginning stage (60 min). The size of the raindrops formed from autoconversion and accretion is relatively small, which can easily evaporate. The melting of frozen particles to form raindrops becomes more significant after ~90 min, which dominates the production of raindrops. As shown in Fig. R6, although the processes still continue at 180 simulation minutes, the microphysics has already fully developed during this simulation period. Thus our 3 simulation hour could cover the characteristics of the formation and evolution of the pyro-convective clouds.

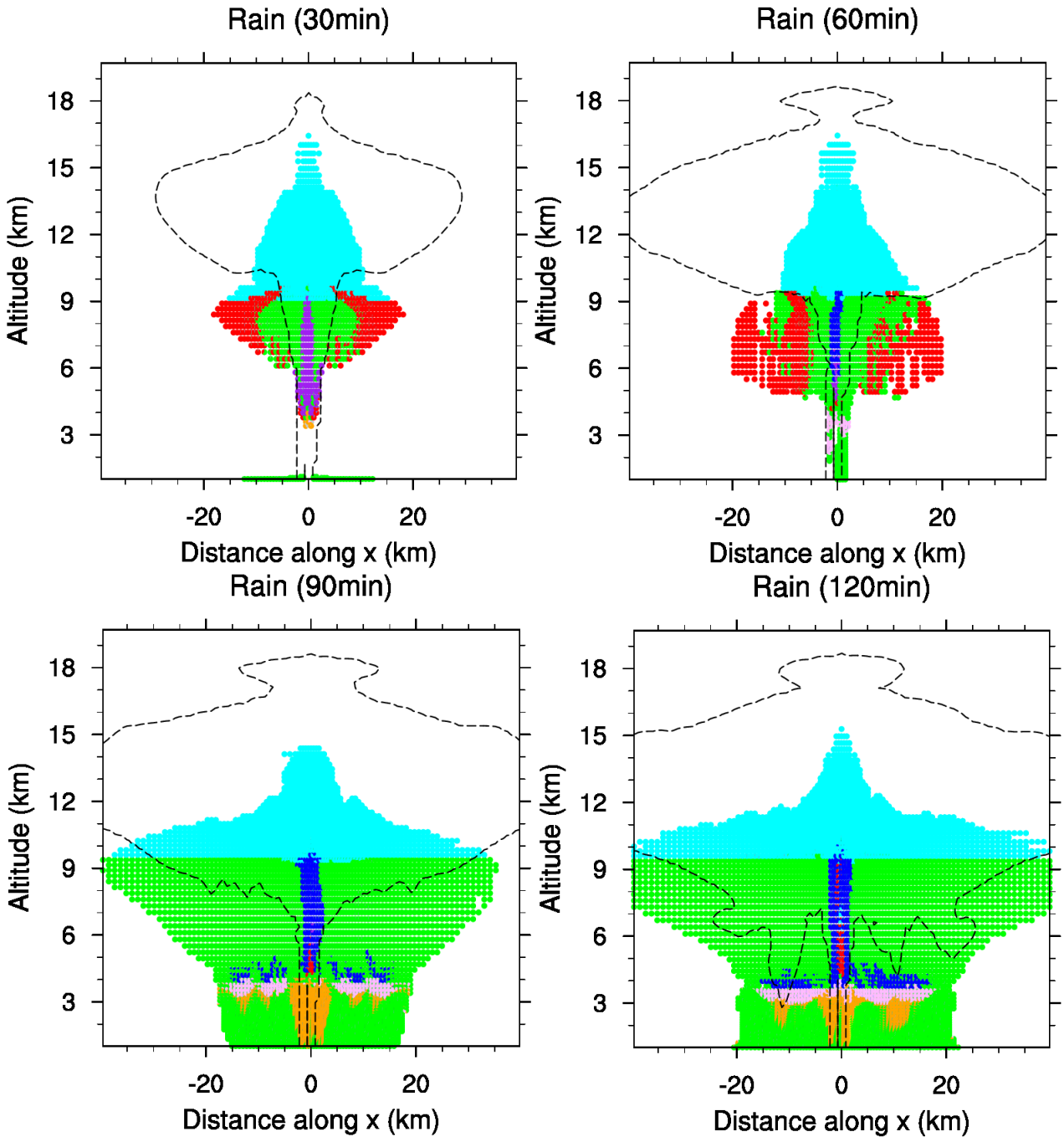
Rain (30min)
Rain (60min)
Rain (90min)
Rain (120min)
Altitude (km)
Distance along x (km)
18
15
12
9
6
3
-20
0
20

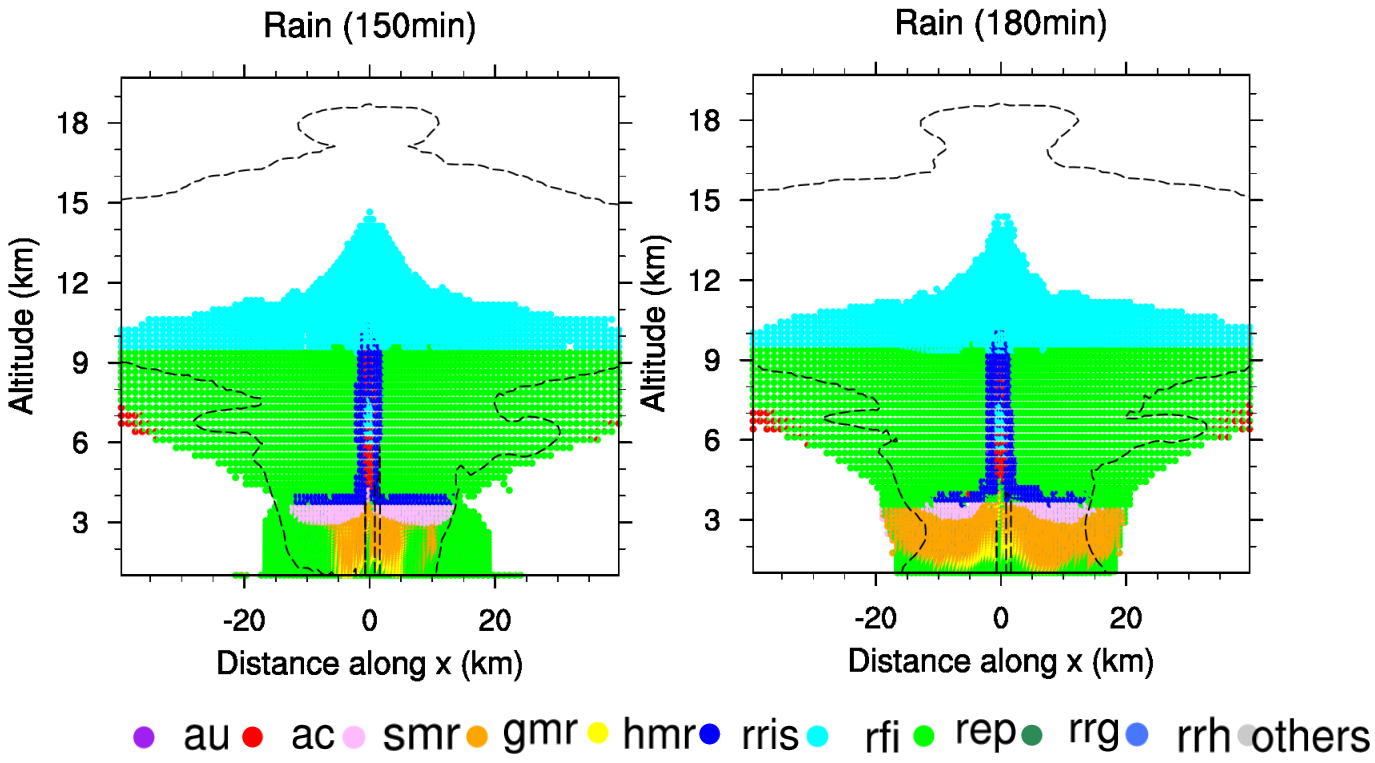

Figure R6. The pie charts summarize the vertical cross sections of the change rate of main microphysical processes contributing to raindrops. Each pie chart shows the averaged contribution over the past 30 min. Colors within each pie chart reflect the percentage of processes in each grid. The black dashed line is the 0.1 μg kg^{-1} isoline of the interstitial aerosol, indicating the shape of smoke plume. Warm colors denote the source, while cold colors denote the sink. The acronyms indicate au: autoconversion; ac: accretion; s/g/hmr: melting of snow/graupel/hail to form raindrops; rris: riming of raindrops to form ice and snow; rfi: freezing of raindrops to form ice crystals; rep: raindrop evaporation; rrg/h: riming of raindrops to form graupel/hail.

For other hydrometeors, please see the revised manuscript (sect. 3.3.1 for cloud droplets, sect. 3.3.2 for raindrops, and sect. 3.3.3 for frozen particles).

11. Section 4, Conclusions. I recommend removing the jargon for those people who just read the conclusions. Explaining the meaning of the results to our understanding of the aerosol-cloud science would be a bonus.

Response: In the new manuscript, we have modified the conclusion part, and reduced the jargon to avoid difficult comprehension. Instead of saying "positive/negative effect", we explain our results in a simple and understandable way. For example, instead of "Larger FF resulted in more precipitation, whereas the effect of aerosols on precipitation was complex and could be either positive or negative" in conclusion 4. The conclusion concerning precipitation is changed to be as follows with detailed explanation: "Larger *FF* resulted in more precipitation, whereas the effect of aerosols on precipitation was complex and could either enhance or suppress the production of precipitation. The suppression on the precipitation is due to the change in the fraction of small frozen particles and total melting rate of frozen particles. The enhancement on the precipitation resulting from increasing N_{CN} under low aerosol condition is a result of changes in the vertical distribution of frozen particles and its evaporation process." Please see 687-692. For other conclusions, we have also revised the language description to avoid the use of jargon.

In addition to interpreting the meaning of the results, we have also described the present limitations of this work and have emphasized that caveats are required in the interpretation of our results.

12. p. 7796, lines 5-12. Isn't conclusion 1 a conclusion of Reutter et al. (2009)? I'm not sure it needs to be repeated here.

Response: Conclusion 1 is the result of the deterministic regimes from our simulations, which consider full microphysics and the larger temporal and spatial scales of a single pyro-convective cloud. Here we intended to emphasize that even when we consider a larger scale for pyro-convective clouds, three-regime structure for the number concentration of cloud droplets still exists.

13. p. 7796, lines 26-27. Conclusion 4 reports a result, but does not explain why it happens. An explanation should be included.

Response: We run more simulations and conduct more analysis to explain Conclusion 4, and add the explanation in the Conclusion part. The text is "(4) Larger FF resulted in more precipitation, whereas the effect of aerosols on precipitation was complex and could be either positive or negative. The negative aerosol effect is due to the change in the fraction of small frozen particles and total melting rate of frozen particles. The positive effect of aerosols under low aerosol condition is a result of changes in the vertical distribution of frozen particles and its evaporation process." Please see lines 687-692.

Technical comments:

p. 7782, line 25. Do the authors mean "soil processes"?

Response: It is the "soil module" inside the ATHAM model, which is not included in our modeling configuration and thus we did not explain it in detail. We make it clear in the main text. Please see line 109.

p. 7785, line 12-13. It may be better to say, "summarizes all the microphysical processes and their acronyms"

Response: Accepted. This sentence is revised to be "Table A1 summarizes all the microphysical processes and their acronyms." Please see lines 190-191.

p. 7787-7790, please state what aerosol and FF (updraft speeds) values constitute the low and high aerosol cases and the low and high updraft cases.

Response: Actually we stated the range of low/high aerosol and *FF* conditions in the figure captions, and the text is "Note that the low/high aerosol and fire forcing conditions (LA, HA, LU, and HU) in these figures refer to a group of N_{CN}/FF conditions. LU: low updrafts (1,000–7,000 W m^{-2}); HU: high updrafts (75,000–300,000 W m^{-2}); LA: low aerosols (200–1,500 cm^{-3}); HA: high aero-

sols (10,000–100,000 cm^{-3})." To make clear of this, we will also add this statement in the main text. Please see lines 276-280.

Figures 2-15, please label individual panels. This can easily be done as part of the panel title.

Response: Accepted. We label each panel in the figures.

p. 7789, line 25. It seems like Rosenfeld's Science paper should be cited here.

Response: Accepted. Rosenfeld et al. (2008) described how the deep convective clouds evolve when more polluted aerosol particles are added in the atmosphere based on the conceptual model. We cite this paper in Line 353-354.

p. 7790, line 10. The Tao et al. Geophys. Res. (2012) review would be very good to cite here. Tao, W.-K., J.-P. Chen, Z. Li, C. Wang, and C. Zhang (2012), Impact of aerosols on convective clouds and precipitation, Rev. Geophys., 50, RG2001, doi:10.1029/2011RG000369.

Response: Accepted. Tao et al. (2012) summarized the aerosol effects on the CCN activation, warm-rain process, mixed-phase clouds, and precipitation in terms of microphysical scale, cloud-resolving scale, and regional scale, which are retrieved from the theoretical analysis, observations, and numerical modeling. The underlying mechanisms and the comparison between the results from different studies was also presented and analyzed. We add this citation in this part. Please see line 377.

p. 7793, line 21. To be consistent, write "rain drops" instead of droplets

Response: Accepted. Please see line 500.

p. 7793, line 22. Should be melted snow (singular)

Response: Accepted. We corrected this word. Please see line 499.

p. 7798, line 14. It may be good to cite Van den Heever and Cotton's work here. I think they were the first to show the aerosol-cloud-precipitation effects at longer time scales (> 12 hours).

Response: Accepted. We have included the Van Den Heever and Cotton (J Appl Meteorol Clim., 2007) for reference here. Please see Line 746.

Figure S2. Could this figure be shown on a skew-T plot and have the horizontal winds included? It may also be useful to show how big of a temperature increase occurs as the fire forcing increases.

Response: (1) The atmospheric radiosonde for the simulations is shown in Fig. R7 by a skewT-logp diagram, which has been included as the new Fig. 2 in the revised manuscript.

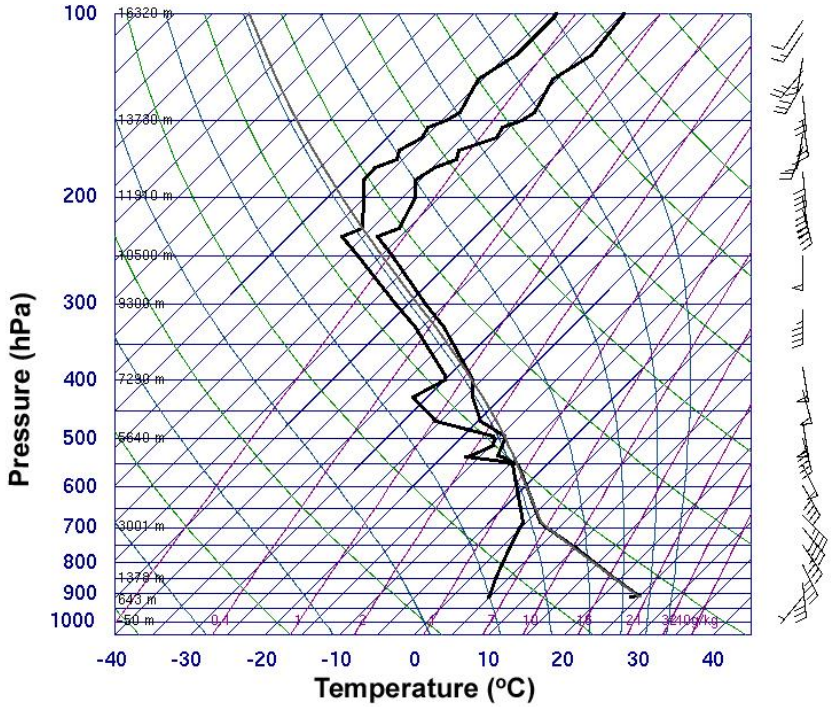

Figure R7. Atmospheric sounding launched near Edmonton, Alberta on 29 May 2001. The right black line represents the temperature, and the left black line corresponds the dew-point temperature. This weather information is from the University of Wyoming Department of Atmospheric Science (http://weather.uwyo.edu/).

(2) We plotted the relationship between fire forcing and the corresponding maximum temperature at cloud base under different aerosol conditions. As the aerosol impact on the temperature is very small, we take N_{CN}=5,000 cm^{-3} for example. The correlation of fire forcing and temperature is shown in Fig. R8. The shaded area indicates the variability of estimation over each simulation period. According to the figure, the temperature at cloud base varies monotonically from 7.6 to 16.4 ℃ as fire forcing increases from 1×10^3 to 3×10^5 W m^{-2}. We have included this discussion in Sect. 3.1. Please see Lines 221-230.

In the discussion section (Sect. 3.2.1), we have added the temperature as the secondary vertical axis in the contour plot for cloud mass concentration for reference (Fig. R9, which is Fig. 7b in the revised manuscript).

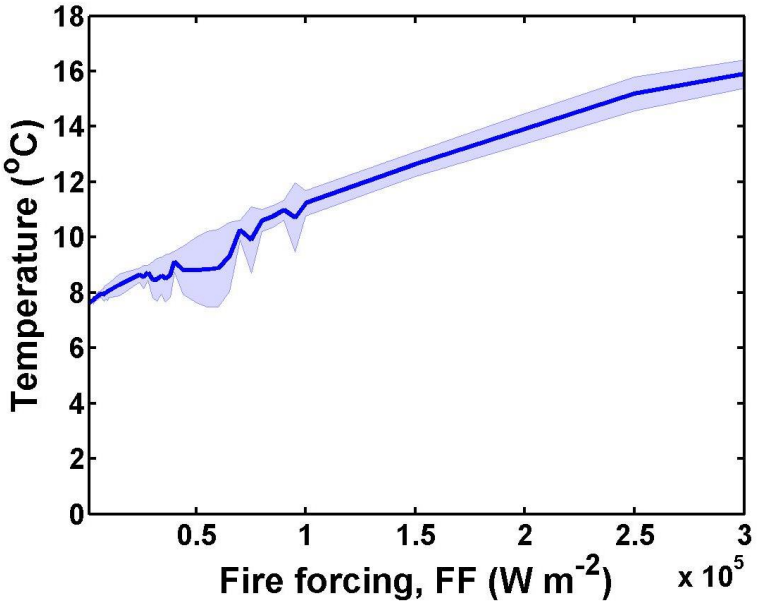

Figure R8. The correlation of fire forcing and the corresponding maximum temperature at cloud base. The shaded area indicates the variability of estimation (±½σ) over each simulation period.

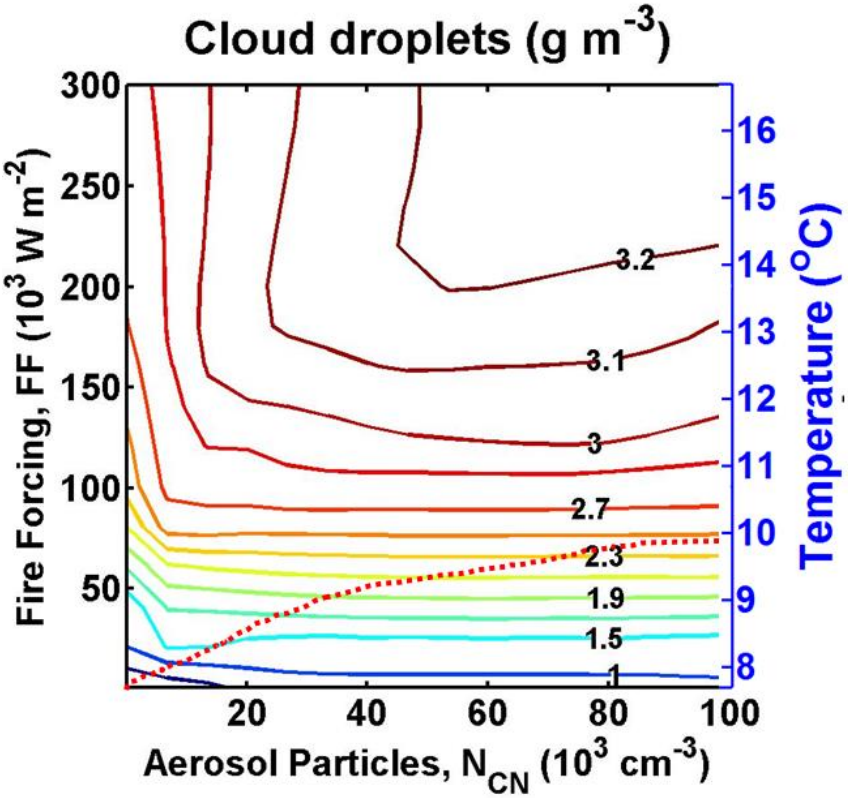

Figure R9. Mass concentration of cloud droplets calculated as a function of aerosol number concentration (N_{CN}) and updraft velocity (represented by *FF*).

References

Fan, J. W., Yuan, T. L., Comstock, J. M., Ghan, S., Khain, A., Leung, L. R., Li, Z. Q., Martins, V. J., and Ovchinnikov, M.: Dominant role by vertical wind shear in regulating aerosol effects on deep convective clouds, J Geophys Res-Atmos, 114, doi: 10.1029/2009jd012352, 2009.

Pruppacher, H. R., and Klett, J. D.: Microphysics of Clouds and Precipitation, Second Revised and Enlarged Edition with an Introduction to Cloud Chemistry and Cloud Electricity, Kluwer Academic Publishers, Reidel, Dordrecht, 954 pp., 1997.

Reutter, P., Su, H., Trentmann, J., Simmel, M., Rose, D., Gunthe, S. S., Wernli, H., Andreae, M. O., and Poschl, U.: Aerosol- and updraft-limited regimes of cloud droplet formation: influence of particle number, size and hygroscopicity on the activation of cloud condensation nuclei (CCN), ATMOSPHERIC CHEMISTRY AND PHYSICS, 9, 7067-7080, 10.5194/acp-9-7067-2009, 2009.

Rosenfeld, D., Lohmann, U., Raga, G. B., O'Dowd, C. D., Kulmala, M., Fuzzi, S., Reissell, A., and Andreae, M. O.: Flood or drought: How do aerosols affect precipitation?, Science, 321, 1309-1313, doi: 10.1126/science.1160606, 2008.

Tao, W. K., Chen, J. P., Li, Z. Q., Wang, C., and Zhang, C. D.: Impact of Aerosols on Convective Clouds and Precipitation, Rev Geophys, 50, doi: 10.1029/2011rg000369, 2012.

Wang, Y., Fan, J. W., Zhang, R. Y., Leung, L. R., and Franklin, C.: Improving bulk microphysics parameterizations in simulations of aerosol effects, J Geophys Res-Atmos, 118, 5361-5379, doi: 10.1002/Jgrd.50432, 2013.

Interactive comment on "Aerosol and dynamic effects on the formation and evolution of pyro-clouds" by D. Chang et al.
MS No.: acp-2014-61

Dear Reviewer,
We would like to thank you for the valuable and constructive comments/suggestions on our manuscript. We have revised the manuscript accordingly and please find our point-to-point responses below (line numbers refer to the new version of manuscript). In addition, the title of the manuscript is revised to be "Regime dependence of aerosol effects on the formation and evolution of pyro-convective clouds".

Response to Anonymous Referee #4

This study used a 2D atmospheric model with a 2-moment microphysical scheme to simulate pyro-clouds. The effects of aerosol and convection intensity on cloud, rain, ice-phase particles, as well as surface rainfall were studied using a test matrix of 31 aerosol concentrations by 42 convection intensities. The authors also carried out process analysis for 4 individual simulations to explore mechanisms of the simulated sensitivities. Results from these process analyses essentially agreed with various previous studies, although nothing new was found. The strength of this study, in my opinion, is the large number of sensitivity simulations which afford more robust sensitivity analyses. However, the authors did not take the full advantage of their simulations. For example, they reverted back to analyzing only 4 individual members in their PA analysis, instead of studying the mean and variations of all available members. Since there is a large room for improvement here, I would recommend publication with major revision. I hope the authors will take full advantage of their large simulation dataset and add more depth to their analyses.

Response: Thanks for the constructive suggestions. In the revised manuscript, we extend the process analysis from four individual cases to the full interested ranges of aerosols and fire forcing in a way as shown in Fig. R1 and Figs. 19, 21, 23 in the revised manuscript.

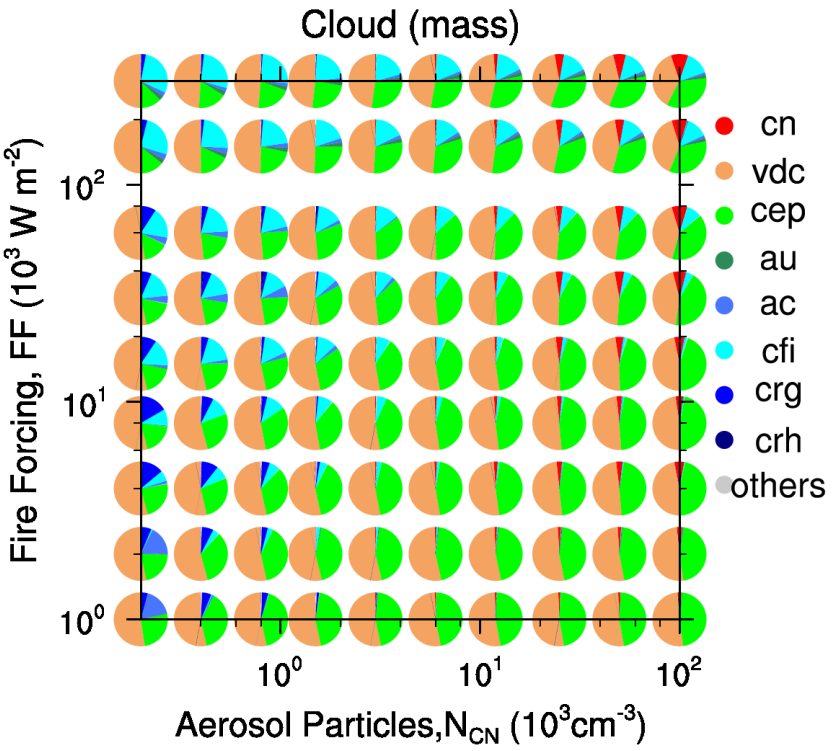

Figure R1. The pie charts summarize the relative percentage of the microphysical processes involving cloud droplets as a function of N_{CN} and fire forcing. Colors within each pie chart reflect the contribution of processes under the specific condition. Warm colors denote the source, while cold colors denote the sink. The acronyms indicate cn: cloud nucleation; vdc: condensational growth of cloud droplets; cep: evaporation of cloud droplets; au: autoconversion; ac: accretion; cfi: freezing of cloud droplets to form ice crystals, including homogeneous and heterogeneous nucleation; crg/h: riming of cloud droplets to form graupel/hail.

The pie charts summarize the relative percentage of the microphysical processes involving cloud droplets as a function of N_{CN} and fire forcing. Colors within each pie chart reflect the contribution of processes under the specific condition. Warm colors denote the source, while cold colors denote the sink. This provides a whole picture that how the contribution of each processes evolve as aerosol concentration or fire forcing increases.

Besides, we also plot the vertical cross sections of the change rate of these microphysical processes contributing to cloud water content in the modeling domain and the temporal evolution of the contributions (e.g., Fig. R2). The

figures for all the simulation period are in Figs. 20, 22 and 24 for cloud droplets, raindrops and frozen particles respectively. The corresponding analysis has been included in Sect. 3.3.

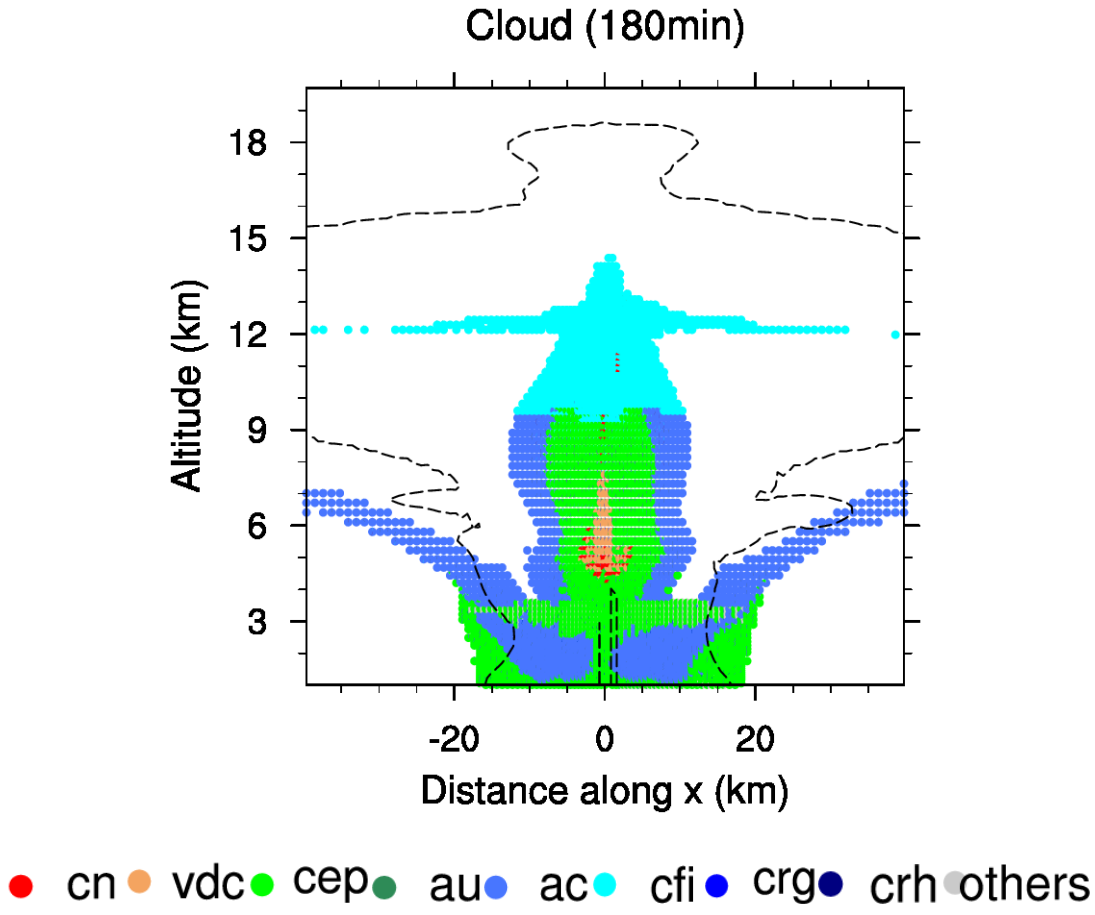

Figure R2. The pie charts summarize the vertical cross sections of the change rate of main microphysical processes contributing to cloud water content. Each pie chart shows the averaged contribution over the past 30 min. Colors within each pie chart reflect the percentage of processes in each grid. The black dashed line is the 0.1 μg kg^{-1} isoline of the interstitial aerosol, indicating the shape of smoke plume. The meaning of the acronyms is the same as in Fig. R1.

Major concerns:

1. Convection is a highly non-linear process. This puts a serious constraint on individual sensitivity studies. One of the ongoing debates is how representative such an individual case study is in elucidating aerosol-cloud interactions. With >1000 simulations and independent variations in two external forcings (aerosol and fire intensity), this study may

be able to shed some light on these debates. For example, if we were to conduct 2 sensitivity tests with high/low CN number (e.g., 2x or10x aerosol concentration), what is the probability that we will be able to get RS within one standard deviation from the mean? Will we be able to at least get the RS sign correctly? How robust is it to apply the mechanisms derived form an individual case with contrasting aerosol scenes to various environmental conditions, in this case, fire intensity? Statistical analysis along this direction will be very helpful in quantifying uncertainties of individual studies. It could also guide designs of future sensitivity tests.

Response: I appreciate the comment very much. As mentioned in the comment, aerosol-cloud interactions are regarded as nonlinear processes. In this case, the local aerosol effects on a cloud relevant parameter Y, i.e., dY/dN_{CN} can be different from $\Delta Y/\Delta N_{CN}$, the dependence derived from two case studies. In Sect. 3.4 of the revised manuscript, we try to answer how much difference can be expected between dY/dN_{CN} and $\Delta Y/\Delta N_{CN}$. In the following, we take the responses of the precipitation to aerosols for example to address this issue.

Figure R3 (Fig. 22 in revised manuscript) shows the statistics of the relative difference between $\Delta Y/\Delta N_{CN}$ and dY/dN_{CN} under LU and HU conditions, in which Y represents the precipitation rate. As precipitation is insensitive to aerosols for N_{CN} >10,000 cm^{-3}, only the cases with N_{CN} of 200~10,000 cm^{-3} are chosen in the calculation. The relative difference is defined as:

$$\text{Relative difference} = \frac{\frac{\Delta Y}{\Delta N_{CN}} - \frac{dY}{dN_{CN}}}{\frac{dY}{dN_{CN}}}$$

and $\frac{\Delta Y}{\Delta N_{CN}}$ is calculated as: $\frac{\Delta Y}{\Delta N_{CN}} = \frac{Y(2N_{CN}) - Y(N_{CN})}{2N_{CN} - N_{CN}}$, in which the aerosol effect is determined by the difference between the reference case and that after doubling N_{CN}. $\frac{dY}{dN_{CN}}$ is the derivative of the precipitation rate at each N_{CN}, representing the local dependence of precipitation on N_{CN}.

The histograms in Fig. R3 demonstrate that $\frac{\Delta Y}{\Delta N_{CN}}$ can deviate considerably from $\frac{dY}{dN_{CN}}$, not only for the absolute value but also for the sign. Statistically, most of the relative differences are in the range of -3.7~0.9 (the 25th and 75th percentiles respectively, with the average difference of -3.0) under LU condition, while are between -1.5 and 0.04 (the 25th and 75th percentiles respectively, with the mean value of 0.02) under HU condition. The fact that individual case studies may not reveal local aerosol effects demonstrates the importance of ensemble studies in determining the real responses of clouds to aerosol perturbations.

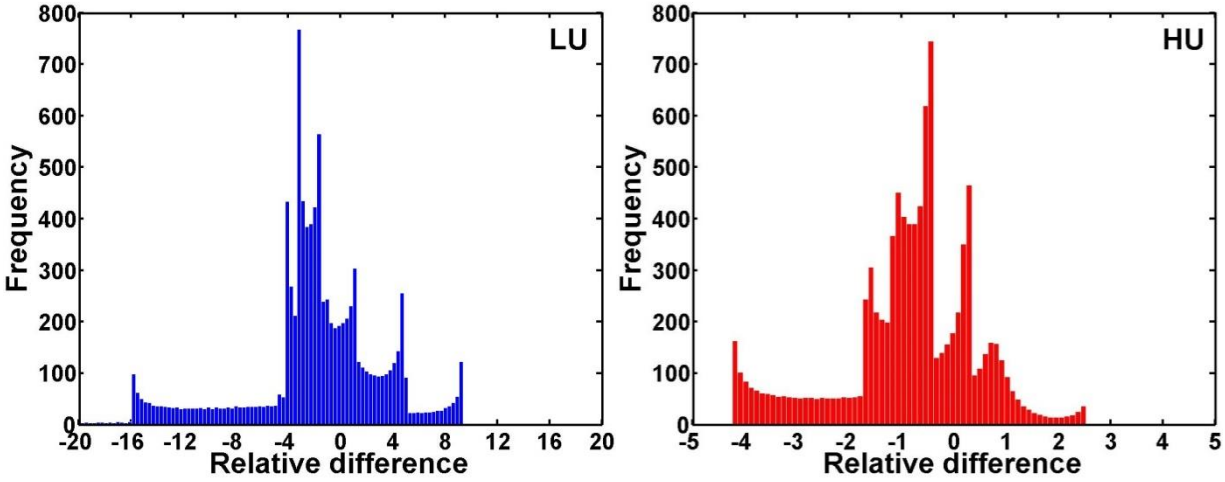

Figure R3. Histograms of the relative difference between $\frac{\Delta Y}{\Delta N_{CN}}$ and $\frac{dY}{dN_{CN}}$ under LU and HU conditions, where Y here denotes precipitation rate. $\frac{\Delta Y}{\Delta N_{CN}} = \frac{Y(2N_{CN}) - Y(N_{CN})}{2N_{CN} - N_{CN}}$, and $\frac{dY}{dN_{CN}}$ is the derivative of the precipitation rate along the variable N_{CN}.

For other hydrometeors, we also get such relative difference figures following this method, and found individual case studies are largely biased from the local derivatives. Different selection of the parameter space may result in different or even opposite conclusions. Therefore, our continuous sensitivity study over a wide range of parameter space shed some lights on these debates. Concerning the length of the manuscript, we just include the discussions for rain rate in the revised manuscript. Please see section 3.4.

2. There is an inconsistency in the RS analysis in the first part, which used 1302 cases, and the PA analysis in the second part, which used only 4 individual simulations. How do we know that mechanisms derived from PA analysis for an individual case are the same mechanisms that produced the mean sensitivities for hundreds of cases? If the authors can prove that the 4 individual cases are representative (see my comments in the previous paragraph), future aerosol-cloud simulations may be greatly simplified. If this cannot be proven, then PA analysis need to be done the same way as RS analysis, using all 1302 simulations.

Response: In the revised manuscript, we extend the process analysis from four individual cases to the full interested ranges of aerosols and fire forcing. The percentage of the microphysical processes under different aerosol and fire forcing conditions would be presented in the revised manuscript. Please see Fig. 19, 21, 23, and the text is in Sect. 3.3. Take cloud droplets for example, the figure is like this:

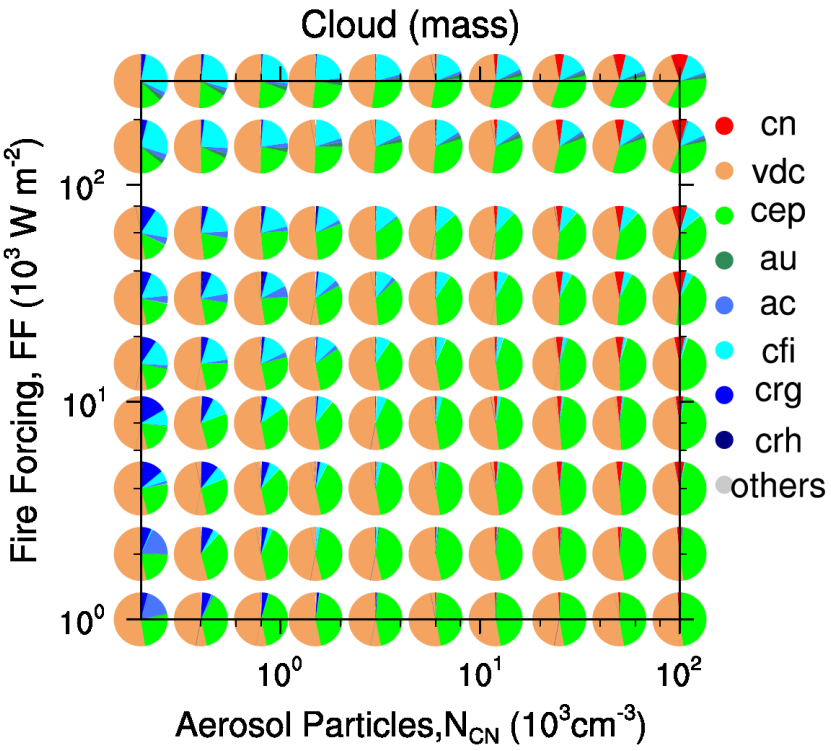

Figure R4. The pie charts summarize the relative percentage of the microphysical processes involving cloud droplets as a function of N_{CN} and fire forcing. Colors within each pie chart reflect the contribution of processes under the specific condition. The acronyms indicate cn: cloud nucleation; vdc: condensational growth of cloud droplets; cep: evaporation of cloud droplets; au: autoconversion; ac: accretion; cfi: freezing of cloud droplets to form ice crystals, including homogeneous and heterogeneous nucleation; crg/h: riming of cloud droplets to form graupel/hail.

Minor points:

1. The current simulation used pyro-cloud set up, e.g., there is a steady heat source at surface. This is fundamentally different from, e.g., a cumulus formed in the atmosphere. The authors should limit their discussions within pyro-clouds. Certain speculative comments, e.g., P7788, L2, P7798, L1, may not be applicable. I would suggest removing them from the discussion.

Response: Thanks for the comments. We have removed these sentences "This strongly suggests that when we evaluate the cloud responses to the changes in the am-

bient aerosol particles for global models or satellite data, we should focus more on the aerosol effect on cloud droplet number concentration, rather than on the liquid water path.", and revised the sentence "For this case study, then, we conclude that aerosol effects on cloud droplet number concentrations and thus cloud radiative properties (first indirect effect) are likely more important than effects on precipitation and thus cloud lifetime (second indirect effect), since precipitation is far less sensitive to aerosol number concentrations than to updraft velocity." to be "For this case study of pyro-convective clouds, then, we conclude that aerosol effects on cloud droplet number concentrations and cloud droplet size are likely more important than effects on precipitation, since precipitation is far less sensitive to N_{CN} than to updraft velocity." Please see Lines 730-733.

In addition, we have also investigated how the cloud and precipitation evolve if the fire forcing was shut down after half hour. The contours for each hydrometeor and precipitation are shown in Figs. R5, R6, R7, and R8 (not shown in the revised main text). For the domain-integrated concentration, the dependences of individual hydrometeor on aerosol concentration and fire forcing ended up showing good agreement with the simulations with persistent fire forcing. We included this information in the revised manuscript: "These results are derived from the simulations with persistent fire forcing over modeling period. We have also examined the case in which the fire forcing was shut down after the first half hour of simulation (not shown). The same regimes were found in these simulations, with boundaries in good agreement with the findings presented in this work." Please see Lines 296-300.

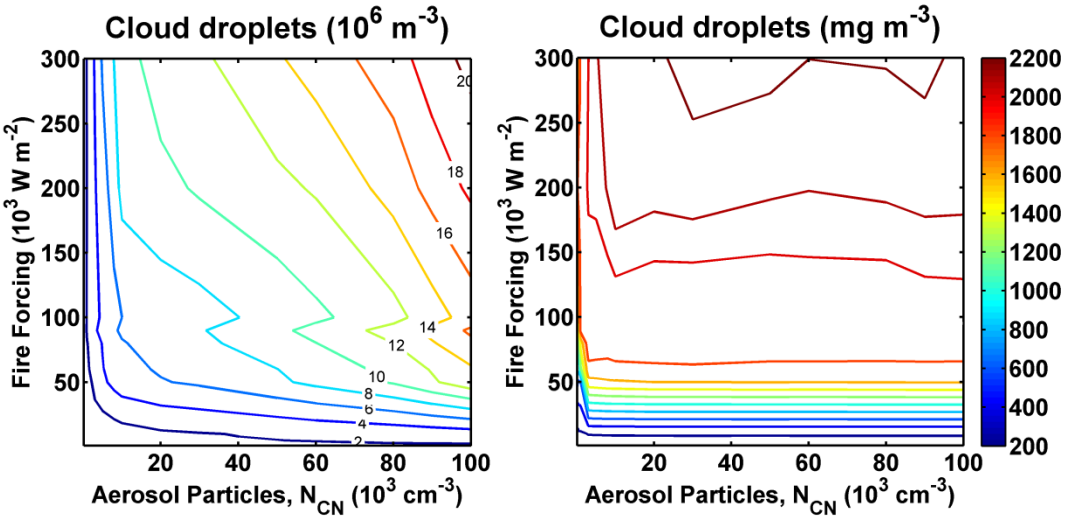

(a) (b)

Figure R5. Number (a) and mass concentration (b) of cloud droplets calculated as a function of aerosol number concentration (N_{CN}) and updraft velocity (represented by FF).

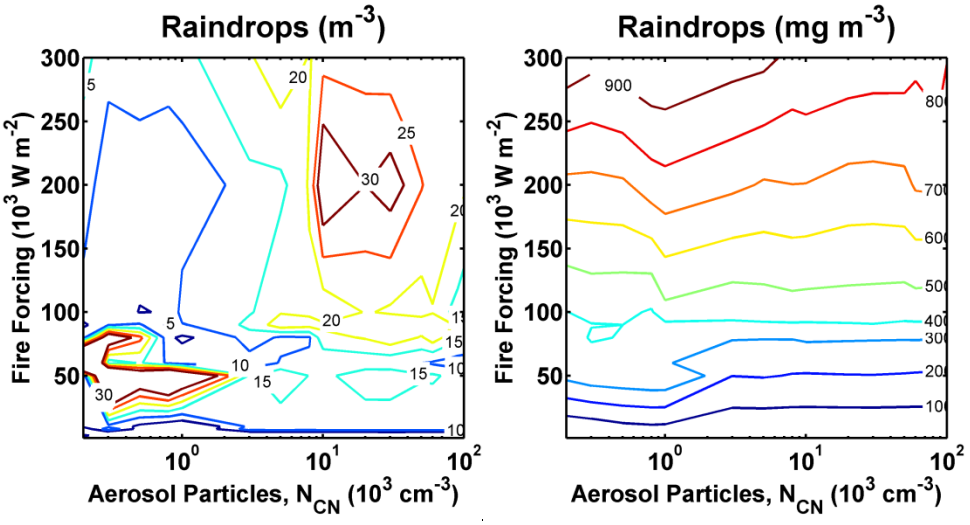

(a) (b)

Figure R6. Same as Fig. R5 but for raindrops.

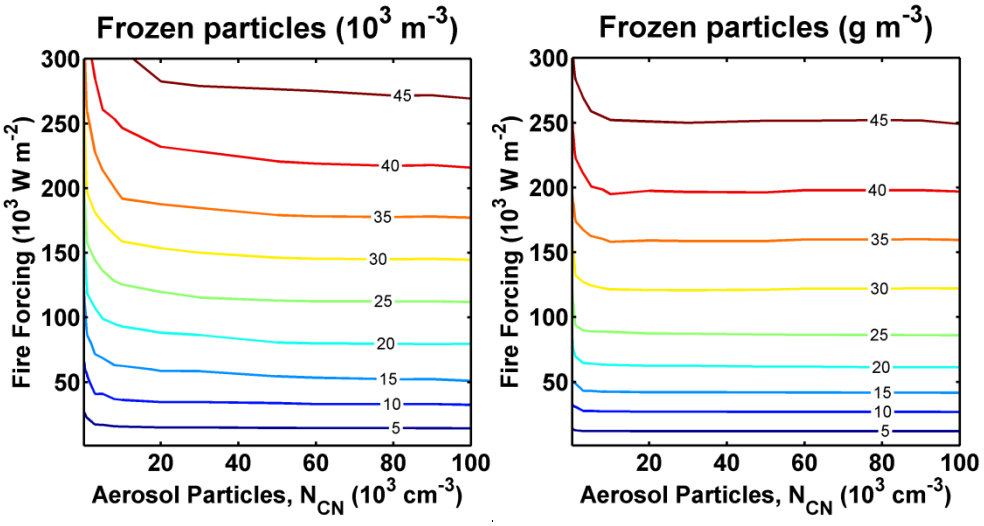

(a) (b)

Figure R7. Same as Fig. R5 but for frozen particles.

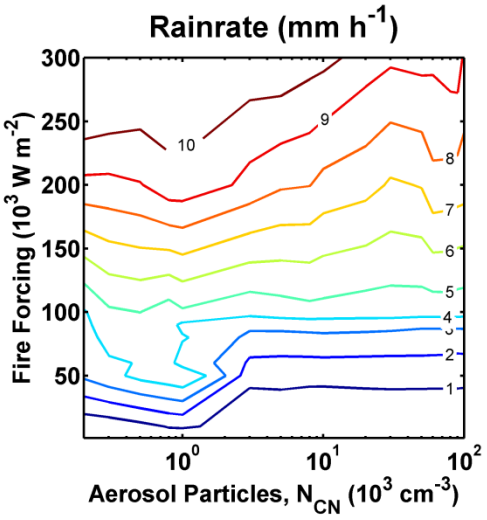

Figure R8. Same as Fig. R5 but for rain rate.

2. In the sensitivity tests, CN concentration ranges from 200 to 100000 per cubic centimeter, fire intensity ranges from 1000 to 100000 W/mˆ2. Can you describe what ranges of CN and fire intensity are realistic? Does higher fire intensity also produce higher CN? Obviously 200 cmˆ-3 is not realistic in any pyro clouds. This can guide the readers to pay

more attention to certain ranges of the parameter space. This information should be added explicitly in section 2.2.

Response: Yes, the condition with low aerosol and weak updrafts is not representative for a real pyro-convective cloud, and is used here for sensitivity studies. More CN will be emitted as fire forcing goes up. We have included the following sentence to avoid misleading the readers: "In reality, the composition and quantity of biomass burning emissions depend on the moisture content of fuels, combustion conditions, weather situation, and fire behavior (Bytnerowicz et al., 2009). What's more, the biomass burning plumes can in turn change the relative humidity as well. The aerosol particle number concentrations in biomass burning plumes usually exceed 10^4 cm^{-3}, and can be up to ~10^5 cm^{-3} (Andreae et al., 2004; Reid et al., 2005). In contrast to regular convection, the updraft velocities in pyro-convective clouds are normally larger than 20~30 m s^{-1} (Khain et al., 2005). On the basis of these facts, within our work more attention is paid to situations with higher aerosol concentration (>10^4 cm^{-3}) and strong updrafts (>20 m s^{-1}), which are more representative of pyro-convective clouds." Please see Lines 170-179.

3. RS values show large fluctuations for fire forcing between 2x10^4 to 1x10^5 (fig. 3,5,7,9). The authors could do more study on why this is the case. For example, do these fluctuations occur during the initial formation of the pyro clouds? Since the model used a steady heating at the surface, using results from the last hour may reduce these fluctuations.

Response: Thanks for the comments. We investigated the temporal evolution of the cloud hydrometeor, and found the fluctuations between 2×10^4 to 1×10^5 W m^{-2} are due to the occurrences of secondary cloud during the simulation period. Take the sensitivity of cloud water content to fire forcing for example, we picked up 4 points along the sensitivity line for HA case to check how the concentration varies. These four points are marked in Fig. R9 by green mark-

ers, which correspond to *FF*= 26,000, 32,000, 34,000 and 36,000 W m^{-2} respectively.

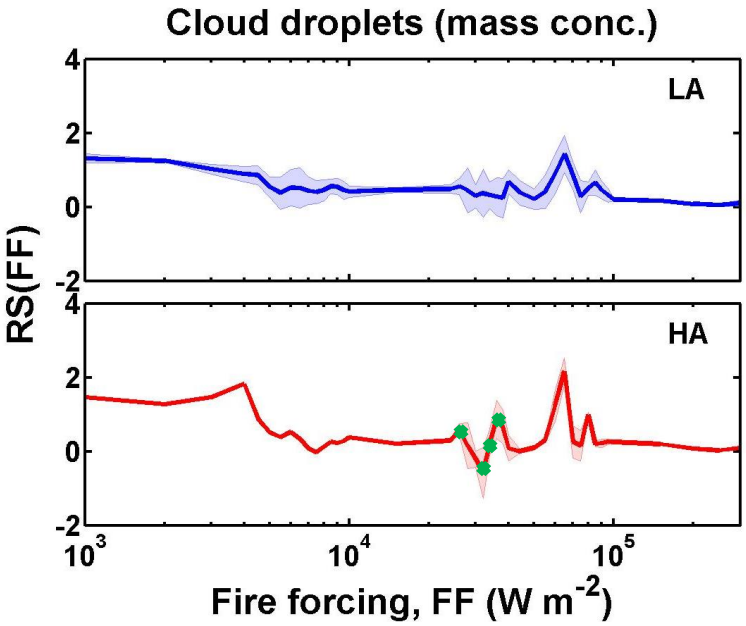

Figure R9. Relative sensitivities with respect to *FF* for mass concentration of cloud droplets under different conditions. The thick solid lines represent the mean values under a given condition, and the shaded areas represent the variability of estimation (±½σ). The acronyms indicate LA: low aerosols (200–1,500 cm^{-3}); HA: high aerosols (10,000–100,000 cm^{-3}).

The temporal evolutions of cloud droplets for these four points are in Fig. 10. It shows that the large fluctuation is caused by the cycling of cloud formation. The simulation covers the whole period of the first cycle but only part of the second cycle. Since we are not integrating the whole cloud period, more fluctuation is introduced.

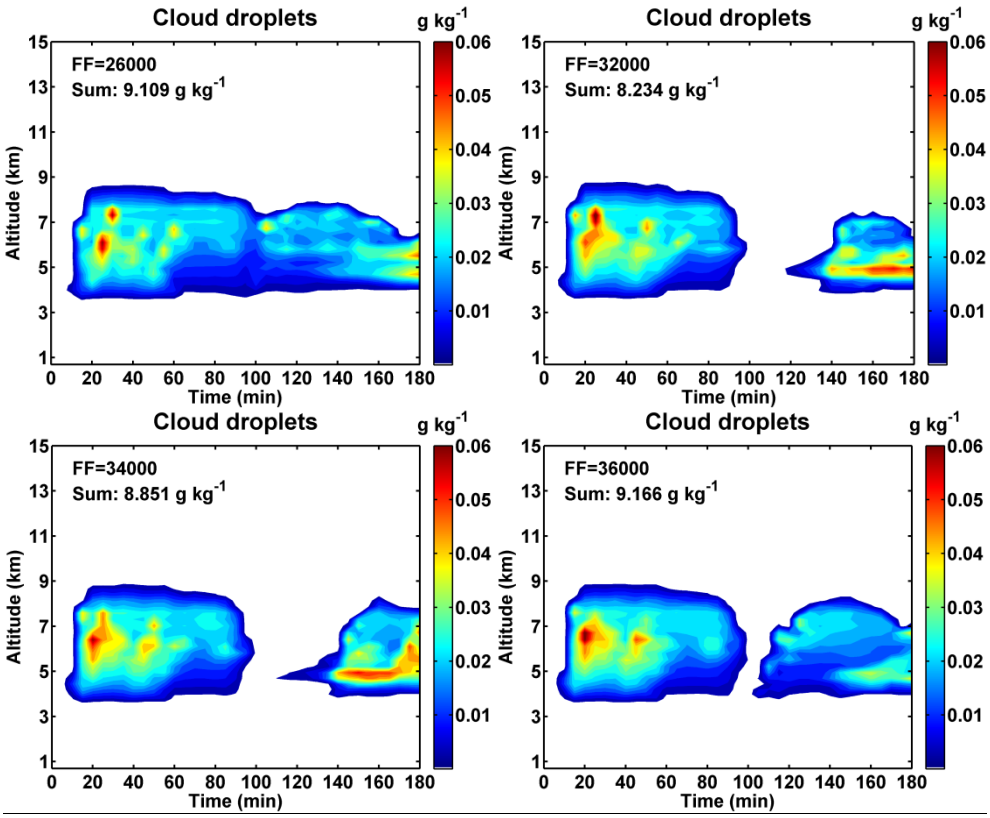

Figure R10. Time evolution of horizontally-averaged cloud water content (g kg^{-1}) as a function of altitude under different fire forcing (*FF*) conditions.

Since it appears that the first cloud usually end around 100 minutes, we plot the sensitivity of each hydrometeor to the fire forcing using the results over 0~100 min (Fig. R11). It is found, compared to the original figures, the sensitivities gets smoother for cloud droplets, raindrops, and frozen particles.

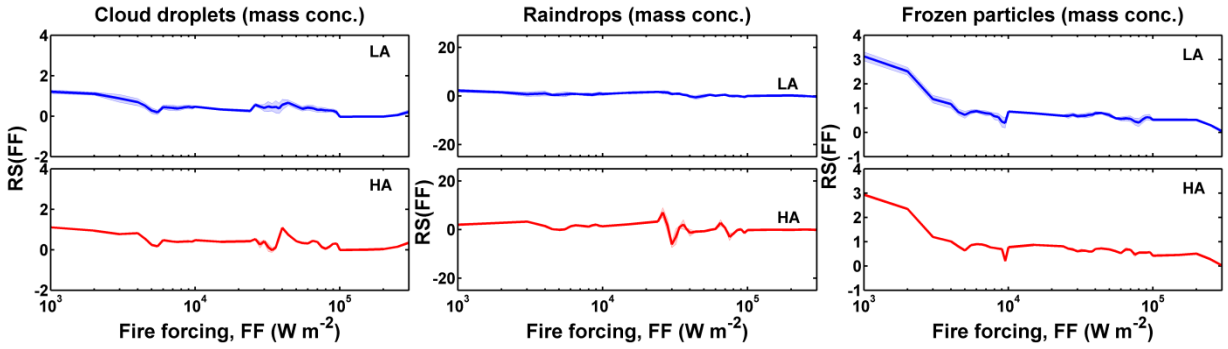

(a) (b) (c)

Figure R11. Relative sensitivities with respect to *FF* for mass concentration of cloud droplets (a), raindrops (b), and frozen particles (c) under different conditions. The thick solid lines represent the mean values under a given condition, and the shaded areas represent the variability of estimation (±½σ). The acronyms indicate LA: low aerosols (200–1,500 cm^{-3}); HA: high aerosols (10,000–100,000 cm^{-3}).

But for the precipitation rate, there remain large fluctuations (Fig. R12). This is probably because that the precipitation usually takes place at the very late period, and needs longer time. The first peak has not completed during 0~100 min.

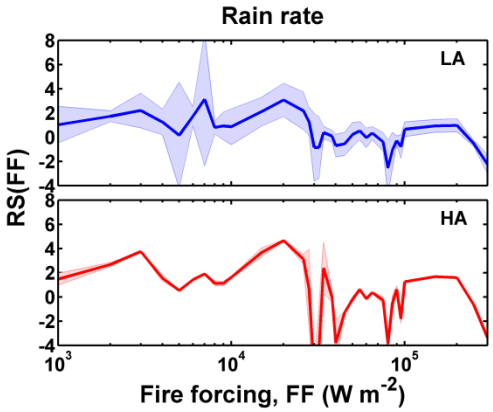

Figure R12. Relative sensitivities with respect to *FF* for rain rate under different conditions.

So far we haven't found a better way of sampling (we also tried the last hour) and thus stick to the original method.

4. P7783, L27, Is the fire forcing at a single point? What are the justifications for using a single point heating? Intuitively I thought forest fires spread to a large area, certainly larger than the 85 km domain size.

Response: The case of pyro-convection modeled in this study is based on the Chisholm forest fire (Luderer, 2007), which is well-documented. The fire front was approximately linear, and extended from south-south-east to north-north-west. The length of fire front is about 25 km, and the width of the fire front was about 500 m. The 2-D simulations within our work were performed at the cross section of the fire front, and thus only the width of the fire front was considered (x axis). Therefore out simulation domain (85 × 26 km in the x and z directions) can cover the fire area.

5. P7780, L12: "When we upscale the activation of a single aerosol…", "extend" should probably replace "upscale".

Response: Accepted.

6. Fig. 11, 13, 15: The scales of y-axis are all different. The authors should point that out explicitly, instead of just tucking them discretely at the corner of each plot. If the authors decided to calculate averages instead of 4 contrasting simulations, as I suggested in my major concern, the mean values might be closer to each other. And the y-axis might be more uniform for labeling.

Response: Thanks for the suggestions. In the revised manuscript, we extend the process analysis from four individual cases to the full interested ranges of aerosols and fire forcing. We plotted the percentage of the microphysical processes under different aerosol and fire forcing conditions in the revised manuscript. Please see Fig. 19, 21, 23, and the text is in Sect. 3.3. The figure was shown at the beginning of this response.

References

Andreae, M. O., Rosenfeld, D., Artaxo, P., Costa, A. A., Frank, G. P., Longo, K. M., and Silva-Dias, M. A. F.: Smoking Rain Clouds over the Amazon, Science, 303, 1337-1342, 2004.

Bytnerowicz, A., Arbaugh, M., Andersen, C., and Riebau, A.: Wildland Fires and Air Pollution, Dev Environm Sci, 8, 1-638, 2009.

Khain, A., Rosenfeld, D., and Pokrovsky, A.: Aerosol impact on the dynamics and microphysics of deep convective clouds, Q J Roy Meteor Soc, 131, 2639-2663, doi: 10.1256/Qj.04.62, 2005.

Luderer, G. G.: Modeling of Deep-Convective Vertical Transport of Foreset Fire Smoke into the Upper Troposphere and Lower Stratosphere, Ph.D, Physics Department, Johannes Gutenberg University Mainz, Mainz, 2007.

Reid, J. S., Koppmann, R., Eck, T. F., and Eleuterio, D. P.: A review of biomass burning emissions part II: intensive physical properties of biomass burning particles, Atmospheric Chemistry and Physics, 5, 799-825, 2005.

Regime dependence of Aerosol Effects on the Formation and Evolution of Pyro-convective clouds

Di Chang[1], Yafang Cheng[1], Philipp Reutter[2], Jörg Trentmann[3], Susannah Burrows[4], Peter Spichtinger[2], Stephan Nordmann[1], Meinrat O. Andreae[5], Ulrich Pöschl[1], and Hang Su[1,*]

[1]Multiphase Chemistry Department, Max Planck Institute for Chemistry, Mainz, Germany

[2]Institute for Atmospheric Physics (IPA), Johannes Gutenberg University Mainz, Mainz, Germany

[3]German Weather Service (DWD), Offenbach, Germany

[4]Pacific Northwest National Laboratory, Richland, WA, USA

[5]Biogeochemistry Department, Max Planck Institute for Chemistry, Mainz, Germany

[*]Correspondence to: h.su@mpic.de

Abstract

A recent parcel model study (Reutter et al., 2009) showed three deterministic regimes of initial cloud droplet formation, characterized by different ratios of aerosol concentrations (N_{CN}) to updraft velocities. This analysis, however, did not reveal how these regimes evolve during the subsequent cloud development. To address this issue, we employed the Active Tracer High Resolution Atmospheric Model (ATHAM) with full microphysics and extended the model simulation from the cloud base to the entire column of a single pyro-convective mixed-phase cloud. A series of 2-D simulations (over 1000) were performed over a wide range of N_{CN} and dynamic conditions. The integrated concentration of hydrometeors over the full spatial and temporal scales was used to evaluate the aerosol and dynamic effects. The results show that: (1) the three regimes for cloud condensation nuclei (CCN) activation in the parcel model (namely aerosol-limited, updraft-limited, and transitional regimes) still exist within our simulations, but net production of raindrops and frozen particles occurs mostly within the updraft-limited regime. (2) Generally, elevated aerosols enhance the formation of cloud droplets and frozen particles. The response of raindrops and precipitation to aerosols is more complex and can be either positive or negative as a function of aerosol concentrations. The most negative effect was found for values of N_{CN} of ~1000 to 3000 cm^{-3}. (3) The nonlinear properties of aerosol-cloud interactions challenge the conclusions drawn from limited case studies in terms of their representativeness, and ensemble studies over a wide range of aerosol concentrations and other influencing factors are strongly recommended for a more robust assessment of the aerosol effects.

Keywords: pyro-convective clouds, precipitation, ATHAM, updrafts, aerosol

1. Introduction

Clouds have a considerable impact on the radiation budget and water cycle of the Earth (IPCC, 2007). Aerosol effects on clouds and precipitation have been suggested to influence the formation, persistence, and ultimate dissipation of clouds and its climate effects (Stevens and Feingold, 2009; Tao et al., 2012), and hence have been studied intensively through cloud-resolving model simulations, analysis of satellite data, and long-term observational data (Tao et al., 2012).

However, aerosol effects are still associated with significant uncertainty in light of the seemingly contradictory results from different studies. For instance, several studies have indicated that increasing aerosol concentrations could reduce cloud fraction and inhibit cloud formation (Albrecht, 1989; Ackerman et al., 2000; Kaufman et al., 2002; Koren et al., 2004), whereas it is suggested that more aerosols can increase the cloud fraction in other studies (Norris, 2001; Kaufman and Koren, 2006; Grandey et al., 2013). Precipitation from stratiform clouds can be inhibited by elevated aerosol concentration (Zhang et al., 2006), while precipitation from convective clouds can be either suppressed or enhanced (Ackerman et al., 2003; Andreae et al., 2004; Altaratz et al., 2008; Lee et al., 2008; Teller and Levin, 2008; Fan et al., 2013; Camponogara et al., 2014). In addition, changing aerosol concentrations have also been found to exert non-monotonic influences (either positive or negative) on a wide range of cloud properties, such as homogeneous freezing (Kay and Wood, 2008), frozen water particles (Saleeby et al., 2009; Seifert et al., 2012), and convection strength (Fan et al., 2009).

One explanation for these seemingly contradictory results is that aerosol effects are regime-dependent, which means that it can vary under different meteorological conditions (updraft velocity, relative humidity, surface temperature, and wind shear), cloud types, aerosol properties (size distribution and chemical composition) and observational or analysis scales (Levin and Cotton, 2007; Tao et al., 2007; Khain et al., 2008; Rosenfeld et al., 2008; Fan et al., 2009; Khain, 2009; Reutter et al., 2009; McComiskey and Feingold, 2012; Tao et al., 2012). It is thus important to investigate the regime-dependence of aerosol-cloud interactions and to improve the representation of cloud re-

gimes in models (Stevens and Feingold, 2009). If we were able to distinguish under which conditions cloud formation is updraft-limited (aerosol-insensitive) as discussed in Reutter et al. (2009), it would have the advantage that in future work one could for many purposes neglect aerosol effects on clouds in areas that are usually updraft limited.

Another challenge in evaluating the aerosol effects lies in the nonlinear properties of aerosol-cloud interactions. Most previous research investigated the response of clouds and precipitation to the perturbation of aerosols based on two or several individual scenarios, by doubling or tripling the number concentration of aerosol particles. This will be fine for the linear dependence. Since aerosol-cloud interaction is a nonlinear process, such method may not reflect the real aerosol effect. An exemplary case is shown in Fig. 1, in which it is clear that the local derivatives (dY/dX) can be different from ΔY/ΔX determined by the difference between A and B cases.

Biomass burning generates significant amounts of smoke aerosols, and the fires loft soil particles that contain minerals (Pruppacher and Klett, 1997), both of which could serve as effective cloud condensation nuclei (CCN) and ice nuclei (IN) (Hobbs and Locatelli, 1969; Hobbs and Radke, 1969; Kaufman and Fraser, 1997; Sassen and Khvorostyanov, 2008), thereby affecting the formation of clouds and precipitation. As an extreme consequence of biomass burning, pyro-clouds feed directly from the smoke and heat released from fires (Andreae et al., 2004; Luderer, 2007) and provide a good example with which to study aerosol-cloud interactions (Reutter et al., 2009).

By taking the pyro-convective clouds as an example, here we demonstrate the ability of ensemble simulations to determine the regime dependence and resolve the nonlinear properties of aerosol-cloud interactions. Aerosol number concentration, updraft velocity (represented by the intensity of fire forcing, which triggers updraft velocities), and key parameters of CCN activation (Reutter et al., 2009) are varied to represent a wide range of aerosol and dynamic conditions. In addition to cloud droplets, the responses of precipitable hydrometeors (raindrops, ice, snow, graupel, and hail) were also investigated. For a better understanding of the mechanisms, we employed the process analysis (PA) method, which documents the rate of change in the mass or number concentration of each

hydrometeor type caused by a particular process, thereby enabling the determination of the relative importance of the major microphysical processes under different dynamic forcing and aerosol conditions.

2. Design of numerical experiments

2.1 ATHAM: model and configuration

The Active Tracer High Resolution Atmospheric Model (ATHAM), a non-hydrostatic model, is used here to study cloud formation and evolution in response to changes in updrafts and aerosol particle concentration. ATHAM was designed initially to investigate high-energy plumes in the atmosphere and applied to simulate volcanic eruptions and fire plumes (Herzog, 1998; Oberhuber et al., 1998). ATHAM has been used to simulate the evolution of pyro-cumulonimbus clouds (pyroCb) caused by a forest fire and shows results consistent with observations (Luderer, 2007).

The model comprises eight modules: dynamics, turbulence, cloud microphysics, ash aggregation, gas scavenging, radiation, chemistry, and soil modules (Herzog et al., 1998; Oberhuber et al., 1998; Graf et al., 1999; Herzog et al., 2003). Cloud microphysical interactions are represented by an extended version of the two-moment scheme developed by Seifert and Beheng (2006), which includes the hail modifications by Blahak (2008), and is able to predict the numbers and mass mixing ratios of six classes of hydrometeors (cloud water, ice crystals, raindrops, snow, graupel, and hail; detailed in Table 1) and water vapor. It has been validated successfully against a comprehensive spectral bin microphysics cloud model (Seifert et al., 2006). The cloud nucleation (CCN activation) module is based on a lookup table derived from parcel model simulations for pyro-convective clouds (Reutter et al., 2009). The ATHAM model can execute both 2-D and 3-D simulations. Results of this study are mainly based on 2-D simulations.

The meteorological conditions were set up to simulate the Chisholm forest fire (Luderer, 2007; Rosenfeld et al., 2007), which is a well-documented case of pyro-convection. All simulations were initialized horizontally homogeneously with radiosonde data from about 200 km south of the fire on 29 May 2001, which is the same as in Luder-

er (2007) (Fig. 2). The vertical profiles of the temperature and dew point temperature reveal a moderate instability in the atmosphere. Open lateral boundaries were used for the model simulations. The means of wind speed and specific humidity were nudged towards the initial profile at the lateral boundaries. The fire forcing was introduced in the middle grid in the bottom layer of the domain, and its intensity remained constant throughout the simulation of each scenario. Each case was run for 3 simulated hours until the clouds were fully developed and had reached steady state.

The 2-D simulations were performed at the cross section of the fire front. The simulation domain was set at 85 × 26 km with 110 × 100 grid boxes in the x and z directions. The horizontal grid box size at the center of the x direction was equal to 500 m, and it enlarged towards the lateral boundaries due to the stretched grid (Fig. 3). Such a process scale with resolution of ca. 1 km has been suggested as the appropriate scale at which to characterize processes related to aerosol-cloud interactions (McComiskey and Feingold, 2012). The vertical grid spacing at the surface and the tropopause was set to 50 and 150 m, respectively. The lowest vertical level in our simulation was placed 766 m above sea level, corresponding to the lowest elevation of the radiosonde data, which is close to the elevation of Chisholm at about 600 m (ASRD, 2001). The results of the 2-D simulations are presented and discussed in Sect. 3.

2.2 Aerosol particles and fire forcing

Atmospheric aerosol particles affect cloud formation through two pathways, by acting as CCN and as IN. Following the previous study of Reutter et al. (2009), we limited the scope of aerosol-cloud interactions to CCN activation only. So, in this study, changes in N_{CN} do not directly influence frozen hydrometeors by providing IN, but do so indirectly through their impact on CCN activation and subsequent processes.

In the 2-D ensemble simulations, 1302 cases (31 N_{CN} × 42 fire forcing values) were simulated to evaluate the interplay of aerosol concentration and updrafts on the formation of clouds and precipitation. The N_{CN} varied from 200 to 100,000 cm^{-3}. In each case, N_{CN} was prescribed (distributed uniformly across the modeling domain and kept identical throughout the simulation). A similar prescribed approach has been used in pre-

vious studies (Seifert et al., 2012; Reutter et al., 2014). Some previous research have pointed out that a prescribed aerosol scheme overestimates the magnitude of CCN concentrations compared to a prognostic aerosol scheme, because it lacks a representation of the efficient removal of particles by nucleation scavenging (Wang et al., 2013).

As mentioned above, we used the lookup table of Reutter et al. (2009) for the CCN activation. This table is determined for fresh biomass burning aerosols with a hygroscopicity parameter κ of 0.2 and a log-normal size distribution (a geometric mean diameter of 120 nm and a geometric standard deviation of 1.5, Reutter et al. 2009). For the present study, the aerosol characteristics, such as size distribution, chemical composition, hygroscopicity and mixing state are in fact rather unimportant, compared with the order-of-magnitude changes in the aerosol number concentration (Reutter et al., 2009; Karydis et al., 2012). Therefore, the effects of variations in aerosol characteristics were not considered in our study.

In all simulations, clouds were triggered by the fire forcing, which was assumed constant during the simulation. The fire forcing intensity varied from 1×10^3 to 3×10^5 W m^{-2}. The correlation between the initial fire forcing and corresponding updraft velocity and temperature at the cloud base was probed and is described in Sect. 3.1.

In reality, the composition and quantity of biomass burning emissions depend on the moisture content of fuels, combustion conditions, weather situation, and fire behavior (Bytnerowicz et al., 2009). What's more, the biomass burning plumes can in turn change the relative humidity as well. The aerosol particle number concentrations in biomass burning plumes usually exceed 10^4 cm^{-3}, and can be up to ~10^5 cm^{-3} (Andreae et al., 2004; Reid et al., 2005). In contrast to regular convection, the updraft velocities in pyro-convective clouds are normally larger than 20~30 m s^{-1} (Khain et al., 2005). On the basis of these facts, within our work more attention is paid to situations with higher aerosol concentration (>10^4 cm^{-3}) and strong updrafts (>20 m s^{-1}), which are more representative of pyro-convective clouds.

2.3 Process analysis

Cloud properties are subject to several tens of microphysical processes, e.g., cloud droplet nucleation, autoconversion, freezing, condensation, evaporation, etc. (Seifert and Beheng, 2006). Elevated concentrations of hydrometeors can be caused either by an increase in their sources or by a decrease in their sinks. To improve the understanding of the aerosol-cloud interactions, we employed the process analysis (PA) method to quantify the causation of changes in the concentrations of individual hydrometeor classes.

In addition to the standard model output (e.g., time and spatial series of mass and number concentrations of hydrometeors, and meteorological output), our PA method archives additional parameters, i.e., the time rate of change of hydrometeors due to individual microphysical processes under different aerosol and fire forcing conditions. Table A1 summarizes all the microphysical processes and their acronyms.

2.4 3-D simulations

In addition, we performed a number of 3-D simulations to investigate its difference to 2-D simulations. As the 3-D simulations are computationally expensive, only 99 cases (11 N_{CN} × 9 fire forcing values) were performed. N_{CN} varied from 200 to 100,000 cm^{-3}, while fire forcing changed from 1×10^3 to 8×10^4 W m^{-2}. The size of the model domain was set at 85 × 65 × 26 km with 110 × 85 × 100 grid boxes in the x, y and z directions. For consistency, the grid resolutions in the x and z directions were the same as for 2-D simulations. The minimum grid box size in the y direction was set to 100 m. The results of the 3-D simulations are presented and discussed in supplementary material.

3. Results and discussion

3.1 Relationship between updraft velocity, temperature, and fire forcing

Fire forcing does not affect the cloud activation of aerosols directly, but it can affect activation indirectly by triggering strong updraft velocities. Updrafts are of importance in the formation of clouds and precipitation for redistributing energy and moisture. In pyro-

convective clouds, the updraft velocities range from ca. 0.25 to 20 m s^{-1} (Reutter et al., 2009), which represent the range found in trade wind cumulus to thunderstorms (Pruppacher and Klett, 1997).

The probability distribution function of vertical velocities (w) at cloud base layer under different fire forcing conditions is shown in Fig. 4a. The velocity on top of the input fire forcing is usually the largest, and decreases towards the lateral sides. As the characteristic velocities, the maximum velocity at cloud base in Fig. 4a, are plotted against the input fire forcing (range of 1×10^3 to 3×10^5 W m^{-2}, $N_{CN} = 1 \times 10^3$ cm^{-3}) in Fig. 4b. The shaded area indicates the variability of estimation over each simulation period. According to the figure, w at cloud base varies monotonically from 1.8 to 27 m s^{-1} as fire forcing increases from 1×10^3 to 3×10^5 W m^{-2}. The positive relationship suggests that fire forcing could be a good indicator of vertical velocity. Because it is a variable of central interest to the cloud research community, the maximum vertical velocity is provided along with the fire forcing values as an additional axis in the following plots.

Another variable of key meteorological interest is the maximum temperature at cloud base. To clarify how temperature is affected by fire forcing in our simulations, the relationship between fire forcing and the corresponding maximum temperature at cloud base is shown in Fig. 5. As variations in aerosol number concentrations have very little effect on the temperature profile, we show this relationship for only one aerosol concentration (N_{CN}=5,000 cm^{-3}) as an example. Based on Fig. 5, the cloud base temperature increases linearly from 7.6 to 16.4 ℃, as fire forcing is enhanced from 1×10^3 to 3×10^5 W m^{-2}. In order to more clearly convey the effect of the heating imposed in the simulation, we have used this linear relationship to add the maximum cloud base temperature as a secondary axis in the figures.

Finally, we note that the horizontal wind shear can also affect the convection strength (Fan et al., 2009), which could be investigated in detail in future studies.

3.2 Aerosol effects and its regime dependence

In this section, the tempo-spatial distribution of each hydrometeor type will be briefly presented, followed by the modeled dependency of various hydrometeors on N_{CN} and fire forcing (*FF*). Note here only the characteristics of dependency are presented, while the underlying mechanisms will be discussed and interpreted in more detail in Sect. 3.3. For an individual hydrometeor type, the averaged concentrations (over the entire domain and simulation period) were used as metrics in our evaluation, and the condensed water reaching the surface was used as a metric for precipitation.

3.2.1 Cloud droplets

Figure 6 shows the temporal evolution of horizontally-averaged mass concentration of cloud droplets (M_{CD}) under the four pairs of *FF* and N_{CN} conditions. Under weak fire forcing conditions (LU), the formation of cloud droplets usually occurs from 20 min, and concentrates at an altitude of 4-7 km. The duration of cloud droplets usually last for a short period (40~60 min). Under strong fire forcing conditions (HU), the cloud droplets form earlier (around 5 min), and most cloud droplets are located at a height of 5-9 km. Besides, the cloud droplets reach steady state because of the cycling of cloud formation.

To investigate the sensitivity of an individual hydrometeor to changes in N_{CN} and *FF*, we adopted the definition of relative sensitivity $RS_Y(X)$ (of one variable Y against the variable X) as

$$RS_Y(X) = \frac{\partial Y / Y}{\partial X / X} = \frac{\partial \ln Y}{\partial \ln X} \quad (1)$$

In this study, X is the factor affecting cloud formation, i.e., N_{CN} and *FF*, and Y is the mass or number concentration of each hydrometeor type (cloud droplets, raindrops, as well as frozen particles). By using a natural logarithmic calculation of the variables (i.e., X, Y), the percentage change of an individual parameter relative to its magnitude could be reflected better. This logarithmic sensitivity evaluation has been applied commonly in the

assessment of aerosol-cloud interactions (Feingold, 2003; McFiggans et al., 2006; Kay and Wood, 2008; Reutter et al., 2009; Sorooshian et al., 2009; Karydis et al., 2012).

Figure 7a shows the dependence of cloud water droplets (N_{CD}) on N_{CN} and *FF*. The shape of the isolines is generally consistent with the regime designations reported by Reutter et al. (2009). Following Reutter et al. (2009), a value of the *RS*(N_{CN}) to *RS*(*FF*) ratio of 4 or 1/4 was taken as the threshold value to distinguish different regimes (the same criteria were employed for rainwater and frozen water content). Red dashed lines in Fig. 7a indicate the borders between different regimes. This resulted in an aerosol-limited regime in the upper left sector of the panel (N_{CD} is sensitive mainly to N_{CN} and is insensitive to fire forcing), an updraft-limited regime in the lower right sector of the panel (N_{CD} displays a linear dependence on *FF* and a very weak dependence on N_{CN}), and the transitional regime along the ridge of the isopleth (*FF* and N_{CN} play comparable roles in the change of N_{CD}). The regimes of Reutter et al. (2009) are derived from simulations of the cloud parcel model of CCN activation at the cloud base. Our results demonstrate that the general regimes for CCN activation still prevail, even when considering full microphysics and the larger temporal and spatial scales of a single pyro-convective cloud system. Figures 7c and 7d display the sensitivity of N_{CD} to variations in N_{CN} and *FF*. Note that the low/high aerosol and fire forcing conditions (LA, HA, LU, and HU) in these figures refer to a group of N_{CN}/*FF* conditions. LU: low updrafts (1,000–7,000 W m^{-2}); HU: high updrafts (75,000–300,000 W m^{-2}); LA: low aerosols (200–1,500 cm^{-3}); HA: high aerosols (10,000–100,000 cm^{-3}). High sensitivities were found for low conditions of N_{CN} and *FF*. While there are some deviations (which appear to be random numerical noise), in general, as either N_{CN} or *FF* increases, the impact on the cloud droplet number concentration of further changes to either the variable becomes weaker (Figs. 7c and 7d). The reduced sensitivity of cloud droplets to aerosols can be explained by the buffering effect of the cloud microphysics, so that the response of the cloud system to aerosols is much smaller than would have been expected.

Compared with N_{CD}, the cloud mass concentration (M_{CD}) is less sensitive to N_{CN}, and an aerosol-limited regime cannot be said to exist for M_{CD} (Fig. 7b and 7e). As a result, there are only two regimes indicated by the red dashed line in the contour plot (Fig. 7b):

290 an updraft-limited regime in the lower right sector of the panel, and a transitional regime
291 in the upper sector (an aerosol- and updraft-sensitive regime). The $RS(N_{CN})$ of N_{CD} is on
292 average 10 times higher than that of M_{CD}, independent of the intensity of the *FF*. As N_{CN}
293 increases, M_{CD} becomes insensitive to the change of N_{CN}. Averaged $RS(FF)$ values over
294 simulated *FF* ranges for N_{CD} (0.60) and M_{CD} (0.50) are commensurate (Fig. 7d and 7f, re-
295 spectively), which implies that both the number and mass concentrations of cloud drop-
296 lets are very sensitive to updrafts. These results are derived from simulations with persis-
297 tent fire forcing over the modeling period. We have also examined the case in which the
298 fire forcing was shut down after the first half hour of simulation (not shown). The same
299 regimes were found in these simulations, with boundaries in good agreement with the
300 findings presented in this work.

301

302 **3.2.2 Raindrops**

303 Figure 8 exhibits the temporal evolution of the horizontally-integrated mass concentration
304 of raindrops under four different conditions. Compared with cloud droplets (Fig. 6), the
305 occurrence of raindrops is much later, especially when N_{CN} and fire forcing are in a high
306 level. Only for LULA case, numerous raindrops can be found in a high altitude (5-7 km),
307 while for other cases, most of raindrops are located below 5 km (~0 ℃).

308 The response of the raindrop number concentration (N_{RD}) to fire forcing and N_{CN}
309 is more complex (Fig. 9a). The impact of *FF* on N_{RD} is non-monotonic. In general, en-
310 hanced *FF* leads to an increase in N_{RD} under weak updraft condition (<~4,000 W m^{-2}),
311 while further increases in *FF* result in the reduction in N_{RD}. The aerosol influence varies
312 in the course of N_{CN} change. Under low aerosol condition (<~1,500 cm^{-3}), increased N_{CN}
313 can enhance the production of N_{RD}. Under high aerosol condition (>~2,000 cm^{-3}), the in-
314 fluence of N_{CN} on N_{RD} is very small.

315 As *FF* increases in magnitude, the amount of rain produced (M_{RD}) increases (Fig.
316 9b), but the size of raindrops varies because of the complex behavior of the response of
317 the rain drop number (N_{RD}) to *FF* (Fig. 9a). The aerosol effect is non-monotonic: M_{RD} in-

creases with aerosols in the lower range of N_{CN} values (<~1000 cm^{-3}), but further increases in N_{CN} result in a decrease in M_{RD}. Combining with the relative sensitivities (Figs. 9e, and 9f), the influence of *FF* is much more significant than that of N_{CN} in most cases. For example, the upper left corner (an aerosol-limited regime for N_{CD}) becomes a transitional regime for M_{RD} with *RS* (*FF*) of 0.1 and *RS* (N_{CN}) of -0.06 (Fig. 9). High sensitivities of M_{RD} to N_{CN} are found at low N_{CN} conditions, but the sensitivity decreases as N_{CN} increases (Fig. 9e). The N_{CN} plays the most negative role in M_{RD} under intermediate N_{CN} conditions (N_{CN} of several 1000 cm^{-3}). In contrast to cloud droplet number concentration, an aerosol-limited regime for M_{RD} hardly exists in our simulations (Fig. 9b). The response of the raindrops to aerosols is much weaker than the response of cloud droplets to aerosols. This finding is consistent with the idea of clouds acting as a buffered system formulated by Stevens and Feingold (2009). Detailed analysis of the microphysical buffering processes will be presented in Sect. 3.3.2.

3.2.3 Frozen water contents

Within our microphysical scheme, frozen water contents are grouped into four main classes: ice crystals, snow, graupel, and hail (Seifert and Beheng, 2006). The time evolution of frozen water content in Fig. 10 suggests that the formation of frozen water content usually occurs in a high level (5-9 km for LU case, and 7-13 km for HU case), and the height of base layer and top layer decreases as time goes by. Under LU condition, the appearance of frozen water content is around 35 min, and lasts for ~120 min, with the peak concentration around 50~70 min. Under HU condition, the frozen particles form around 10 min, and keep in a steady state.

Aerosols exert influence on the frozen water contents via the process of ice nucleation (*in*), but the processes that convert between the different hydrometeor classes and water vapor play a greater role in changing the concentrations of frozen particles, especially the processes of drop freezing to form ice (*cfi*) and the vapor condensational growth of ice and snow (*vdi* and *vds* respectively). Figure 11 illustrates the percentage mass contributions of the individual frozen hydrometeor classes to the total frozen mass.

The percentages of each hydrometeor are calculated based on average values over the entire simulation period. Generally, greater concentrations of aerosols result in more snow and less graupel. This is in agreement with previous studies on convective clouds (Seifert et al., 2012; Lee and Feingold, 2013), and can be explained by the suppression of the warm rain processes under high aerosol condition. High N_{CN} delays the conversion of the cloud water to form raindrops, so that more cloud water content can ascend to altitudes with sub-zero temperatures, hence freeze into small frozen particles (Rosenfeld et al., 2008). Other research has suggested that elevated aerosols could increase the concentration of large frozen particles (graupel/hail) in the convective system (Khain et al., 2009; Wang et al., 2011), which was attributed to the competing effects of aerosols on graupel formation. Since graupel is mainly formed by the accretion of supercooled droplets by ice or snow, the smaller but more abundant supercooled drops under polluted conditions could be either favorable or unfavorable for graupel formation. The percentage of ice crystals does not change much, with ice crystals contributing approximately 20% on average to total frozen particle mass (Fig. 11). It is worth noting that stronger *FF* leads to increasing absolute concentration of hail. But compared to other hydrometeors, its contribution is not important and the relative percentage is very low.

The dependence of total frozen particles on *FF* and N_{CN} is summarized in Fig. 12. With the enhancement in *FF* and N_{CN}, both the number and mass concentrations of the frozen water particles (N_{FP} and M_{FP}, respectively) increase. High $RS(N_{CN})$ and $RS(FF)$ values were found under low N_{CN} and *FF* conditions (Fig. 12), respectively. As N_{CN} or *FF* increases, their impact becomes weaker, as indicated by a decreasing *RS*. According to the ratio of $RS(FF)/RS(N_{CN})$, both N_{FP} and M_{FP} are within the updraft-limited regime. Again, smaller $RS(N_{CN})$ values for M_{FP}, compared with N_{CD}, illustrate the weaker impact of N_{CN} on the production of frozen particles.

3.2.4 Precipitation rate

Surface precipitation rate is a key factor in climate and hydrological processes. Many field measurements, remote sensing studies, and modeling simulations have attempted to

evaluate the magnitude of aerosol-induced effects on the surface rainfall rate (Rosenfeld, 1999, 2000; Tao et al., 2007; Li et al., 2008; Sorooshian et al., 2009; Tao et al., 2012). Fig. 13a shows the response of surface precipitation rate (averaged over each 3 h simulation) to *FF* and N_{CN}. The response of surface precipitation to these forcings is similar to that of raindrops (Fig. 9b). The *FF* play a positive role in the precipitation, and *RS*(*FF*) shows a decreasing trend as *FF* increases (Fig. 13c).

The effect of N_{CN} is more complex. Both positive and negative *RS* (N_{CN}) were found in our study. There are generally two different regimes: a precipitation-invigorated regime and a precipitation-inhibited regime. In the precipitation-invigorated regime (N_{CN} < ~1000 cm^{-3}), an increase in N_{CN} leads to an increase in the precipitation rate, and a reduction in *RS* (N_{CN}) (Fig. 13b). In the precipitation-inhibited regime (N_{CN} > ~1000 cm^{-3}), aerosols start to reduce the precipitation, which is reflected in a negative *RS*(N_{CN}). Within the precipitation-inhibited regime, there is also an extreme *RS*(N_{CN}) at a value of N_{CN} of a few thousand particles per cm^3 (Fig. 13b). The threshold to distinguish these two regimes is derived from the current simulated pyro-convective clouds. The cumulus cloud investigation in Li et al. (2008) also suggested this non-monotonic trend, with the threshold aerosol value around 3000 cm^{-3}. The existence of threshold N_{CN} in both studies implies that similar cloud types may have a similar regime dependence, of which the exact shape may differ due to difference in the meteorological conditions, aerosol properties, etc.

Based on the ensemble studies, we found that individual case studies result in large uncertainties in evaluating the response of precipitation to perturbations, e.g., N_{CN}. Different selections of the parameter space may result in different or even opposite conclusions. Therefore, our ensemble study over a wide range of parameter space sheds some lights on these debates.

Within our simulations, melting of frozen particles is the biggest contributor to precipitation, and the rain rate is well correlated with the melting rate (Fig. 14). For N_{CN} > 1,000 cm^{-3}, increasing N_{CN} results in more small frozen particles (i.e., snow) with low fall velocities. These small frozen particles cannot fall into the warm areas and melt efficiently, resulting in a reduced melting rate. For N_{CN}< 1,000 cm^{-3}, the ratio between large and

small frozen particles is not sensitive to N_{CN} anymore and the vertical distribution of frozen particles becomes important. Increasing N_{CN} leads to earlier formation of frozen particles at low altitude, which evaporate less and result in more rainfall.

In the literature, both positive (Tao et al., 2007) and negative (Altaratz et al., 2008) relationship between aerosols and rain rate have been reported in previous case studies. Our simulations suggest that this apparently contradictory phenomenon might be the expression of the same physical processes under different aerosol and dynamic conditions.

Regarding the temporal evolution, low N_{CN} results in earlier rainfall (Fig. 15), which is consistent with current understanding, observations (e.g., Rosenfeld, 1999, 2000), and modeling evidence (e.g., the convective cumulus cloud study by Li et al. (2008)). Note that the general relationship between precipitation and aerosols described in this study is based on simulations over a period of 3 hours. Simulations for a longer period should be carried out in future studies to investigate the influence of aerosols on precipitation over longer time scales as in Fan et al. (2013) and Wang et al. (2014).

3.3 Process Analysis

In our simulations, the evolution of hydrometeor concentrations is determined by multiple microphysical processes. It is often difficult to tell exactly how aerosol particles affect clouds and precipitation. Here we introduce a process analysis method to help understand the aerosol effects.

3.3.1 Clouds

Figure 16 summarizes the contribution of the microphysical processes that act as the main sources (warm color) and sinks (cold color) for cloud droplets under different aerosol and fire forcing conditions. For N_{CD}, the dominant source term is the cloud nucleation (CCN activation) process, in which aerosols are activated under supersaturated water vapor and form cloud droplets. As cloud nucleation happens mostly at the cloud base and so is not strongly affected by cloud dynamical feedbacks, the response of N_{CD} shows similar

regimes to cloud parcel models (Reutter et al., 2009). To help explain the regime designation, we divide N_{CD} into two factors: an ambient aerosol number concentration (N_{CN}) and an activated fraction (N_{CD}/N_{CN}). Given the aerosol size distributions, the N_{CD}/N_{CN} ratio is determined approximately by the critical activation diameter (D_c) above which the aerosols can be activated into cloud droplets. The D_c is a function of ambient supersaturation. Stronger updrafts result in higher supersaturation, smaller D_c and hence, larger N_{CD}/N_{CN} ratios. Under high updraft conditions (>15 m s^{-1}), N_{CD}/N_{CN} is already close to unity (Reutter et al., 2009). A further increase in the updraft velocity will still change the supersaturation and D_c, but it will not significantly influence the N_{CD}/N_{CN} ratios and N_{CD}. In this case, N_{CD} is approximately proportional to N_{CN}.

Under weak updrafts, the N_{CD}/N_{CN} ratio is sensitive to ambient supersaturations. In this case, a larger supersaturation induced by stronger updrafts can effectively change the N_{CD}/N_{CN} ratio and thus N_{CD} is sensitive to the updraft velocity. On the other hand, the stronger dependence of N_{CD}/N_{CN} on the supersaturation also changes the role of aerosols. As more aerosols reduce supersaturation, increasing N_{CN} tends to reduce the activated fraction, N_{CD}/N_{CN}. Taking N_{CN} = 60,000 cm^{-3} (FF = 2,000 W m^{-2}), for example, a 10% increase in N_{CN} causes a 4% decrease in N_{CD}/N_{CN}, whereas a 10% decrease in N_{CN} leads to an 8% increase in N_{CD}/N_{CN}. The impact of changing N_{CN} on the N_{CD}/N_{CN} ratio counteracts partly or mostly the positive effect of N_{CN} on cloud droplet formation.

The changes of M_{CD} are influenced mainly by the following sources: (1) the condensation of water vapor on the present cloud droplets (*vdc*) and (2) the cloud nucleation process (*cn*), and by the following sinks: (3) cloud droplet evaporation (*cep*) and (4) the accretion of cloud droplets (*ac*), and (5) the freezing of cloud droplets to form cloud ice (*cfi*), which includes heterogeneous (Seifert and Beheng, 2006) and homogeneous freezing processes (Jeffery and Austin, 1997; Cotton and Field, 2002). Concerning their relative contributions, the net change of condensational growth of droplets (*vdc*) and cloud droplet evaporation (*cep*) dominates the change of M_{CD}. As N_{CN} increases, the condensation rate (*vdc*) does not change much, while the evaporation rate (*cep*) is raised greatly owing to increased surface-to-volume ratio of smaller cloud droplets. Condensation increases M_{CD} and evaporation reduces M_{CD}. In our study, the net effects are negative. A

similar result has been reported by Khain et al. (2005) for deep convective clouds. They found that high CCN concentrations led to both greater heating and cooling, and that the net convective heating became smaller as CCN increased. However, the cloud nucleation rate is enhanced and the loss of cloud water due to other sinks (*ac* for weak *FF* condition, and *cfi* for strong *FF* condition) decreases at the same time. This leads to an increasing trend in the total cloud water content with the increase in N_{CN}.

Concerning the absolute contribution, increasing *FF* enhances the change rate of the conversion of water vapor to the condensed phase (R_{vdc} and R_{cn}), whose effect is straightforward. The processes of autoconversion (*au*) and accretion (*ac*) are the major sinks at weak updrafts. As *FF* increases, the conversion of cloud droplets to frozen particles, especially to ice (the *cfi* process), becomes increasingly important.

The contribution of the microphysical processes in each modeling grid could be observed from the pie charts in Fig. 17 (take HUHA (w = 27 m s^{-1}; N_{CN}=100,000 cm^{-3}) for example, which is representative of the pyro-convective clouds). Each plot shows the vertical cross sections of the averaged change rate of main processes contributing to cloud water content over 30 simulation minutes. Colors within each pie chart reflect the percentage of processes in each grid. CCN activation usually starts at cloud base, followed by *vdc* in the center of the cloud. Towards both sides, cloud droplets convert to water vapor via evaporation. It is worth noting that the pie charts only represent the relative importance of each process at individual simulation grid, not the absolute amount. Though there are fewer *vdc*-dominated grids than *cep*-dominated grids, the total cloud formation rate from *vdc* is still similar to or higher than the *cep* processes. At cloud top with sub-freezing temperature, cloud droplets are frozen to ice crystals via homogeneous and heterogeneous nucleation. At the beginning stage of the cloud (30 min), the cloud droplets concentrate at the center of the modeling domain. As the evolution of the cloud, it starts to expand, and at the same time the margin area dissipates due to the sink processes (i.e., *cep*, *cfi*, and *ac*).

We are aware that the exact process rates may vary depending on the microphysical schemes used in the simulation (Muhlbauer et al., 2010). Therefore, we stress that the

process analysis here is based on the Seifert microphysical scheme (Seifert and Beheng, 2006). In the future, further observations from laboratory and field measurements are needed to improve the understanding of aerosol-cloud interactions and to better constrain microphysical parametrizations.

3.3.2 Rain

Dynamic conditions strongly influence the pathways of rain formation and dissipation. For weak updraft cases, the warm rain processes, i.e., autoconversion (*au*) and accretion (*ac*) play a big role. Together with melting of snow (*smr*) or graupel (*gmr*), they are the main sources for raindrops (Fig. 18). Under this condition, raindrops may appear at altitudes as high as 5–7 km (e.g., Fig. 8a). For high updraft cases, strong updrafts deliver cloud droplets to higher freezing altitudes (Fig. 6). The cloud droplets then turn directly into frozen particles (cloud→ice crystals), without formation of raindrops as an intermediate stage (cloud→rain→larger frozen particles). Most raindrops are formed from melted frozen droplets and consequently, they appear below ~4 km (Figs. 8c, d). The weaker cloud→rain conversion with higher updrafts also influences the conversion of rain to frozen particles, and is the reason why the *rrg* process (riming of raindrops to form graupel) becomes relatively less important as *FF* increases under low aerosol condition.

The aerosols also modify the pathways of rain formation. Taking weak updraft cases for example, the accretion process (*ac*) dominates the cloud→rain conversion under low aerosol concentrations, but is replaced by autoconversion (*au*) under high aerosol concentrations (Fig. 18b). The reason for this is that *au* is the process that initializes rain formation. Once rain embryos are produced, accretion of cloud droplets by raindrops is triggered and becomes the dominant process of rainwater production, as observed for shallow clouds (Stevens and Seifert, 2008) and stratiform clouds (Wood, 2005). High aerosol loading delays the occurrence of *au*, inhibiting the initialization of rain and the following accretion processes at the early stage (0–100 min). Melted frozen particles are also a major source of raindrops. Under low N_{CN} conditions, most of them form from melted graupel particles, whereas under high N_{CN} condition, melting of snowflakes be-

520 comes more important. This is consistent with the aerosol impact on the relative abun-
521 dance of frozen particles shown in Fig. 11. A higher aerosol concentration leads to a
522 higher fraction of smaller frozen particles (ice crystals and snowflakes). The main differ-
523 ence between low and high updrafts is that cloud conversion is the main source in the
524 former case, whereas in the latter case, melted graupel/snow particles become the main
525 contributors.

526 Figure 19 illustrates the temporal evolution of the contribution of each process at
527 individual simulation grid (HUHA case). As mentioned before, the warm rain process is
528 quite unimportant under strong *FF* condition (Fig. 18b). However, it is observed that the
529 warm rain process is the leading source of raindrops at the beginning stage (60 min). The
530 raindrops formed from *au* and *ac* are relatively small, which can easily evaporate. The
531 melting of frozen particles to form raindrops becomes more significant after ~90 min,
532 which dominates the production of raindrops. As shown in Fig. 19, although the process-
533 es still continue at 180 simulation minutes, the microphysics has already fully developed
534 during this simulation period. Thus our 3 simulation hour could cover the characteristics
535 of the formation and evolution of the pyro-convective clouds. What is more, it should be
536 paid attention that long-term simulation may conceal some detailed information, leading
537 to the bias in prediction of hydrometeors.

538 The PA clearly demonstrates that aerosols could significantly alter the microphys-
539 ical pathways and their intensities. Although the variation in individual microphysical
540 process is remarkable, the net result of all processes is not obvious and even insusceptible
541 to aerosol perturbations. This is especially obvious when we consider the aerosol effect
542 on rain water: it is observed that as aerosols is enhanced by a factor of 500, the intensities
543 of the source processes only decrease by a factor of 10; however, there is only a two-fold
544 change in the net rain water content. This implies that the microphysical scheme itself is a
545 self-regulatory system, which can produce equilibrium and buffers the effect of aerosol
546 disturbance (negative feedback).

547 The sensitivity of raindrops to aerosols mainly depends on autoconversion param-
548 eterization, and the melting processes, etc. All those parameterizations have very large

549 uncertainties, especially with bulk microphysical parameterizations. For example, most of
550 the autoconversion schemes were developed or evaluated for stratocumulus clouds,
551 which may not be appropriate for convective clouds. Based on the simulations during the
552 convective phase of squall-line development, van Lier-Walqui et al. (2012) presented the
553 uncertainty in the microphysical parameterization by the posterior probability density
554 functions (PDFs) of parameters, observations, and microphysical processes. With the
555 purpose to improve the representation of microphysics, it is of significance to quantify
556 the parameterization uncertainty by using observation data to constrain parameterization.

557

558 **3.3.3 Frozen water content**

559 In this section, we only focus on the interactions between liquid water phase and solid
560 water phase. As the selfcollection and internal conversion between different frozen hy-
561 drometeors could also cause the change in number concentration of total frozen particles,
562 the process analysis for its number concentration is not discussed. As shown in Fig. 20,
563 the effect of *FF* is straightforward, boosting vapor deposition (*vdi*) and cloud droplet
564 freezing on ice (*cfi*). The *vdi* is always the most important pathway for the formation of
565 frozen particles in our simulations, whereas *cfi* shows comparable contribution in the
566 HULA case. Over a wide range of N_{CN} and updraft velocities, our results have extended
567 and generalized the results of Yin et al. (2005), in which *vdi* and *cfi* were suggested as the
568 dominant processes controlling the formation of ice crystals in individual mixed-phase
569 convective clouds. Although snow is the dominant constituent of frozen particle mass
570 (Fig. 11), the condensation of vapor on ice (*vdi*) rather than on snow is the major pathway
571 for frozen particles. The increase of snow mass is mostly caused by collecting of ice (*ics*)
572 and ice self-collection (coagulation of ice particles, *iscs*), which are internal conversions
573 not counted as either a source or a sink of frozen water content. The ice crystals used for
574 conversion to snow derive mostly from the *vdi* process. Increasing *FF* enhances the up-
575 ward transport of water vapor and liquid water to higher altitudes where frozen particles
576 can be formed effectively through *vdi* and *cfi*. On the other hand, stronger *FF* reduces the
577 residence time of cloud droplets in the warm environment (to form raindrops), which

could explain the attenuation of *rrg* (riming of raindrops to form graupel) as fire forcing increases under low aerosol condition.

Positive relationship between aerosols and the frozen water content have been demonstrated in Sect. 3.2.3. As shown in Fig. 20, the increase in frozen water content is achieved through the enhancement of the *vdi* process. The condensational growth rate R_{vdi} is a function of the number concentration (N_{ice}) and size (D_{ice}) of ice, together with the ambient supersaturation over ice (S_{ice}). In our simulations, the averaged S_{ice} and D_{ice} are not sensitive to the aerosol disturbance; it is the N_{ice} that has been increased significantly because of elevated aerosol concentrations. Higher N_{ice} provides a larger surface area for water vapor deposition on the existing ice crystals and increases R_{vdi}. Lee and Penner (2010) have suggested similar mechanisms for cirrus clouds, which was based on the double-moment bulk representation of Saleeby and Cotton (2004).

The process of the formation and dissipation of frozen water content in the modeling area is illustrated in Fig. 21. The ice crystals form firstly at a higher height, followed by the snow production at a lower level. Downdraughts in the margin region are caused mainly by evaporation and melting. Massive melting takes place at the late stage (after 90 min), when large frozen particles (i.e., graupel) form. This is in agreement with the fact that the raindrops appear at a late stage and at a lower altitude under strong *FF* condition (Figs. 8c and d).

As shown aforementioned, drop freezing parameterizations and ice nucleation parameterizations influence frozen water content dramatically, which involve large uncertainties. Ice microphysics is significantly more complicated due to the wide variety of ice particle characteristics. On one hand, the intensities of these processes differ greatly among different microphysical schemes. Eidhammer et al. (2009) have compared three different ice nucleation parameterizations, and found that different assumptions could result in similar qualitative conclusions although with distinct absolute values. The parameterization with observational constraints agrees well with the measurements. On the other hand, van Lier-Walqui et al. (2012) suggested the processes contributing to frozen parti-

cles are dependent on both particle size distribution and density parameters. Parameterization improvement based on observations could help to reduce the uncertainties.

3.3.4 Contribution of individual microphysical processes

The ATHAM model consists of several tens of microphysical processes. However, based on the calculation of their relative contributions, only a few processes play dominant roles in regulating the number and mass concentrations of cloud hydrometeors, suggesting a possibility for the simplification of microphysical schemes.

For the number concentration of cloud droplets, the cloud nucleation (*cn*) and *cfi* (freezing of cloud droplets to form ice) processes contribute most to its budget, while other processes together account for less than 10%. For the mass concentration, the net change of *vdc* (condensational growth of cloud droplets by deposition) and *cep* (evaporation of cloud droplets) processes determines the variations in the cloud water content. The *cfi* process could contribute ~50% of the sink under LAHU condition. Therefore, when we simulate the mass of cloud droplets, four microphysical processes, i.e., *cn*, *vdc*, *cep*, and *cfi*, account for a large fraction of the budget.

The dominant processes that contribute ~90% to the raindrop number concentration under specific conditions are autoconversion (*au*), selfcollection (*rsc*), evaporation (*rep*), melting of ice, snow, and graupel (*imr*, *smr*, and *gmr*). For the raindrop mass concentration, the contribution of three processes accounts for ~90% under most conditions, which are rain evaporation (*rep*), melting of snow and graupel (*smr*, and *gmr*).

For the frozen water content, under weak fire forcing condition, *vdi* (condensational growth of ice crystals by deposition) and *sep* (snow evaporation) contribute ~90% of the source and sink respectively. Under strong fire forcing condition, *vdi* and *cfi* together contribute 90% of the source, while *sep* and *gmr* together are the most important sink (90%).

These major processes can capture most of the qualitative and quantitative features of pyro-convection processes and this complex model can thus be simplified for many purposes to improve the computational capacity. Comparison between the comprehensive model and simplified framework will be performed and validated in future studies.

3.4 Uncertainties due to nonlinearity

Aerosol-cloud interactions are regarded as nonlinear processes. In this case, the local aerosol effects on a cloud relevant parameter Y, i.e., $d\mathrm{Y}/dN_{\mathrm{CN}}$ can be different from $\Delta\mathrm{Y}/\Delta N_{\mathrm{CN}}$, the dependence derived from two case studies. Fig. 1 has shown such an example: depending on the case selection, a positive (or negative) $d\mathrm{Y}/dN_{\mathrm{CN}}$ can correspond to a $\Delta\mathrm{Y}/\Delta N_{\mathrm{CN}}$ of 0. Then the question arises, how much difference can be expected between $d\mathrm{Y}/dN_{\mathrm{CN}}$ and $\Delta\mathrm{Y}/\Delta N_{\mathrm{CN}}$? In the following, we take the responses of the precipitation to aerosols as an example to address this issue.

Figure 22 shows the statistics of the relative difference between $\Delta\mathrm{Y}/\Delta N_{\mathrm{CN}}$ and $d\mathrm{Y}/dN_{\mathrm{CN}}$ under LU and HU conditions, in which Y represents the precipitation rate. As precipitation is insensitive to aerosols for N_{CN} >10,000 cm^{-3}, only the cases with N_{CN} of 200~10,000 cm^{-3} are chosen in the calculation. The relative difference is defined as:

$$\text{Relative difference} = \frac{\frac{\Delta Y}{\Delta N_{CN}} - \frac{dY}{dN_{CN}}}{\frac{dY}{dN_{CN}}} \quad (2)$$

and $\frac{\Delta Y}{\Delta N_{CN}}$ is calculated as: $\frac{\Delta Y}{\Delta N_{CN}} = \frac{Y(2N_{CN}) - Y(N_{CN})}{2N_{CN} - N_{CN}}$, in which the aerosol effect is determined by the difference between the reference case and that after doubling N_{CN}. $\frac{dY}{dN_{CN}}$ is the derivative of the precipitation rate at each N_{CN}, representing the local dependence of precipitation on N_{CN}.

655 The histograms in Fig. 22 demonstrate that $\frac{\Delta Y}{\Delta N_{CN}}$ can deviate considerably from

656 $\frac{dY}{dN_{CN}}$, not only for the absolute value but also for the sign. Statistically, most of the rela-

657 tive differences are in the range of -3.7~0.9 (the 25th and 75th percentiles respectively,

658 with the average difference of -3.0) under LU condition, while are between -1.5 and 0.04

659 (the 25th and 75th percentiles respectively, with the mean value of 0.02) under HU condi-

660 tion. The fact that individual case studies may not reveal local aerosol effects demon-

661 strates the importance of ensemble studies in determining the real responses of clouds to

662 aerosol perturbations.

663

664 **4. Conclusions**

665 In this study, the regime dependence of aerosol effects on the formation and evolution of

666 pyro-convective clouds have been studied in detail (Fig. 23). The main conclusions are

667 summarized as follows:

668 (1) As N_{CN} and *FF* increase, the number concentration of cloud droplets increases.

669 There are three distinct regimes for the cloud number concentration: an updraft-limited

670 regime (high $RS(FF)/RS(N_{CN})$ ratio), an aerosol-limited regime (low $RS(FF)/RS(N_{CN})$ ra-

671 tio), and a transitional regime (intermediate $RS(FF)/RS(N_{CN})$ ratio), which agrees well

672 with the regimes derived from a parcel model (Reutter et al., 2009). The cloud mass con-

673 centration is less sensitive to aerosols, and there are two regimes for mass concentration:

674 an updraft-limited regime, and a transitional regime.

675 (2) The production of rain water content (i.e., M_{RD}) was enhanced with increase in

676 updrafts, and the aerosols could either slightly increase M_{RD} with low N_{CN} or decrease

677 M_{RD} with large N_{CN}. The N_{CN} plays a mostly negative role in M_{CD} under intermediate N_{CN}

678 conditions (N_{CN} of several 1000 cm^{-3}). M_{RD} was generally within an updraft-limited re-

679 gime, i.e., M_{RD} was very sensitive to changes in updrafts, but insensitive to aerosol con-

centrations ($RS(FF)/RS(N_{CN})>4$). The aerosol and *FF* effects on raindrop number concentrations (N_{RD}) are quite complicated; both of them play the non-monotonic role in the N_{RD}.

(3) As updrafts and aerosols increase, the domain-averaged number and mass concentrations of frozen particles (N_{FP} and M_{FP} respectively) were enhanced. N_{FP} and M_{FP} were also within the updraft-limited regime, which is characterized by large $RS(FF)/RS(N_{CN})$ ratio. In this regime, N_{FP} and M_{FP} were directly proportional to fire forcing, and independent of aerosols.

(4) Larger *FF* resulted in more precipitation, whereas the effect of aerosols on precipitation was complex and could either enhance or suppress the production of precipitation. The suppression on the precipitation is due to the change in the fraction of small frozen particles and total melting rate of frozen particles. The enhancement on the precipitation resulting from increasing N_{CN} under low aerosol condition is a result of changes in the vertical distribution of frozen particles and its evaporation process.

(5) In addition, when N_{CN} and *FF* became too large, their impact became weaker, as indicated by a decreasing *RS*.

The PA provided further insight into the mechanisms of aerosol-cloud interactions. By evaluating the contribution of the relevant microphysical processes to the formation of an individual hydrometeor, the PA revealed the dominant factors responsible for the changes in hydrometeor number and mass. (1) Cloud nucleation (*cn*) initializes cloud droplet formation and is the major factor that controls the number concentration of cloud droplets. As expected, the increase in cloud droplet mass can be attributed mostly to the condensational growth (*vdc*). (2) Under weak *FF*, autoconversion (*au*) and accretion (*ac*) are the main sources of rain droplets. Under strong *FF*, the major source is the melting of frozen particles. (3) For the frozen content, the condensation of water vapor on existing ice crystals (*vdi*) is the most important contributor. In addition to CCN activation, the PA also highlights the importance of other microphysical processes in regulating cloud evolution, which is worthy of further scrutiny. By identifying the contribution from individual processes, PA may also provide an opportunity for the simplification of microphysical schemes. For example, out of 24 microphysical processes that are directly related to the

budget of cloud droplets and raindrops, over 90% of the mass and number changes are attributed to only 10 processes.

While the general trend is clear, the inclusion of nonlinear (dynamic and microphysical) processes leads to a complex and unstable response of clouds to aerosol perturbations. This applies to the response of all hydrometeors and precipitation, as indicated by the large standard deviation of *RS* in Figs. 7, 9, 12 and 13. This should also hold when variations in other parameters (e.g., meteorological conditions) are introduced. Compared with our results, the *RS* derived from cloud parcel modeling is much smoother (Fig. 8 in Reutter et al. (2009)). The difference is probably caused by complex interactions between cloud microphysics and dynamics (Khain et al., 2008; Fan et al., 2009). These highly nonlinear processes result in a more unstable and chaotic response of cloud evolution to aerosol and dynamic perturbations. Because of this non-linearity, sensitivities of clouds based on limited case studies may require caveats, because they may not be as representative as expected, and so cannot safely be extrapolated to conditions outside of the range explored. To understand better the role of aerosols in cloud formation, we recommend high-resolution ensemble sensitivity studies over a wide range of dynamic and aerosol conditions.

General current understanding and global modelling studies suggest that for cloud droplet number concentration, the updraft-limited regime may be more characteristic of continental clouds, while the aerosol-limited regime may be more characteristic of marine clouds (e.g., Karydis et al., 2012), suggesting that aerosol effects are generally more important for the marine environment. For this case study of pyro-convective clouds, then, we conclude that aerosol effects on cloud droplet number concentrations and cloud droplet size are likely more important than effects on precipitation, since precipitation is far less sensitive to N_{CN} than to updraft velocity. This is in agreement with other studies (e.g., Seifert et al., 2012). A recent long-term convective cloud investigation found that microphysical effects driven by aerosol particles dominate the properties and morphology of deep convective clouds, rather than updraft-related dynamics (Fan et al., 2013). Therefore, it must still be determined whether this conclusion applies to other cloud types and over longer time scales.

In this study, we demonstrate the performance of ensemble simulations in determining the regime dependence of aerosol effects. The use of such regime dependence requires caveats because it may differ for different cloud types, aerosol properties, meteorological conditions and model configurations (e.g., microphysical schemes, dynamic schemes, dimensionality, etc.; the 3-D results are in the supplementary material).

In future work, we intend to extend the current studies to: (1) include other types of clouds with other meteorological or atmospheric conditions; (2) investigate the cloud response over longer timescales (Van Den Heever and Cotton, 2007), as different observational scales could introduce biases in the quantification of aerosol effects on clouds (McComiskey and Feingold, 2012); and (3) evaluate the relative contribution of microphysical and dynamic effects to cloud buffering effects (Stevens and Feingold, 2009; Seifert et al., 2012).

Table A1. Symbols and acronyms for individual microphysical process.

Symbol	Process
cn	Cloud nucleation
cri/s/g/h	Riming of cloud droplets to form ice crystals/snow/graupel/hail
cfi[(1)]	Freezing of cloud water to form ice crystals
imc/r	Melting of ice crystals to form cloud water/raindrops
au	Autoconversion of cloud water to form rain
ac	Accretion of cloud water by rain
vdc/i/g/s	Condensational growth of cloud droplets/ice crystals/graupel/snow by vapor deposition
in	Ice nucleation
s/g/hmr	Melting of snow/graupel/hail to form raindrops
rsc	Self-collection of raindrops
rfi/s/g/h	Freezing of raindrops to form ice crystals/snow/graupel/hail
rri/s/g/h	Riming of raindrops to form ice crystals/snow/graupel/hail
c/r/i/s/gep	Evaporation of cloud droplets/raindrops/ice/snow/graupel

[(1)] Here, *cfi* process includes both heterogeneous and homogeneous freezing processes.

Acknowledgements

This work was supported by the Max Planck Society (MPG), Max Planck Graduate Center (MPGC), and EU project BACCHUS (No. 603445). Susannah Burrows was supported by the Office of Science Biological and Environmental Research Program of the U.S. Department of Energy as part of the Earth System Modelling Program. We thank A. Seifert, P. Spichtinger and P. Neis for helpful discussions and model setup.

763 **References**

764 Ackerman, A. S., Toon, O. B., Stevens, D. E., Heymsfield, A. J., Ramanathan, V., and
765 Welton, E. J.: Reduction of tropical cloudiness by soot, Science, 288, 1042-1047, doi:
766 10.1126/science.288.5468.1042, 2000.
767 Ackerman, A. S., Toon, O. B., Stevens, D. E., and Coakley, J. A.: Enhancement of cloud
768 cover and suppression of nocturnal drizzle in stratocumulus polluted by haze, Geophys
769 Res Lett, 30, 1381, doi: 10.1029/2002gl016634, 2003.
770 Albrecht, B. A.: Aerosols, Cloud Microphysics, and Fractional Cloudiness, Science, 245,
771 1227-1230, doi: 10.1126/science.245.4923.1227, 1989.
772 Altaratz, O., Koren, I., Reisin, T., Kostinski, A., Feingold, G., Levin, Z., and Yin, Y.:
773 Aerosols' influence on the interplay between condensation, evaporation and rain in warm
774 cumulus cloud, Atmospheric Chemistry and Physics, 8, 15-24, 2008.
775 Andreae, M. O., Rosenfeld, D., Artaxo, P., Costa, A. A., Frank, G. P., Longo, K. M., and
776 Silva-Dias, M. A. F.: Smoking Rain Clouds over the Amazon, Science, 303, 1337-1342,
777 2004.
778 ASRD: Final documentation report-Chisholm Fire (LWF-063), Forest Protection
779 Division, Alberta Sustainable Resource Development, 2001.
780 Blahak, U.: Towards a Better Representation of High Density Ice Particles in a State-of-
781 the-Art Two-Moment Bulk Microphysical Scheme, 15th International Conf. on Clouds
782 and Precipitation, Cancun, Mexico, July 7–11, 2008.
783 Bytnerowicz, A., Arbaugh, M., Andersen, C., and Riebau, A.: Wildland Fires and Air
784 Pollution, Dev Environm Sci, 8, 1-638, 2009.
785 Camponogara, G., Dias, M. A. F. S., and Carrio, G. G.: Relationship between Amazon
786 biomass burning aerosols and rainfall over the La Plata Basin, Atmospheric Chemistry
787 and Physics, 14, 4397-4407, doi: 10.5194/acp-14-4397-2014, 2014.
788 Cotton, R. J., and Field, P. R.: Ice nucleation characteristics of an isolated wave cloud, Q
789 J Roy Meteor Soc, 128, 2417-2437, doi: 10.1256/Qj.01.150, 2002.
790 Eidhammer, T., DeMott, P. J., and Kreidenweis, S. M.: A comparison of heterogeneous
791 ice nucleation parameterizations using a parcel model framework, J Geophys Res-Atmos,
792 114, doi: 10.1029/2008jd011095, 2009.

793 Fan, J. W., Yuan, T. L., Comstock, J. M., Ghan, S., Khain, A., Leung, L. R., Li, Z. Q.,
794 Martins, V. J., and Ovchinnikov, M.: Dominant role by vertical wind shear in regulating
795 aerosol effects on deep convective clouds, J Geophys Res-Atmos, 114, doi:
796 10.1029/2009jd012352, 2009.
797 Fan, J. W., Leung, L. R., Rosenfeld, D., Chen, Q., Li, Z. Q., Zhang, J. Q., and Yan, H. R.:
798 Microphysical effects determine macrophysical response for aerosol impacts on deep
799 convective clouds, P Natl Acad Sci USA, 110, E4581-E4590, doi:
800 10.1073/pnas.1316830110, 2013.
801 Feingold, G.: Modeling of the first indirect effect: Analysis of measurement requirements,
802 Geophys Res Lett, 30, doi: 10.1029/2003gl017967, 2003.
803 Graf, H. F., Herzog, M., Oberhuber, J. M., and Textor, C.: Effect of environmental
804 conditions on volcanic plume rise, J Geophys Res-Atmos, 104, 24309-24320, 1999.
805 Grandey, B. S., Stier, P., and Wagner, T. M.: Investigating relationships between aerosol
806 optical depth and cloud fraction using satellite, aerosol reanalysis and general circulation
807 model data, Atmospheric Chemistry and Physics, 13, 3177-3184, doi: 10.5194/acp-13-
808 3177-2013, 2013.
809 Herzog, M.: Simulation der dynamik eines multikomponentensystems am beispiel
810 vulkanischer eruptionswolken, Ph. D, University of Hamburg, Hamburg, Germany, 153
811 pp., 1998.
812 Herzog, M., Graf, H. F., Textor, C., and Oberhuber, J. M.: The effect of phase changes of
813 water on the development of volcanic plumes, J Volcanol Geoth Res, 87, 55-74, 1998.
814 Herzog, M., Oberhuber, J. M., and Graf, H. F.: A prognostic turbulence scheme for the
815 nonhydrostatic plume model ATHAM, J Atmos Sci, 60, 2783-2796, 2003.
816 Hobbs, P. V., and Locatelli, J. D.: Ice nuclei from a natural forest fire, J Appl Meteorol, 8,
817 833-834, 1969.
818 Hobbs, P. V., and Radke, L. F.: Cloud Condensation Nuclei from a Simulated Forest Fire,
819 Science, 163, 279-280, 1969.
820 IPCC: Climate change 2007: The physical science basis, Contribution of Working Group
821 I to the Fourth Assessment Report of the Intergovernmental Panel on Climate Change,
822 edited by: Solomon, S., Qin, D., Manning, M., Chen, Z., Marquis, M., Averyt, K. B.,

823 Tignor, M., and Miller, H. L., Cambridge University Press, Cambridge and New York,
824 2007.
825 Jeffery, C. A., and Austin, P. H.: Homogeneous nucleation of supercooled water: Results
826 from a new equation of state, J Geophys Res-Atmos, 102, 25269-25279, doi:
827 10.1029/97jd02243, 1997.
828 Karydis, V. A., Capps, S. L., Russell, A. G., and Nenes, A.: Adjoint sensitivity of global
829 cloud droplet number to aerosol and dynamical parameters, Atmospheric Chemistry and
830 Physics, 12, 9041-9055, doi: 10.5194/acp-12-9041-2012, 2012.
831 Kaufman, Y. J., and Fraser, R. S.: The effect of smoke particles on clouds and climate
832 forcing, Science, 277, 1636-1639, 1997.
833 Kaufman, Y. J., Tanre, D., and Boucher, O.: A satellite view of aerosols in the climate
834 system, Nature, 419, 215-223, doi: 10.1038/Nature01091, 2002.
835 Kaufman, Y. J., and Koren, I.: Smoke and pollution aerosol effect on cloud cover,
836 Science, 313, 655-658, doi: 10.1126/science.1126232, 2006.
837 Kay, J. E., and Wood, R.: Timescale analysis of aerosol sensitivity during homogeneous
838 freezing and implications for upper tropospheric water vapor budgets, Geophys Res Lett,
839 35, doi: 10.1029/2007gl032628, 2008.
840 Khain, A., Rosenfeld, D., and Pokrovsky, A.: Aerosol impact on the dynamics and
841 microphysics of deep convective clouds, Q J Roy Meteor Soc, 131, 2639-2663, doi:
842 10.1256/Qj.04.62, 2005.
843 Khain, A. P., BenMoshe, N., and Pokrovsky, A.: Factors determining the impact of
844 aerosols on surface precipitation from clouds: An attempt at classification, J Atmos Sci,
845 65, 1721-1748, doi: 10.1175/2007jas2515.1, 2008.
846 Khain, A. P.: Notes on state-of-the-art investigations of aerosol effects on precipitation: a
847 critical review, Environ Res Lett, 4, doi: 10.1088/1748-9326/4/1/015004, 2009.
848 Khain, A. P., Leung, L. R., Lynn, B., and Ghan, S.: Effects of aerosols on the dynamics
849 and microphysics of squall lines simulated by spectral bin and bulk parameterization
850 schemes, J Geophys Res-Atmos, 114, doi: 10.1029/2009jd011902, 2009.
851 Koren, I., Kaufman, Y. J., Remer, L. A., and Martins, J. V.: Measurement of the effect of
852 Amazon smoke on inhibition of cloud formation, Science, 303, 1342-1345, doi:
853 10.1126/science.1089424, 2004.

Lee, S. S., Donner, L. J., Phillips, V. T. J., and Ming, Y.: The dependence of aerosol effects on clouds and precipitation on cloud-system organization, shear and stability, J Geophys Res-Atmos, 113, doi: 10.1029/2007jd009224, 2008.

Lee, S. S., and Penner, J. E.: Aerosol effects on ice clouds: can the traditional concept of aerosol indirect effects be applied to aerosol-cloud interactions in cirrus clouds?, Atmospheric Chemistry and Physics, 10, 10345-10358, doi: 10.5194/acp-10-10345-2010, 2010.

Lee, S. S., and Feingold, G.: Aerosol effects on the cloud-field properties of tropical convective clouds, Atmospheric Chemistry and Physics, 13, 6713-6726, doi:10.5194/acp-13-6713-2013, 2013.

Levin, Z., and Cotton, W.: Aerosol Pollution Impact on Precipitation: A Scientific Review, World Meteorol. Organ, Geneva, Switzerland, 2007.

Li, G. H., Wang, Y., and Zhang, R. Y.: Implementation of a two-moment bulk microphysics scheme to the WRF model to investigate aerosol-cloud interaction, J Geophys Res-Atmos, 113, doi: 10.1029/2007jd009361, 2008.

Luderer, G. G.: Modeling of Deep-Convective Vertical Transport of Foreset Fire Smoke into the Upper Troposphere and Lower Stratosphere, Ph.D, Physics Department, Johannes Gutenberg University Mainz, Mainz, 2007.

McComiskey, A., and Feingold, G.: The scale problem in quantifying aerosol indirect effects, Atmospheric Chemistry and Physics, 12, 1031-1049, doi: 10.5194/acp-12-1031-2012, 2012.

McFiggans, G., Artaxo, P., Baltensperger, U., Coe, H., Facchini, M. C., Feingold, G., Fuzzi, S., Gysel, M., Laaksonen, A., Lohmann, U., Mentel, T. F., Murphy, D. M., O'Dowd, C. D., Snider, J. R., and Weingartner, E.: The effect of physical and chemical aerosol properties on warm cloud droplet activation, Atmospheric Chemistry and Physics, 6, 2593-2649, 2006.

Muhlbauer, A., Hashino, T., Xue, L., Teller, A., Lohmann, U., Rasmussen, R. M., Geresdi, I., and Pan, Z.: Intercomparison of aerosol-cloud-precipitation interactions in stratiform orographic mixed-phase clouds, Atmospheric Chemistry and Physics, 10, 8173-8196, doi: 10.5194/acp-10-8173-2010, 2010.

884 Norris, J. R.: Has northern Indian Ocean cloud cover changed due to increasing
885 anthropogenic aerosol?, Geophys Res Lett, 28, 3271-3274, doi: 10.1029/2001gl013547,
886 2001.
887 Oberhuber, J. M., Herzog, M., Graf, H. F., and Schwanke, K.: Volcanic plume simulation
888 on large scales, J Volcanol Geoth Res, 87, 29-53, 1998.
889 Pruppacher, H. R., and Klett, J. D.: Microphysics of Clouds and Precipitation, Second
890 Revised and Enlarged Edition with an Introduction to Cloud Chemistry and Cloud
891 Electricity, Kluwer Academic Publishers, Reidel, Dordrecht, 954 pp., 1997.
892 Reid, J. S., Koppmann, R., Eck, T. F., and Eleuterio, D. P.: A review of biomass burning
893 emissions part II: intensive physical properties of biomass burning particles, Atmospheric
894 Chemistry and Physics, 5, 799-825, 2005.
895 Reutter, P., Su, H., Trentmann, J., Simmel, M., Rose, D., Gunthe, S. S., Wernli, H.,
896 Andreae, M. O., and Poschl, U.: Aerosol- and updraft-limited regimes of cloud droplet
897 formation: influence of particle number, size and hygroscopicity on the activation of
898 cloud condensation nuclei (CCN), Atmospheric Chemistry and Physics, 9, 7067-7080,
899 10.5194/acp-9-7067-2009, 2009.
900 Reutter, P., Trentmann, J., Seifert, A., Neis, P., Su, H., Chang, D., Herzog, M., Wernli, H.,
901 Andreae, M. O., and Poschl, U.: 3-D model simulations of dynamical and microphysical
902 interactions in pyro-convective clouds under idealized conditions, Atmospheric
903 Chemistry and Physics, 14, 7573-7583, doi:10.5194/acp-14-7573-2014, 2014.
904 Rosenfeld, D.: TRMM observed first direct evidence of smoke from forest fires inhibiting
905 rainfall, Geophys Res Lett, 26, 3105-3108, 1999.
906 Rosenfeld, D.: Suppression of rain and snow by urban and industrial air pollution,
907 Science, 287, 1793-1796, 2000.
908 Rosenfeld, D., Fromm, M., Trentmann, J., Luderer, G., Andreae, M. O., and Servranckx,
909 R.: The Chisholm firestorm: observed microstructure, precipitation and lightning activity
910 of a pyro-cumulonimbus, Atmos Chem Phys, 7, 645-659, 2007.
911 Rosenfeld, D., Lohmann, U., Raga, G. B., O'Dowd, C. D., Kulmala, M., Fuzzi, S.,
912 Reissell, A., and Andreae, M. O.: Flood or drought: How do aerosols affect precipitation?,
913 Science, 321, 1309-1313, doi: 10.1126/science.1160606, 2008.

914 Saleeby, S. M., and Cotton, W. R.: A large-droplet mode and prognostic number
915 concentration of cloud droplets in the Colorado State University Regional Atmospheric
916 Modeling System (RAMS). Part I: Module descriptions and supercell test simulations, J
917 Appl Meteorol, 43, 182-195, doi: 10.1175/1520-0450(2004)043, 2004.
918 Saleeby, S. M., Cotton, W. R., Lowenthal, D., Borys, R. D., and Wetzel, M. A.: Influence
919 of Cloud Condensation Nuclei on Orographic Snowfall, J Appl Meteorol Clim, 48, 903-
920 922, doi: 10.1175/2008jamc1989.1, 2009.
921 Sassen, K., and Khvorostyanov, V. I.: Cloud effects from boreal forest fire smoke:
922 evidence for ice nucleation from polarization lidar data and cloud model simulations,
923 Environ Res Lett, 3, 12, doi: 10.1088/1748-9326/3/2/025006, 2008.
924 Seifert, A., and Beheng, K. D.: A two-moment cloud microphysics parameterization for
925 mixed-phase clouds. Part 1: Model description, Meteorol Atmos Phys, 92, 45-66, doi:
926 10.1007/s00703-005-0112-4, 2006.
927 Seifert, A., Khain, A., Pokrovsky, A., and Beheng, K. D.: A comparison of spectral bin
928 and two-moment bulk mixed-phase cloud microphysics, Atmos Res, 80, 46-66, doi:
929 10.1016/j.atmosres.2005.06.009, 2006.
930 Seifert, A., Kohler, C., and Beheng, K. D.: Aerosol-cloud-precipitation effects over
931 Germany as simulated by a convective-scale numerical weather prediction model,
932 Atmospheric Chemistry and Physics, 12, 709-725, doi: 10.5194/acp-12-709-2012, 2012.
933 Sorooshian, A., Feingold, G., Lebsock, M. D., Jiang, H. L., and Stephens, G. L.: On the
934 precipitation susceptibility of clouds to aerosol perturbations, Geophys Res Lett, 36,
935 L13803, doi: 10.1029/2009gl038993, 2009.
936 Stevens, B., and Seifert, A.: Understanding macrophysical outcomes of microphysical
937 choices in simulations of shallow cumulus convection, J Meteorol Soc Jpn, 86, 143-162,
938 2008.
939 Stevens, B., and Feingold, G.: Untangling aerosol effects on clouds and precipitation in a
940 buffered system, Nature, 461, 607-613, doi: 10.1038/Nature08281, 2009.
941 Tao, W. K., Li, X. W., Khain, A., Matsui, T., Lang, S., and Simpson, J.: Role of
942 atmospheric aerosol concentration on deep convective precipitation: Cloud-resolving
943 model simulations, J Geophys Res-Atmos, 112, D24S18, doi: 10.1029/2007jd008728,
944 2007.

945 Tao, W. K., Chen, J. P., Li, Z. Q., Wang, C., and Zhang, C. D.: Impact of Aerosols on
946 Convective Clouds and Precipitation, Rev Geophys, 50, doi: 10.1029/2011rg000369,
947 2012.
948 Teller, A., and Levin, Z.: Factorial method as a tool for estimating the relative
949 contribution to precipitation of cloud microphysical processes and environmental
950 conditions: Method and application, J Geophys Res-Atmos, 113, doi:
951 10.1029/2007jd008960, 2008.
952 Van Den Heever, S. C., and Cotton, W. R.: Urban aerosol impacts on downwind
953 convective storms, J Appl Meteorol Clim, 46, 828-850, doi: 10.1175/Jam2492.1, 2007.
954 van Lier-Walqui, M., Vukicevic, T., and Posselt, D. J.: Quantification of Cloud
955 Microphysical Parameterization Uncertainty Using Radar Reflectivity, Mon Weather Rev,
956 140, 3442-3466, doi: 10.1175/Mwr-D-11-00216.1, 2012.
957 Wang, M., Ghan, S., Ovchinnikov, M., Liu, X., Easter, R., Kassianov, E., Qian, Y., and
958 Morrison, H.: Aerosol indirect effects in a multi-scale aerosol-climate model PNNL-
959 MMF, Atmospheric Chemistry and Physics, 11, 5431-5455, doi: 10.5194/acp-11-5431-
960 2011, 2011.
961 Wang, Y., Fan, J. W., Zhang, R. Y., Leung, L. R., and Franklin, C.: Improving bulk
962 microphysics parameterizations in simulations of aerosol effects, J Geophys Res-Atmos,
963 118, 5361-5379, doi: 10.1002/Jgrd.50432, 2013.
964 Wang, Y., Zhang, R. Y., and Saravanan, R.: Asian pollution climatically modulates mid-
965 latitude cyclones following hierarchical modelling and observational analysis, Nat
966 Commun, 5, doi: 10.1038/Ncomms4098, 2014.
967 Wood, R.: Drizzle in stratiform boundary layer clouds. Part II: Microphysical aspects, J
968 Atmos Sci, 62, 3034-3050, doi: 10.1175/Jas3530.1, 2005.
969 Yin, Y., Carslaw, K. S., and Feingold, G.: Vertical transport and processing of aerosols in
970 a mixed-phase convective cloud and the feedback on cloud development, Q J Roy Meteor
971 Soc, 131, 221-245, doi: 10.1256/qj.03.186, 2005.
972 Zhang, L. M., Michelangeli, D. V., and Taylor, P. A.: Influence of aerosol concentration
973 on precipitation formation in low-level, warm stratiform clouds, J Aerosol Sci, 37, 203-
974 217, doi: 10.1016/j.jaerosci.2005.04.002, 2006.

Table captions

Table 1. Typical characterizations of the frozen hydrometeor classes.

Table 1. Typical characterizations of the frozen hydrometeor classes.

		Diameter (mm)	Density (g cm^{-3})	Terminal velocity (m s^{-1})
Cloud ice	Columnar cystals	0.01—1[(1)]	0.36—0.7 [(2)]	0.013—0.055[(2)]
	Plate-like	0.01—1[(1)]	~0.9[(1)]	0.02—0.06[(2)]
	Dendrites	0.1—3[(1)]	0.3—1.4[(1)]	0.25—0.7[(3)]
Snowflakes		2—5[(1)]	0.05—0.89[(1)]	0.5—3[(1)]
Graupel		0.5—5[(1)]	~0.4[(1)]	3—14[(1)]
Hail		5—80[(1)]	0.8—0.9[(1)]	10—40[(1)]

[(1)] Pruppacher H.R. (1978).

[(2)]Jayaweer and Ryan (1972).

[(3)]Mitchell and Heymsfield (2005).

Figure captions

Figure 1. Conceptual model of the nonlinear relationship between aerosol concentrations and rain rate (Data are from 2-D simulation results of this work).

Figure 2. Atmospheric sounding launched near Edmonton, Alberta on 29 May 2001. The right black line represents the temperature, and the left black line corresponds to the dew-point temperature. This weather information is from the University of Wyoming Department of Atmospheric Science (http://weather.uwyo.edu/).

Figure 3. The 110×100 grid points in the computational domain.

Figure 4. Probability distribution function of vertical velocities (w) at cloud base layer under different fire forcing conditions (a); Relationship between input fire forcing (FF) and induced vertical velocity (w) at cloud base (b). The aerosol concentration is 1,000 cm^{-3}. The shaded area represents the variability of estimation (±½σ).

Figure 5. The correlation of fire forcing and the corresponding maximum temperature at cloud base. The shaded area indicates the variability of estimation (±½σ) over each simulation period.

Figure 6. Time evolution of horizontally-averaged cloud water content (g kg^{-1}) as a function of altitude for four extreme cases, which are referred to as (1) LULA: low updrafts (2,000 W m^{-2}) and low aerosols (200 cm^{-3}); (2) LUHA: low updrafts (2,000 W m^{-2}) and high aerosols (100,000 cm^{-3}); (3) HULA: high updrafts (300,000 W m^{-2}) and low aerosols (200 cm^{-3}); (4) HUHA: high updrafts (300,000 W m^{-2}) and high aerosols (100,000 cm^{-3}). Maximum values for each episode are also shown.

Figure 7. Number (a) and mass concentration (b) of cloud droplets calculated as a function of aerosol number concentration (N_{CN}) and updraft velocity (represented by FF). Red dashed lines indicate the borders between different regimes defined by RS (N_{CN})/RS(FF)=4 or 1/4, respectively. Relative sensitivities with respect to N_{CN} (left) and FF (right) for number (panels (c) and (d)) and mass (panels (e) and (f)) concentration of cloud droplets under different conditions. The thick dashed or solid lines represent the mean values under a given condition, and the shaded areas represent the variability of estimation (±½σ). The acronyms indicate LU: low updrafts (1,000–7,000 W m^{-2}); HU: high updrafts (75,000–300,000 W m^{-2}); LA: low aerosols (200–1,500 cm^{-3}); HA: high aerosols (10,000–100,000 cm^{-3}).

Figure 8. Same as Figure 6 but for raindrops.

Figure 9. Same as Figure 7 but for raindrops.

Figure 10. Same as Figure 6 but for the frozen particles.

Figure 11. Contributions of individual frozen hydrometeor to total frozen water content under four extreme conditions which are referred to as (1) LULA: low updrafts (2,000 W m^{-2}) and low aerosols (200 cm^{-3}); (2) LUHA: low updrafts (2,000 W m^{-2}) and high aerosols (100,000

cm^{-3}); (3) HULA: high updrafts (300,000 W m^{-2}) and low aerosols (200 cm^{-3}); (4) HUHA: high updrafts (300,000 W m^{-2}) and high aerosols (100,000 cm^{-3}).

Figure 12. Same as Figure 7 but for total frozen particles.

Figure 13. Same as Figure 7 but for surface rain rate.

Figure 14. The correlation of rain rate and the melting rate of the frozen particles. The green diamond points are the averaged rain rate under different aerosol concentrations (FF= 10^5 W m^{-2}). The columns represent the integrated melting rate from individual frozen particles.

Figure 15. Time evolution of surface rain rates for the three aerosol episodes (N_{CN} = 200; 1,000; and 100,000 cm^{-3} respectively) under LU (low updrafts, FF=2,000 W m^{-2}) and HU (high updrafts, FF=50,000 W m^{-2}) conditions.

Figure 16. The pie charts summarize the relative percentage of the microphysical processes involving cloud droplets as a function of N_{CN} and fire forcing (a: number concentration; b: mass concentration). Colors within each pie chart reflect the contribution of processes under the specific condition. Warm colors denote the sources, while cold colors denote the sinks. The acronyms indicate cn: cloud nucleation; vdc: condensational growth of cloud droplets; cep: evaporation of cloud droplets; au: autoconversion; ac: accretion; cfi: freezing of cloud droplets to form ice crystals, including homogeneous and heterogeneous nucleation; crg/h: riming of cloud droplets to form graupel/hail.

Figure 17. The pie charts summarize the vertical cross sections of the change rate of main microphysical processes contributing to cloud water content. Each pie chart shows the averaged contribution over the past 30 min. Colors within each pie chart reflect the percentage of processes in each grid. The black dashed line is the 0.1 μg kg^{-1} isoline of the interstitial aerosol, indicating the shape of smoke plume. The meaning of the acronyms is the same as in Figure 16. Warm colors denote the sources, while cold colors denote the sinks.

Figure 18. Same as Figure 16 but for raindrops. The acronyms indicate au: autoconversion; ac: accretion; i/s/g/hmr: melting of ice/snow/graupel/hail to form raindrops; rsc: self-collection of raindrops; ismr: melting of ice and snow to form raindrops; rfi/h: freezing of raindrops to form ice crystals/hail; rep: raindrop evaporation; rrg: riming of raindrops to form graupel; rris: riming of raindrops to form ice and snow.

Figure 19. Same as Figure 17, but for raindrops.

Figure 20. Same as Figure 16 but for the total frozen water content. The acronyms indicate in: ice nucleation; cfi: freezing of cloud droplets to form ice crystals, including homogeneous and heterogeneous nucleation; rfh: freezing of raindrops to form hail; vdi/s/g: condensational growth of ice crystals/snow/graupel by water vapor; rrg: riming of raindrops to form graupel; i/s/gep: evaporation of ice/snow/graupel; s/g/hmr: melting of snow/graupel/hail to form raindrops.

Figure 21. Same as Figure 17 but for frozen particles.

Figure 22. Histograms of the relative difference between $\frac{\Delta Y}{\Delta N_{CN}}$ and $\frac{dY}{dN_{CN}}$ under LU and HU conditions, where *Y* here denotes precipitation rate. $\frac{\Delta Y}{\Delta N_{CN}} = \frac{Y(2N_{CN}) - Y(N_{CN})}{2N_{CN} - N_{CN}}$, and $\frac{dY}{dN_{CN}}$ is the derivative of the precipitation rate along the variable N_{CN}.

Figure 23. Overview of the research approaches on multi-scale cloud initialization and development.

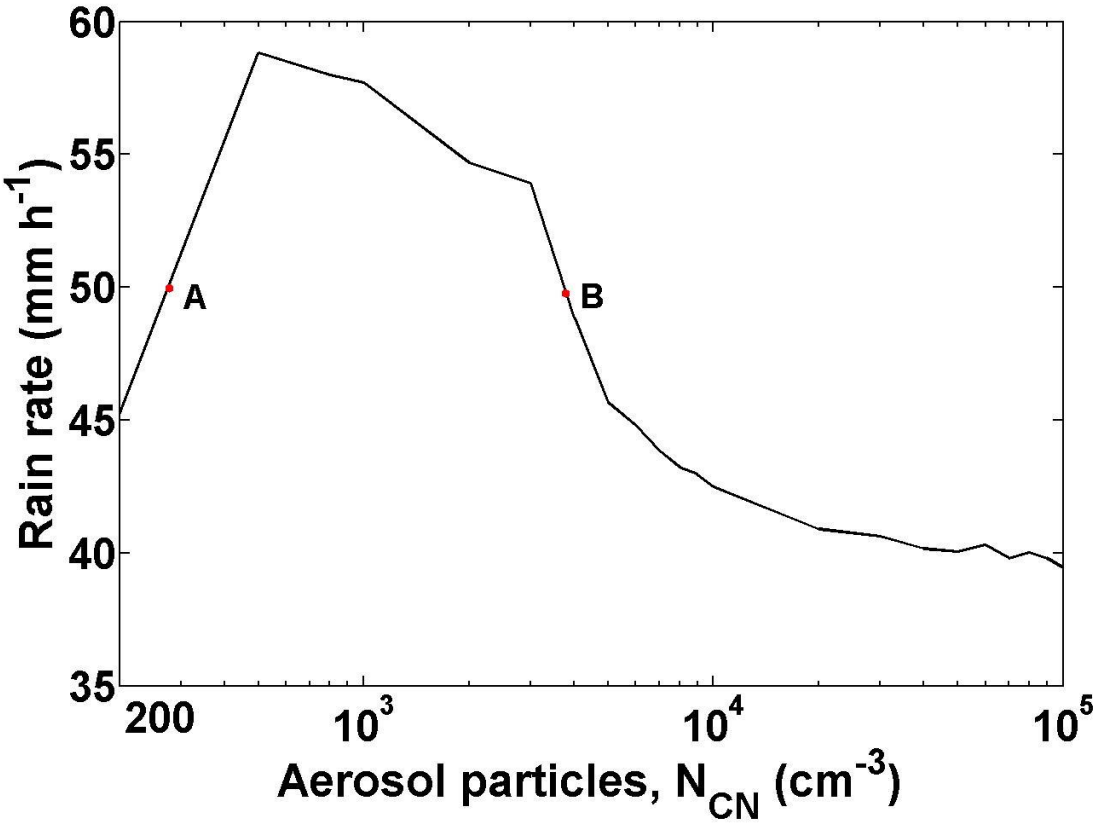

Figure 1. Conceptual model of the nonlinear relationship between aerosol concentrations and rain rate (Data are from 2-D simulation results of this work).

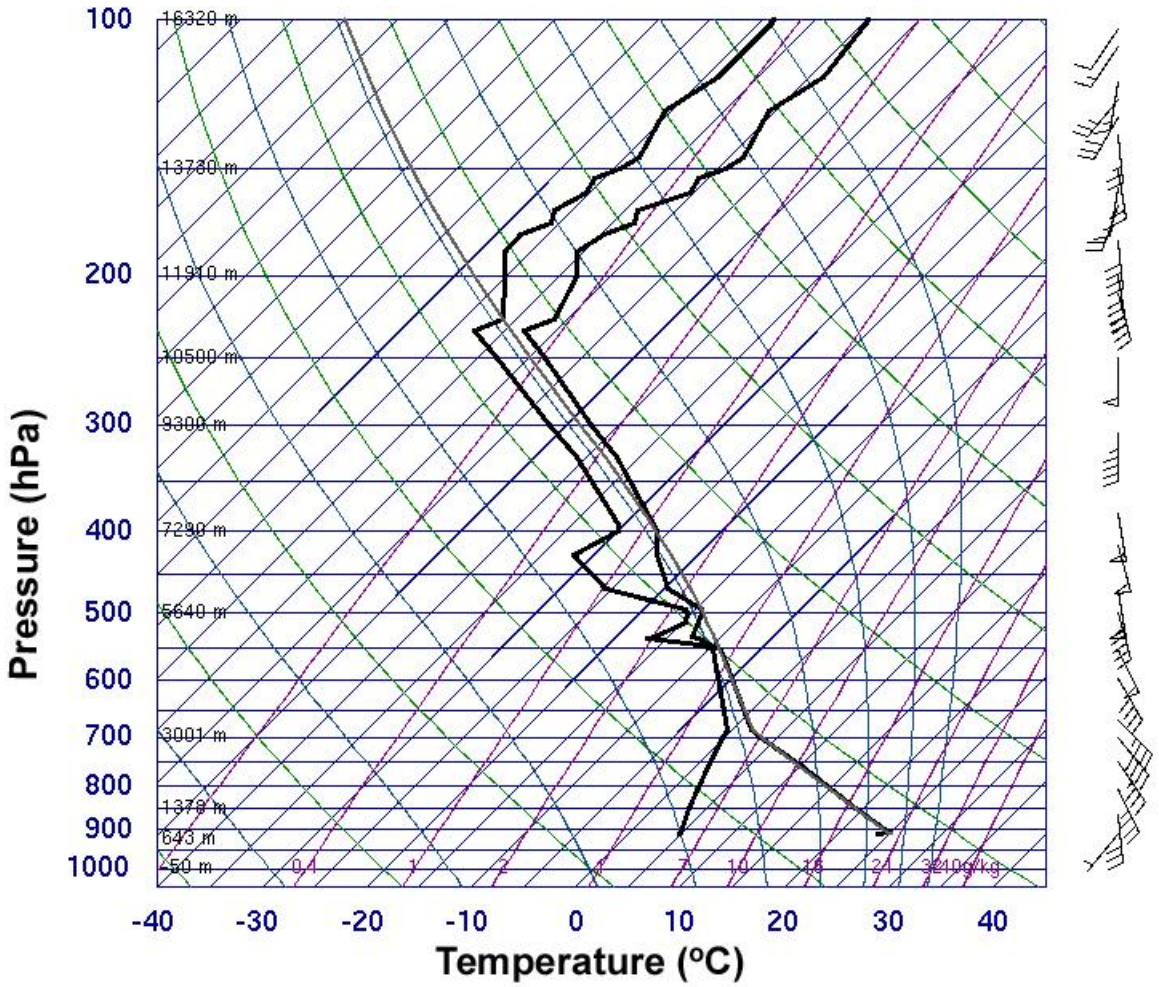

Figure 2. Atmospheric sounding launched near Edmonton, Alberta on 29 May 2001. The right black line represents the temperature, and the left black line corresponds to the dew-point temperature. This weather information is from the University of Wyoming Department of Atmospheric Science (http://weather.uwyo.edu/).

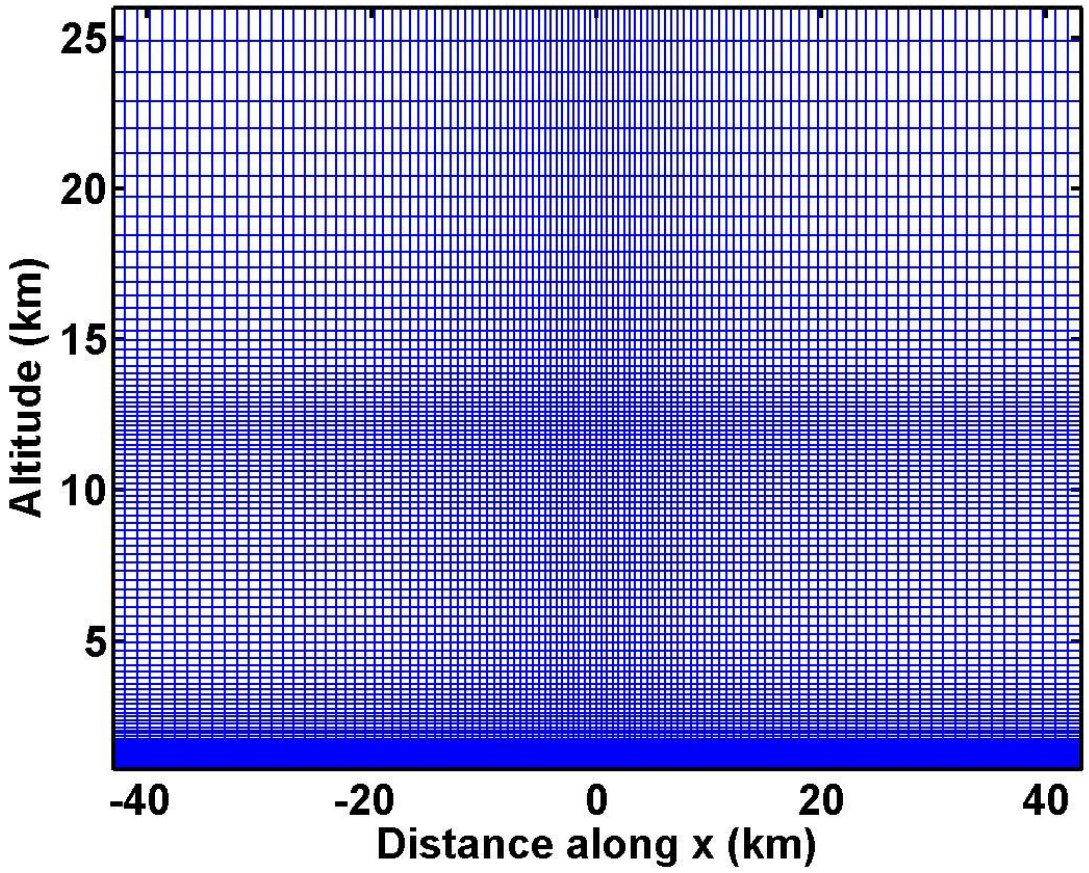

Figure 3. The 110×100 grid points in the computational domain.

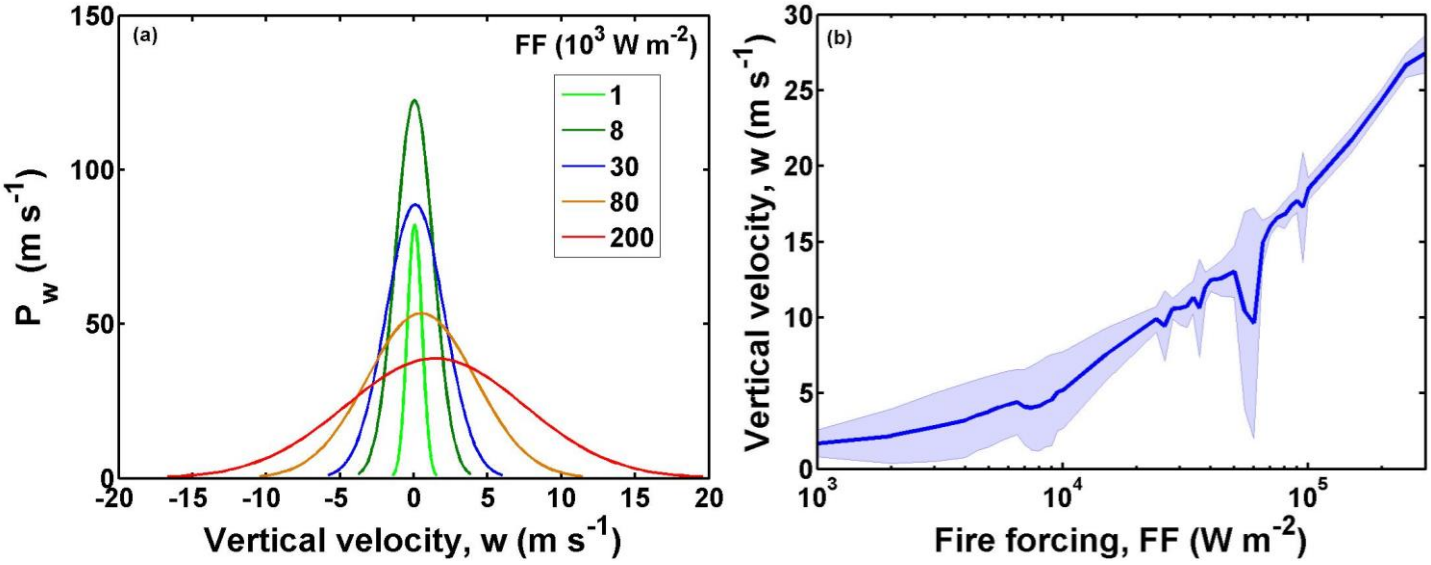

Figure 4. Probability distribution function of vertical velocities (*w*) at cloud base layer under different fire forcing conditions (a); Relationship between input fire forcing (*FF*) and induced vertical velocity (*w*) at cloud base (b). The aerosol concentration is 1,000 cm^{-3}. The shaded area represents the variability of estimation (±½σ).

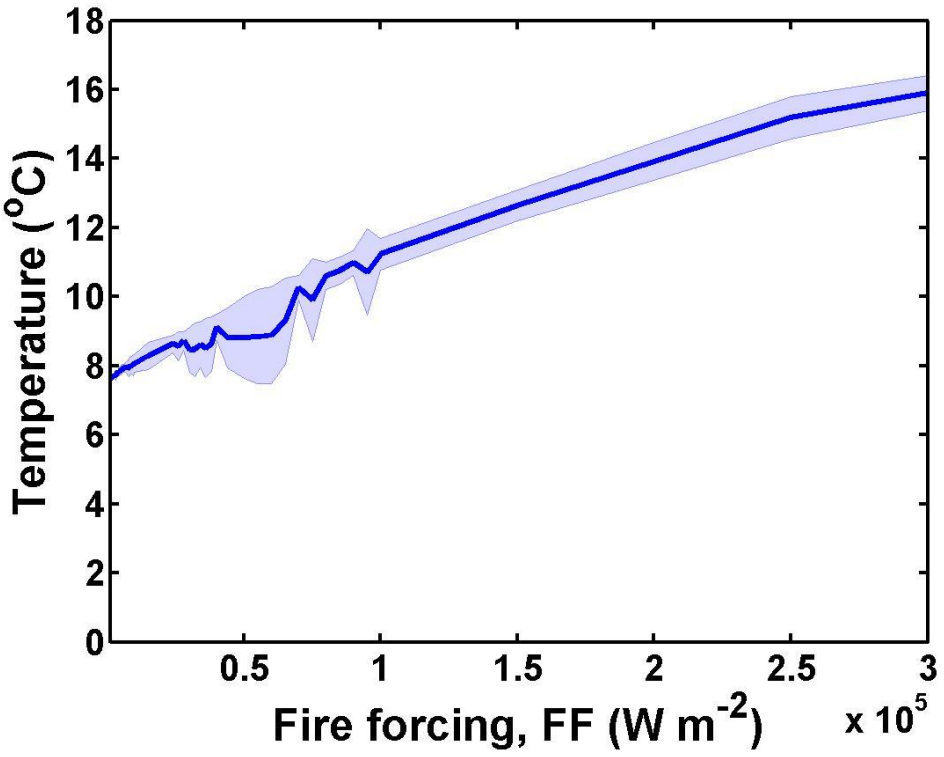

Figure 5. The correlation of fire forcing and the corresponding maximum temperature at cloud base. The shaded area indicates the variability of estimation (±½σ) over each simulation period.

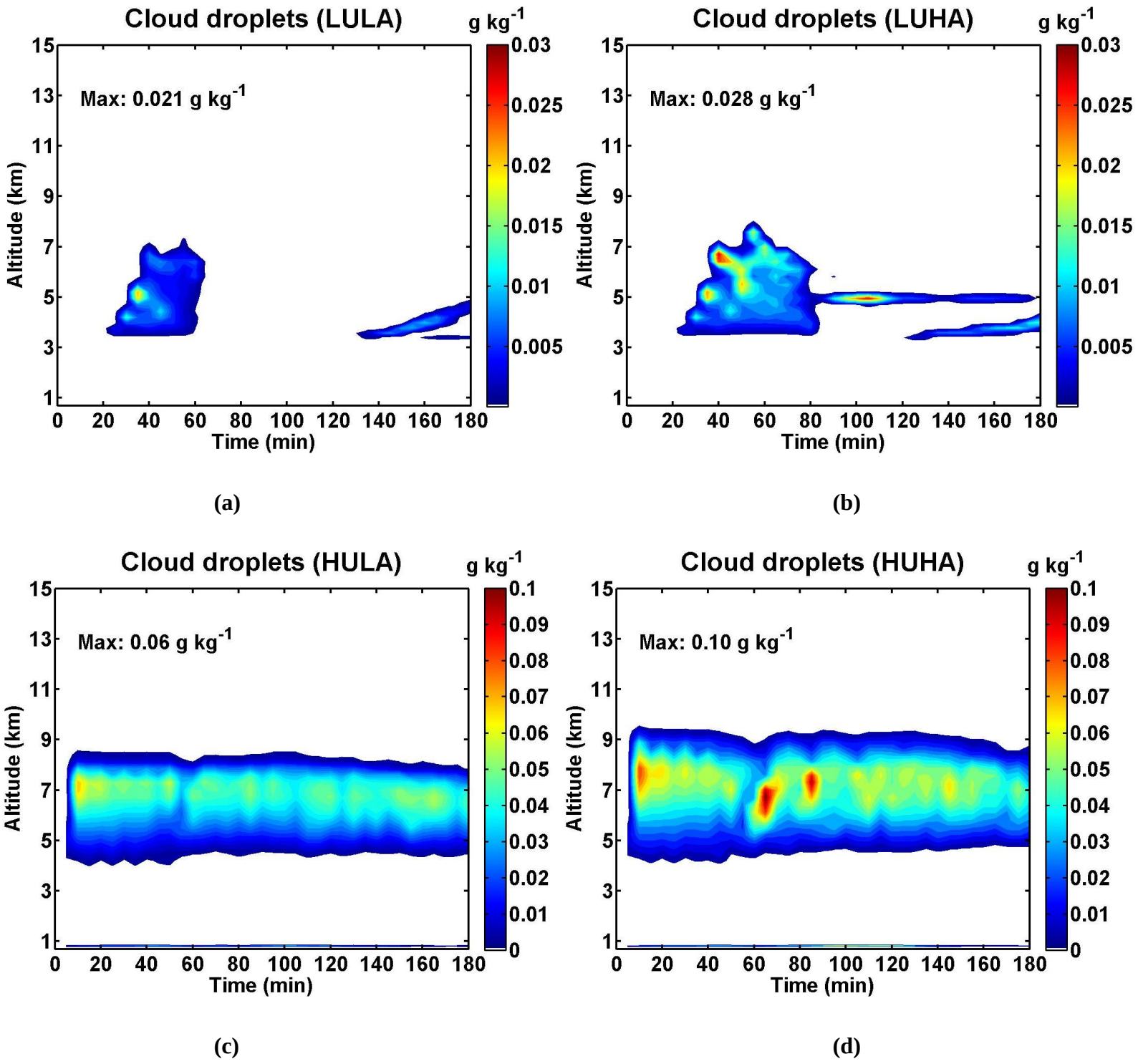

Figure 6. Time evolution of horizontally-averaged cloud water content (g kg^{-1}) as a function of altitude for four extreme cases, which are referred to as (1) LULA: low updrafts (2,000 W m^{-2}) and low aerosols (200 cm^{-3}); (2) LUHA: low updrafts (2,000 W m^{-2}) and high aerosols (100,000 cm^{-3}); (3) HULA: high updrafts (300,000 W m^{-2}) and low aerosols (200 cm^{-3}); (4) HUHA: high updrafts (300,000 W m^{-2}) and high aerosols (100,000 cm^{-3}). Maximum values for each episode are also shown.

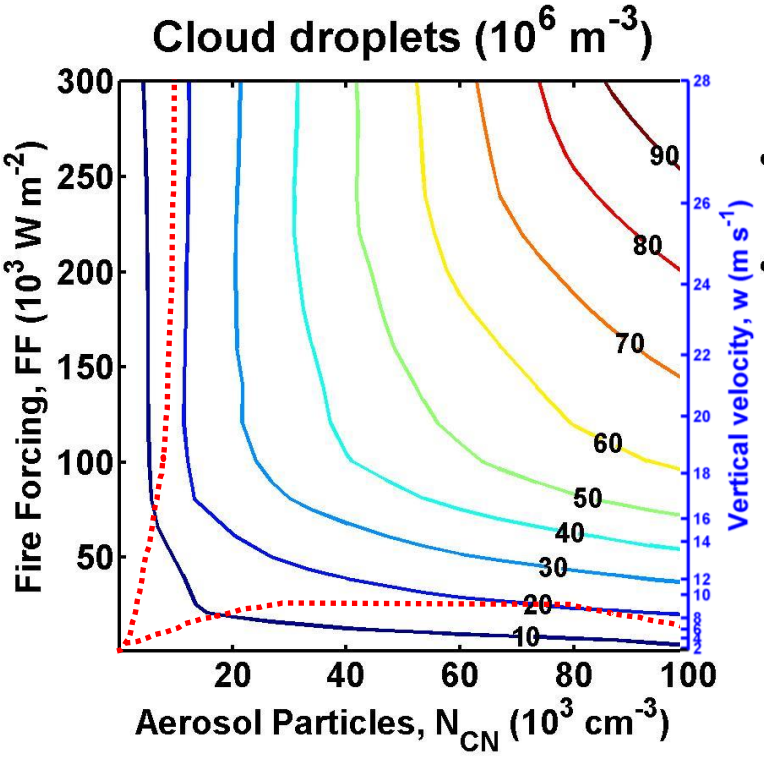
Cloud droplets (10^6 m^{-3})
Fire Forcing, FF (10^3 W m^{-2})
Vertical velocity, w (m s^{-1})
Aerosol Particles, N_{CN} (10^3 cm^{-3})
90
80
70
60
50
40
30
20
10

(a)

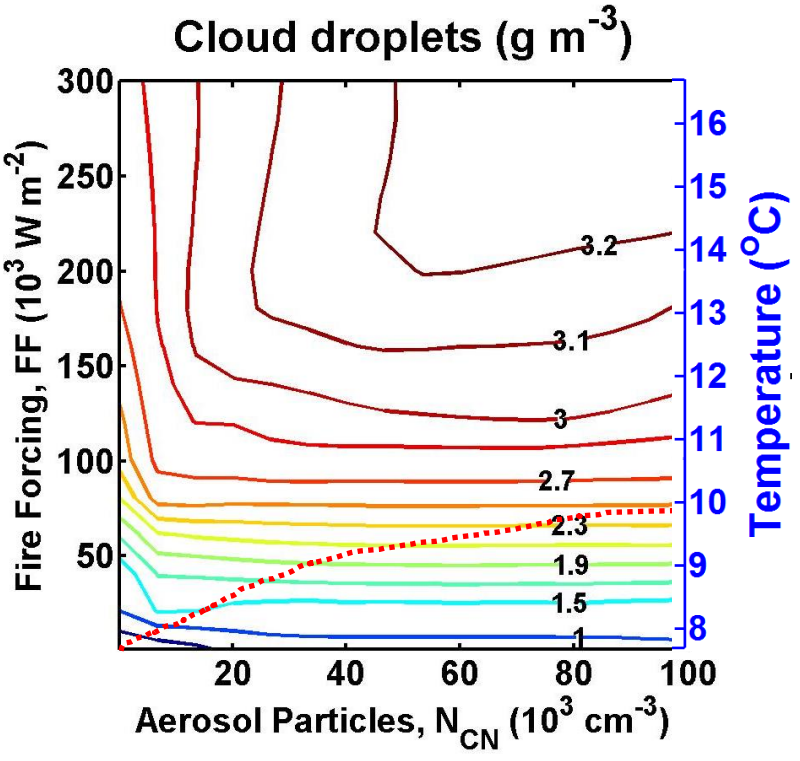
Cloud droplets (g m^{-3})
Fire Forcing, FF (10^3 W m^{-2})
Temperature (^{o}C)
Aerosol Particles, N_{CN} (10^3 cm^{-3})
3.2
3.1
3
2.7
2.3
1.9
1.5
1

(b)

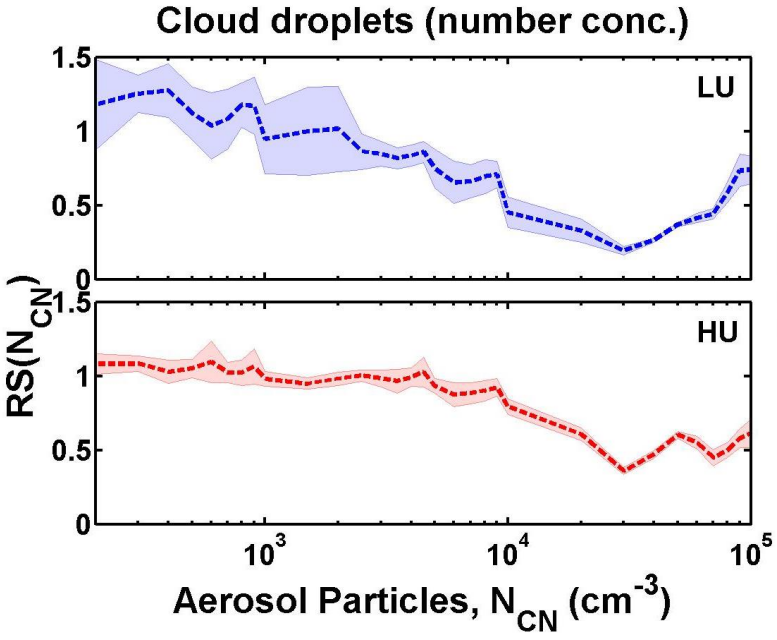
Cloud droplets (number conc.)
LU
HU
RS(N_{CN})
Aerosol Particles, N_{CN} (cm^{-3})

(c)

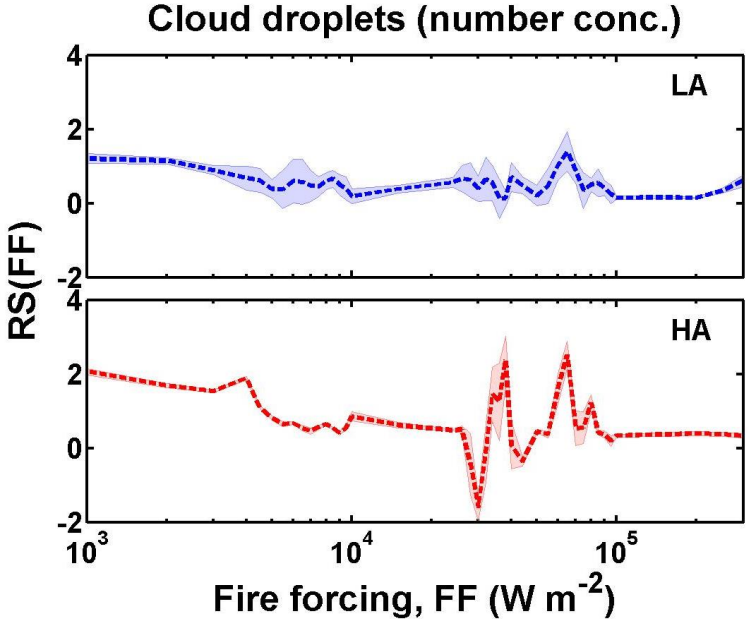
Cloud droplets (number conc.)
LA
HA
RS(FF)
Fire forcing, FF (W m^{-2})

(d)

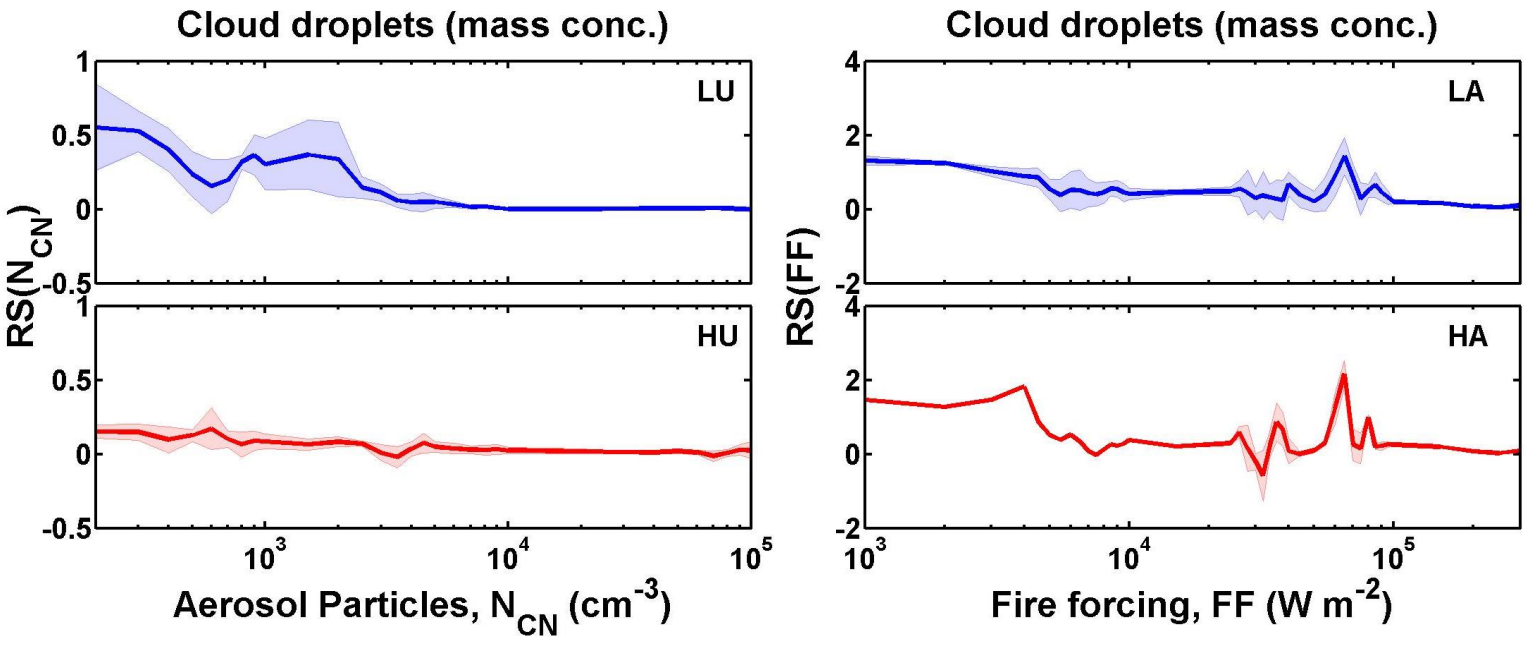

(e) **(f)**

Figure 7. Number (a) and mass concentration (b) of cloud droplets calculated as a function of aerosol number concentration (N_{CN}) and updraft velocity (represented by *FF*). Red dashed lines indicate the borders between different regimes defined by *RS* (N_{CN})/*RS*(*FF*)=4 or 1/4, respectively. Relative sensitivities with respect to N_{CN} (left) and *FF* (right) for number (panels (c) and (d)) and mass (panels (e) and (f)) concentration of cloud droplets under different conditions. The thick dashed or solid lines represent the mean values under a given condition, and the shaded areas represent the variability of estimation (±½σ). The acronyms indicate LU: low updrafts (1,000–7,000 W m^{-2}); HU: high updrafts (75,000–300,000 W m^{-2}); LA: low aerosols (200–1,500 cm^{-3}); HA: high aerosols (10,000–100,000 cm^{-3}).

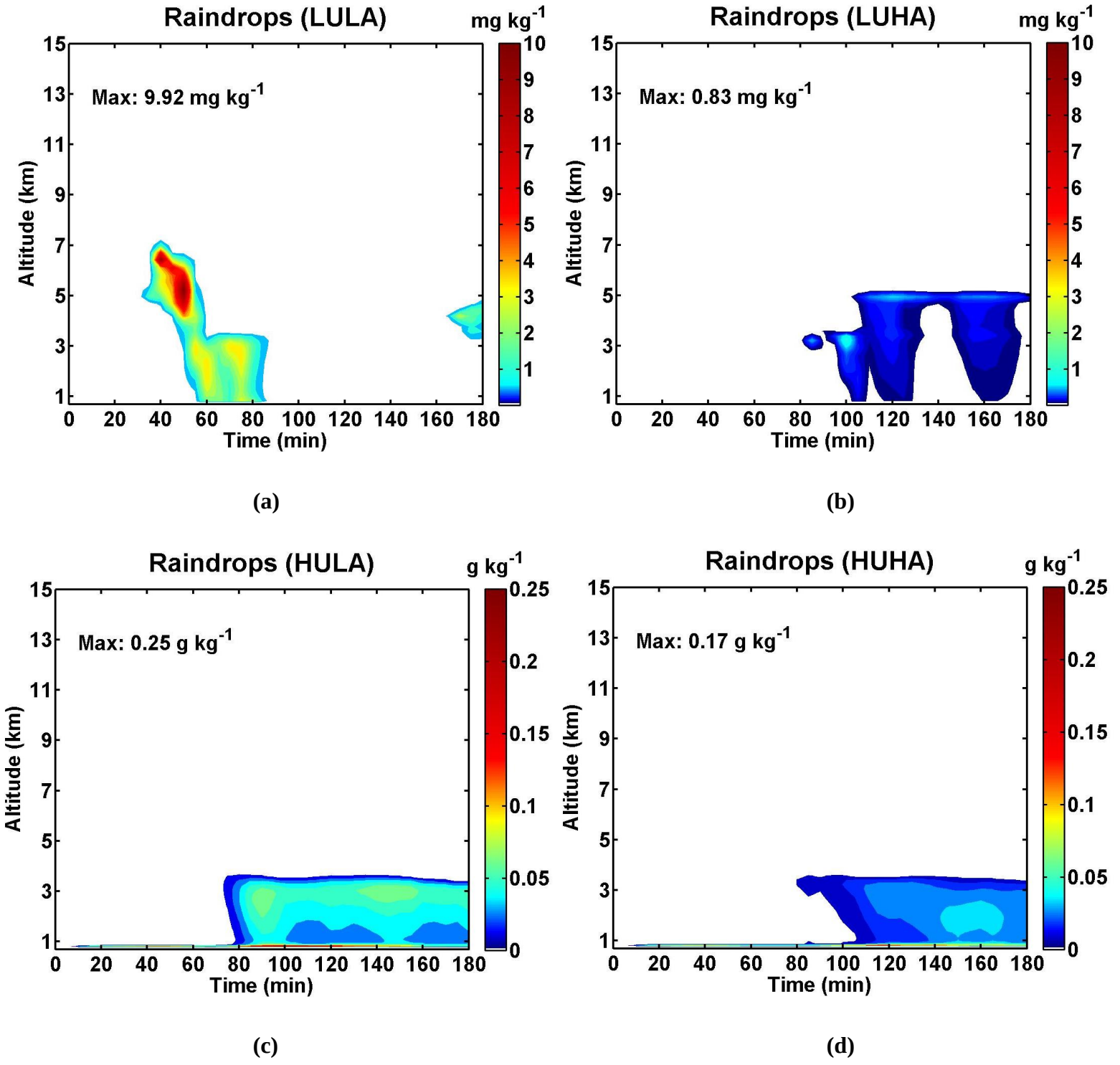

Figure 8. Same as Figure 6 but for raindrops.

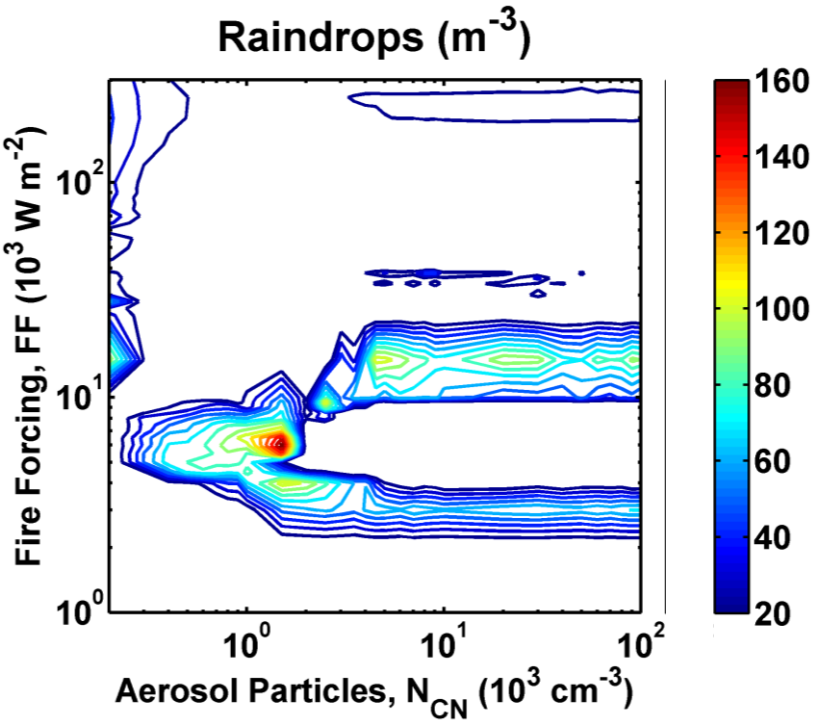
Raindrops (m-3)
Fire Forcing, FF (10^3 W m^-2)
Aerosol Particles, N_CN (10^3 cm^-3)
160
140
120
100
80
60
40
20

(a)

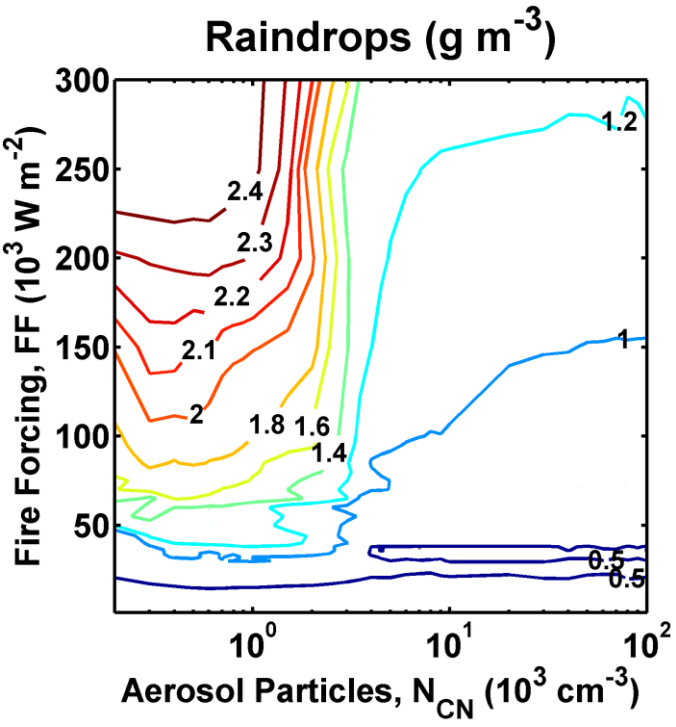
Raindrops (g m-3)
Fire Forcing, FF (10^3 W m^-2)
Aerosol Particles, N_CN (10^3 cm^-3)
2.4
2.3
2.2
2.1
2
1.8
1.6
1.4
1.2
1
0.5
0.5

(b)

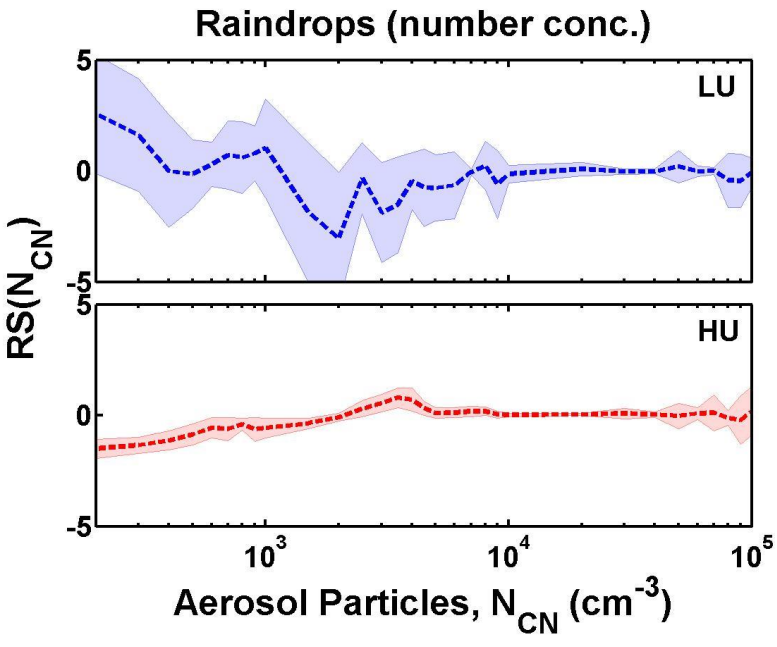
Raindrops (number conc.)
RS(N_CN)
LU
HU
Aerosol Particles, N_CN (cm^-3)

(c)

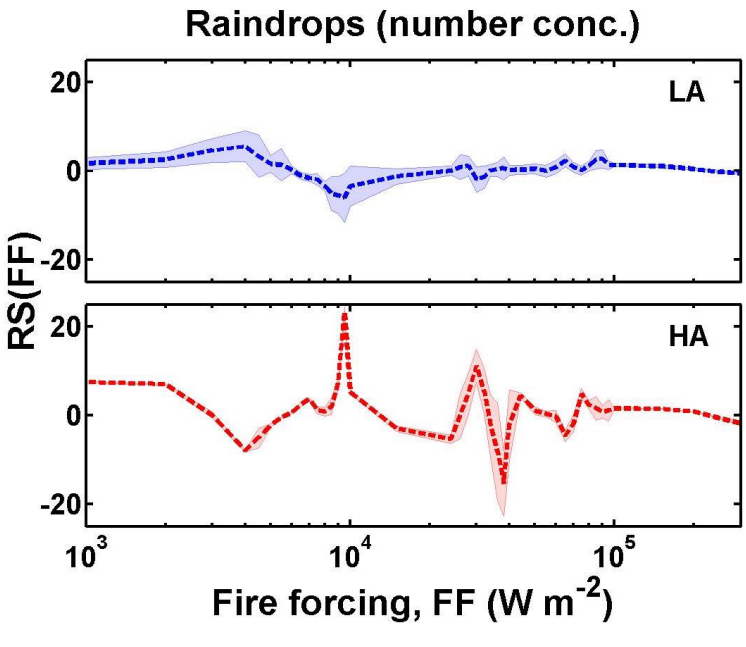
Raindrops (number conc.)
RS(FF)
LA
HA
Fire forcing, FF (W m^-2)

(d)

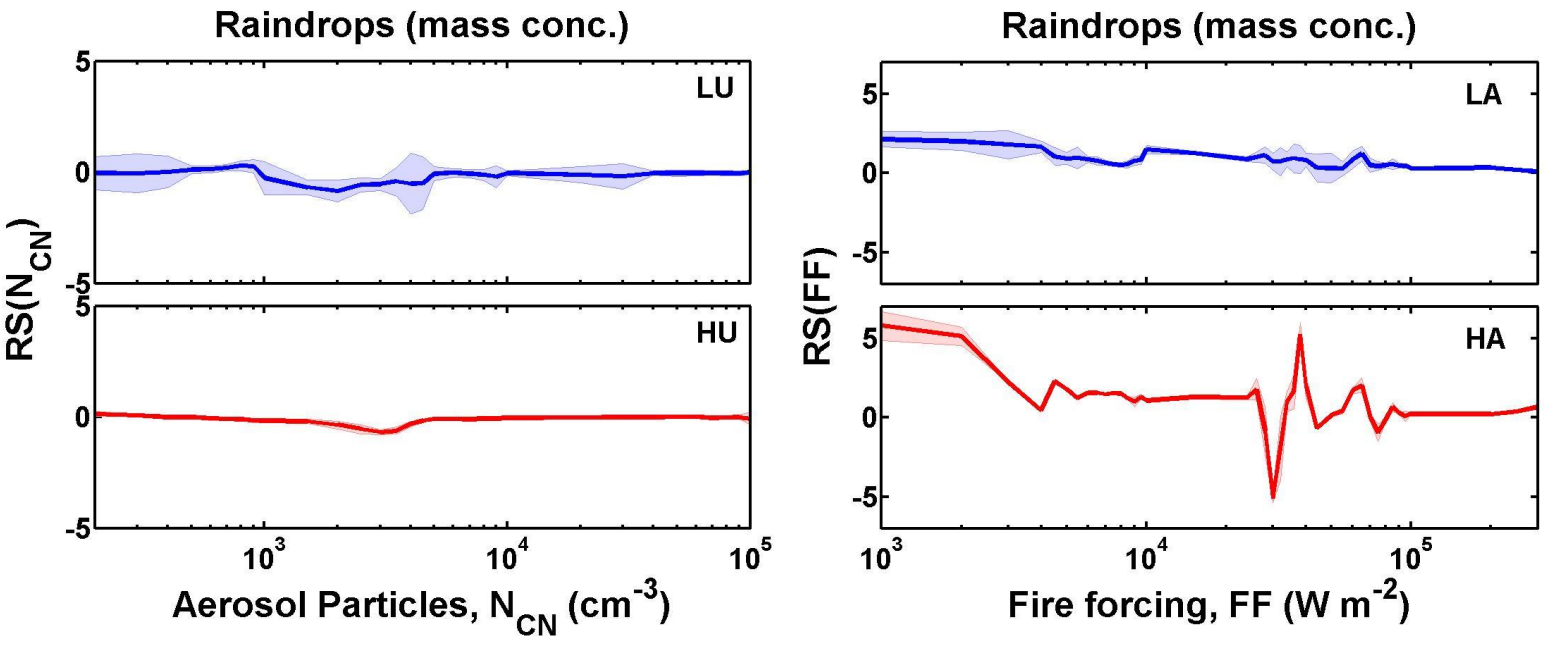

(e) **(f)**

Figure 9. Same as Figure 7 but for raindrops.

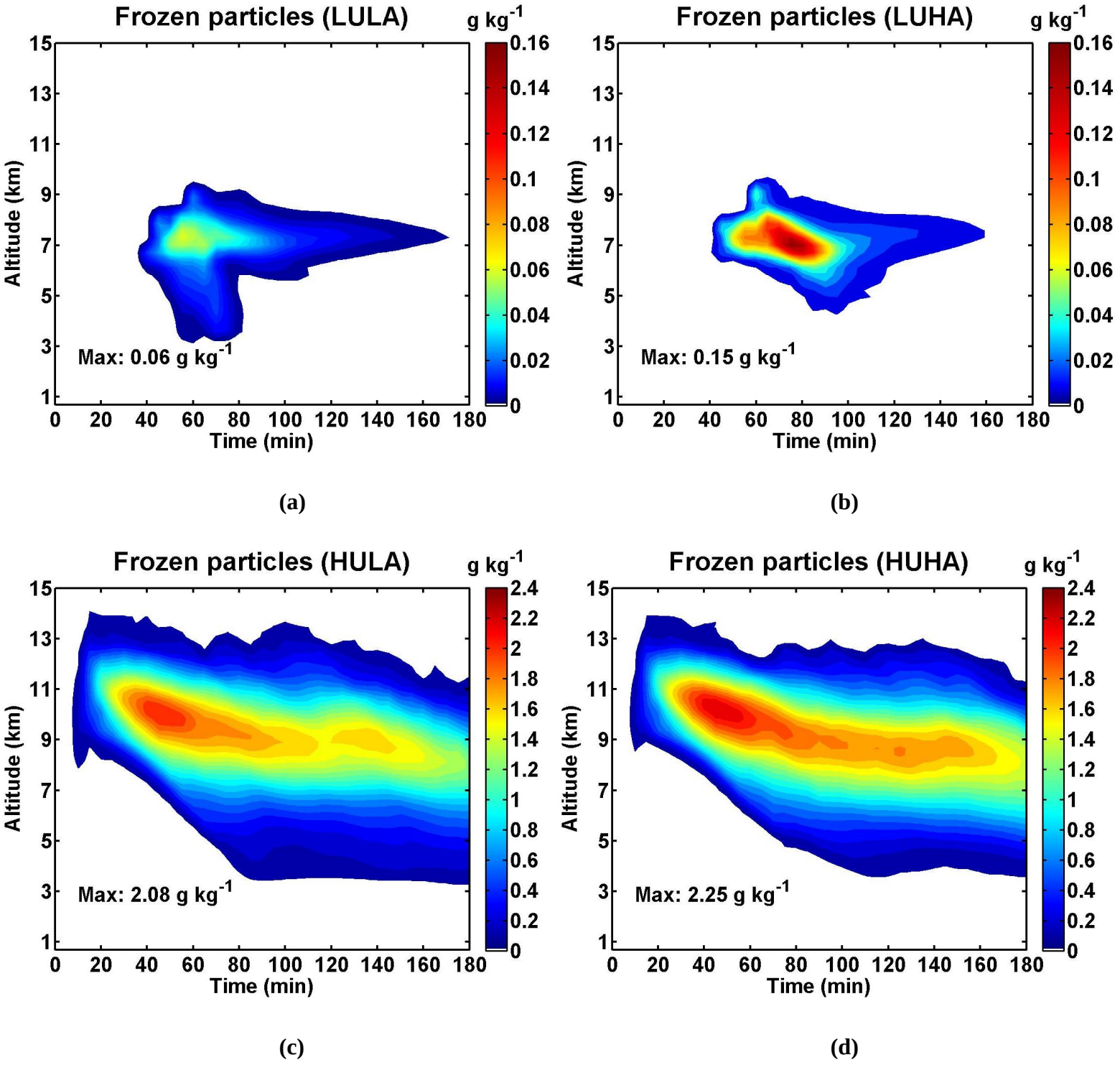

Figure 10. Same as Figure 6 but for the frozen particles.

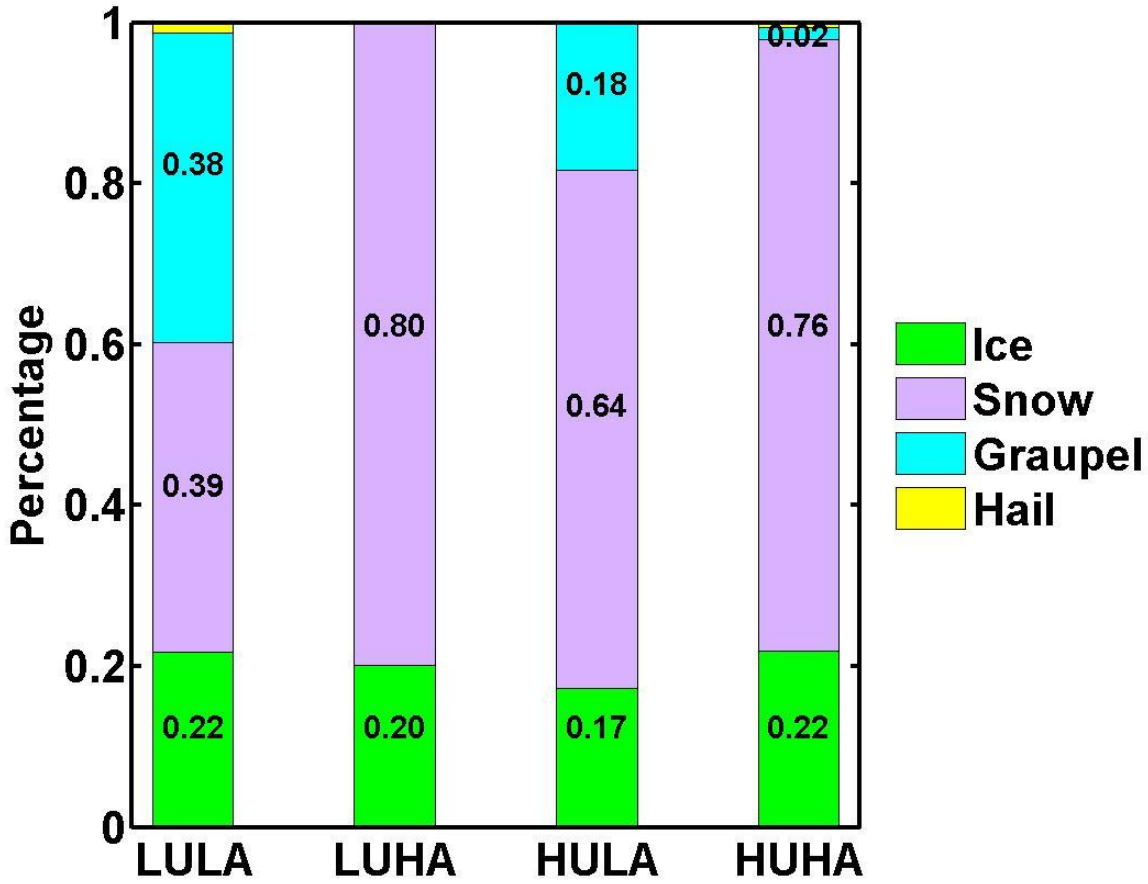

Figure 11. Contributions of individual frozen hydrometeor to total frozen water content under four extreme conditions which are referred to as (1) LULA: low updrafts (2,000 W m^{-2}) and low aerosols (200 cm^{-3}); (2) LUHA: low updrafts (2,000 W m^{-2}) and high aerosols (100,000 cm^{-3}); (3) HULA: high updrafts (300,000 W m^{-2}) and low aerosols (200 cm^{-3}); (4) HUHA: high updrafts (300,000 W m^{-2}) and high aerosols (100,000 cm^{-3}).

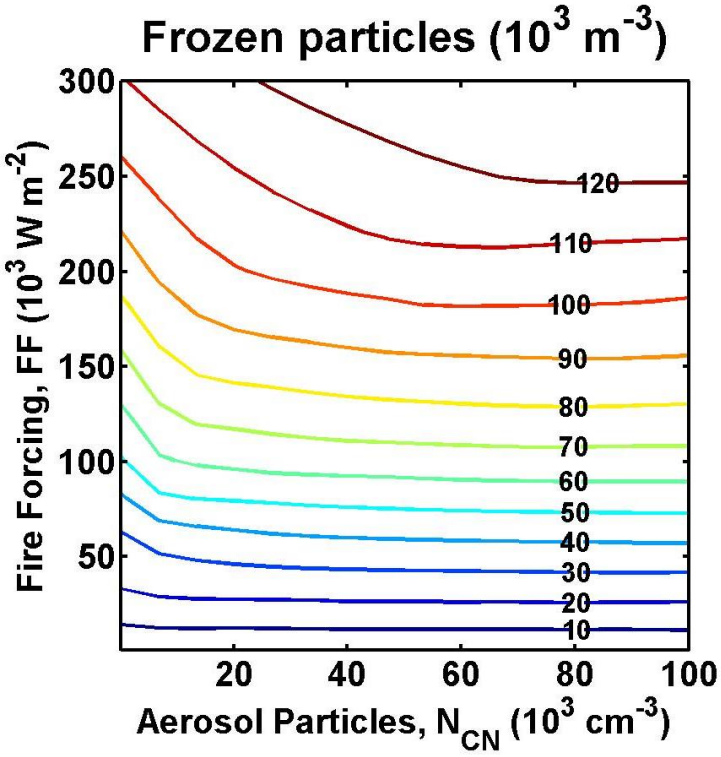
Frozen particles (10^3 m^{-3})
Fire Forcing, FF (10^3 W m^{-2})
Aerosol Particles, N_{CN} (10^3 cm^{-3})
120
110
100
90
80
70
60
50
40
30
20
10

(a)

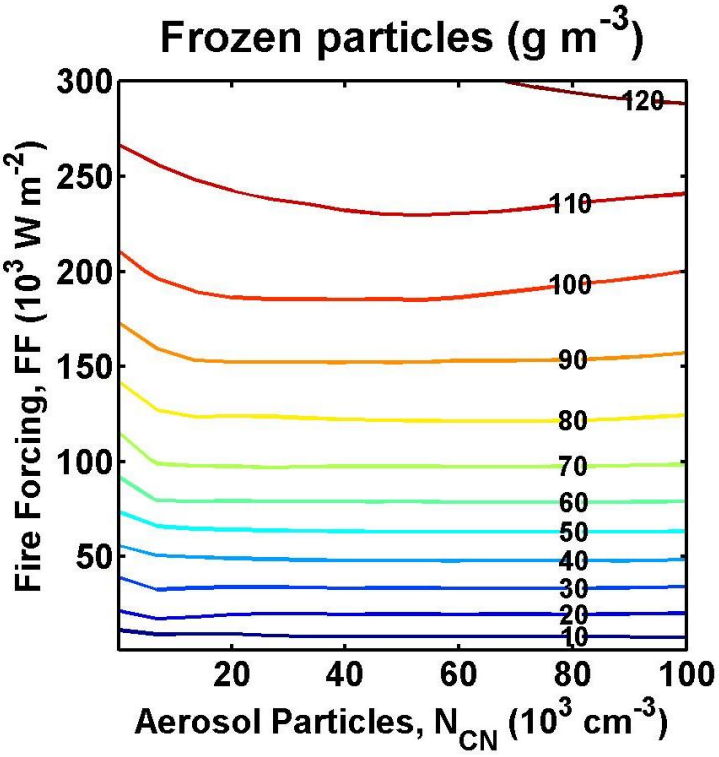
Frozen particles (g m^{-3})
Fire Forcing, FF (10^3 W m^{-2})
Aerosol Particles, N_{CN} (10^3 cm^{-3})
120
110
100
90
80
70
60
50
40
30
20
10

(b)

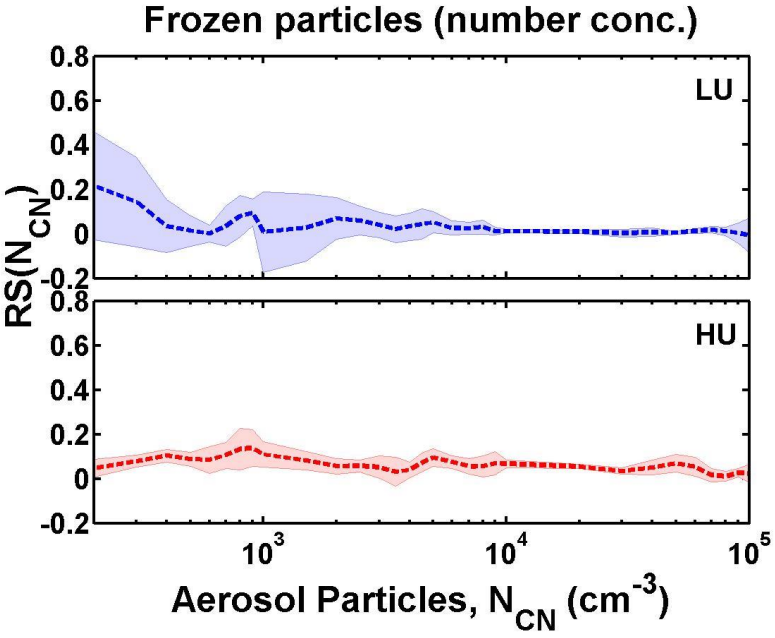
Frozen particles (number conc.)
LU
HU
RS(N_{CN})
Aerosol Particles, N_{CN} (cm^{-3})

(c)

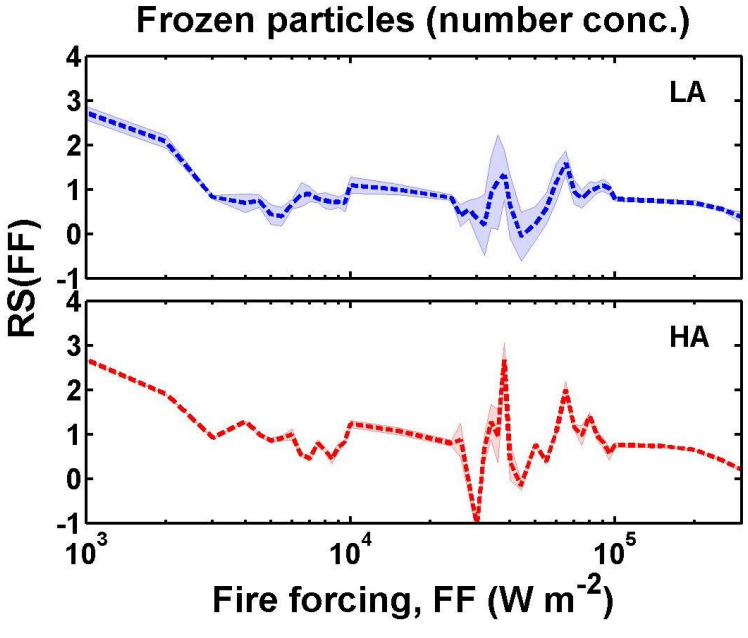
Frozen particles (number conc.)
LA
HA
RS(FF)
Fire forcing, FF (W m^{-2})

(d)

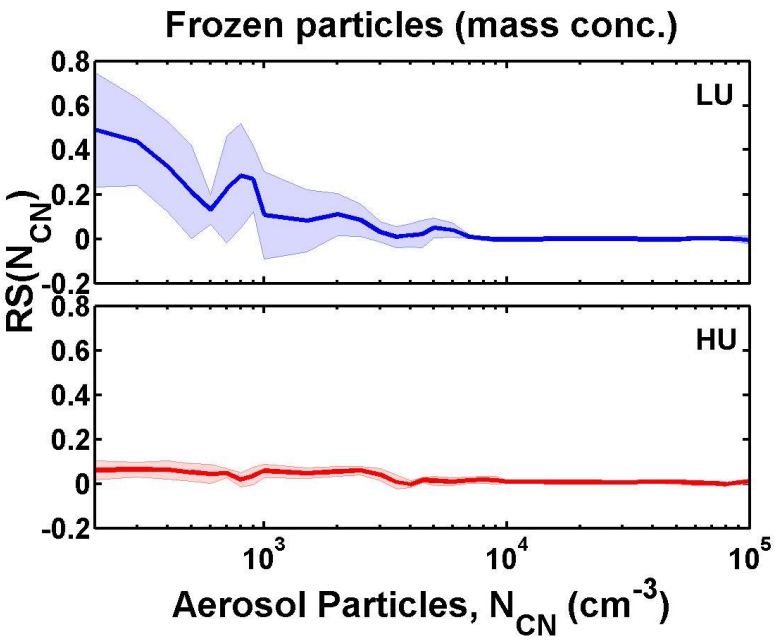

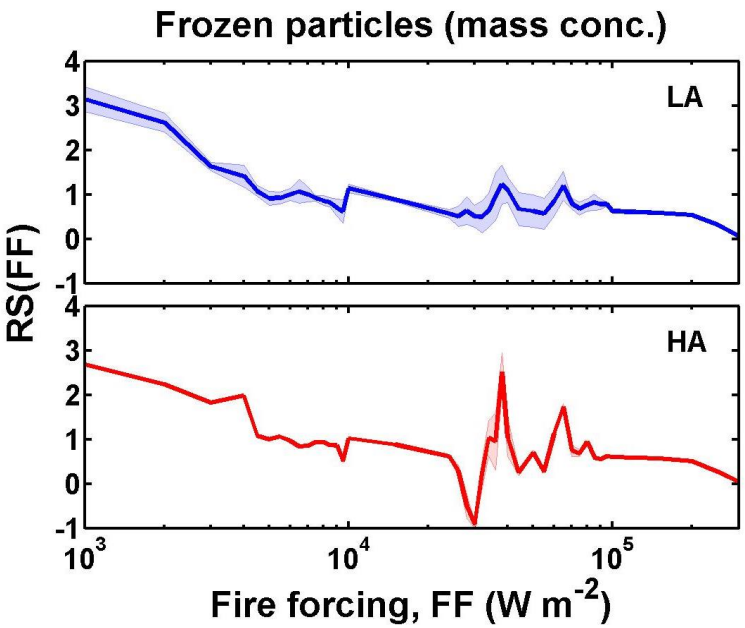

(e) **(f)**

Figure 12. Same as Figure **7** but for total frozen particles.

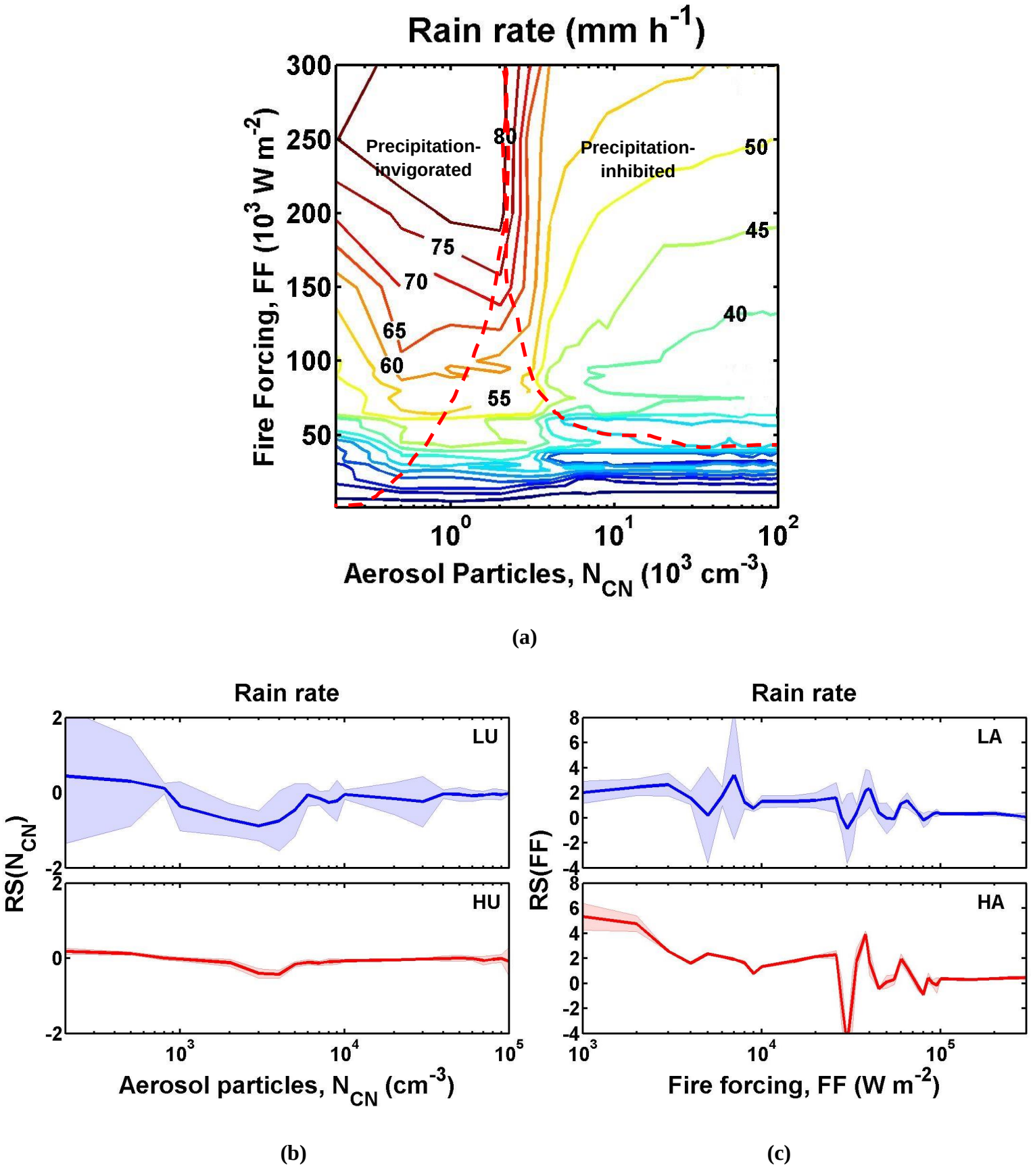

Figure 13. Same as Figure 7 but for surface rain rate.

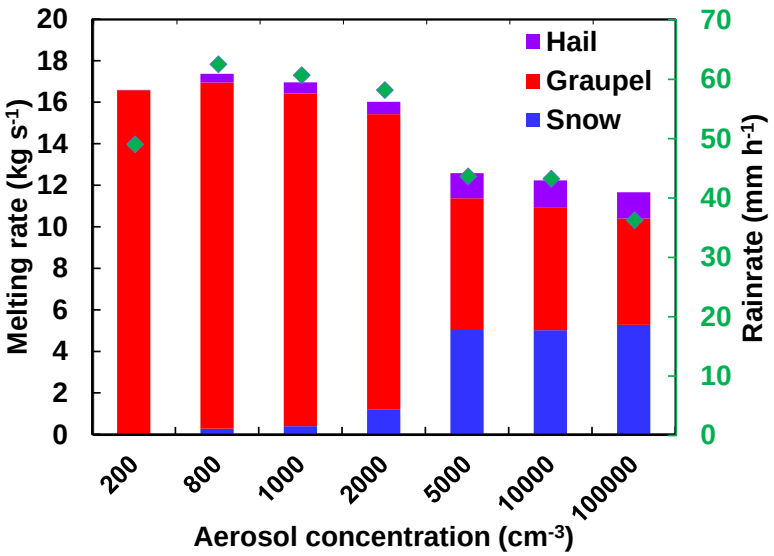

Figure 14. The correlation of rain rate and the melting rate of the frozen particles. The green diamond points are the averaged rain rate under different aerosol concentrations (FF= 10^5 W m^{-2}). The columns represent the integrated melting rate from individual frozen particles.

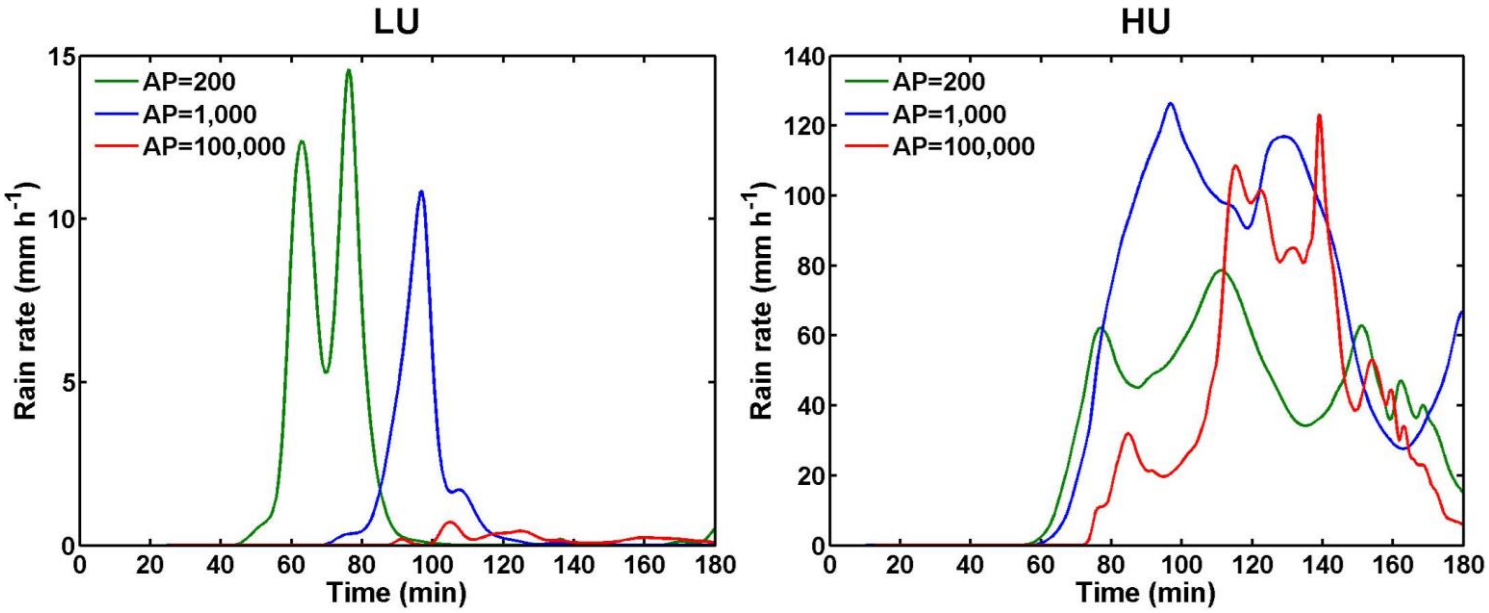

Figure 15. Time evolution of surface rain rates for the three aerosol episodes (N_{CN} = 200; 1,000; and 100,000 cm^{-3} respectively) under LU (low updrafts, FF=2,000 W m^{-2}) and HU (high updrafts, FF=50,000 W m^{-2}) conditions.

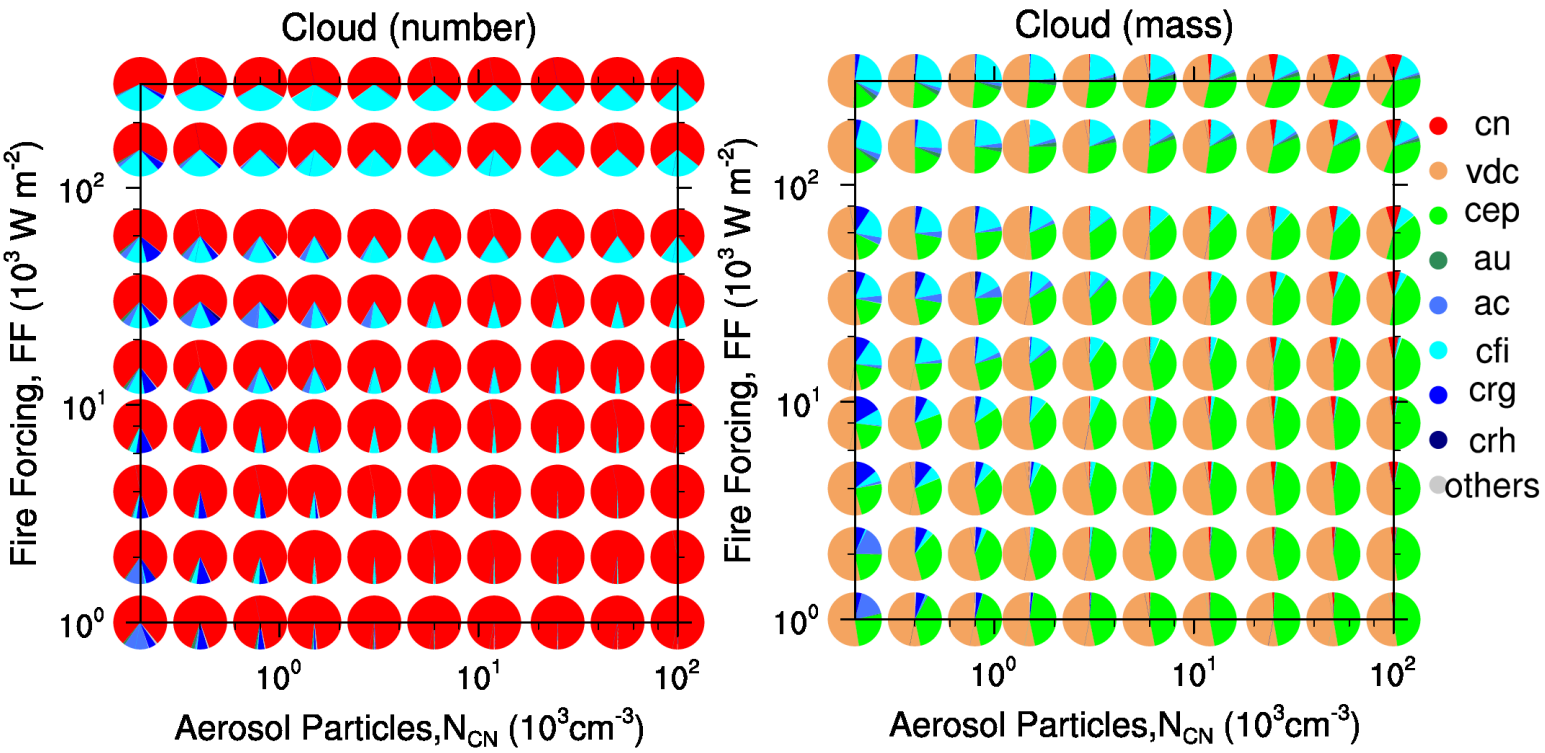

(a) (b)

Figure 16. The pie charts summarize the relative percentage of the microphysical processes involving cloud droplets as a function of N_{CN} and fire forcing (a: number concentration; b: mass concentration). Colors within each pie chart reflect the contribution of processes under the specific condition. Warm colors denote the sources, while cold colors denote the sinks. The acronyms indicate cn: cloud nucleation; vdc: condensational growth of cloud droplets; cep: evaporation of cloud droplets; au: autoconversion; ac: accretion; cfi: freezing of cloud droplets to form ice crystals, including homogeneous and heterogeneous nucleation; crg/h: riming of cloud droplets to form graupel/hail.

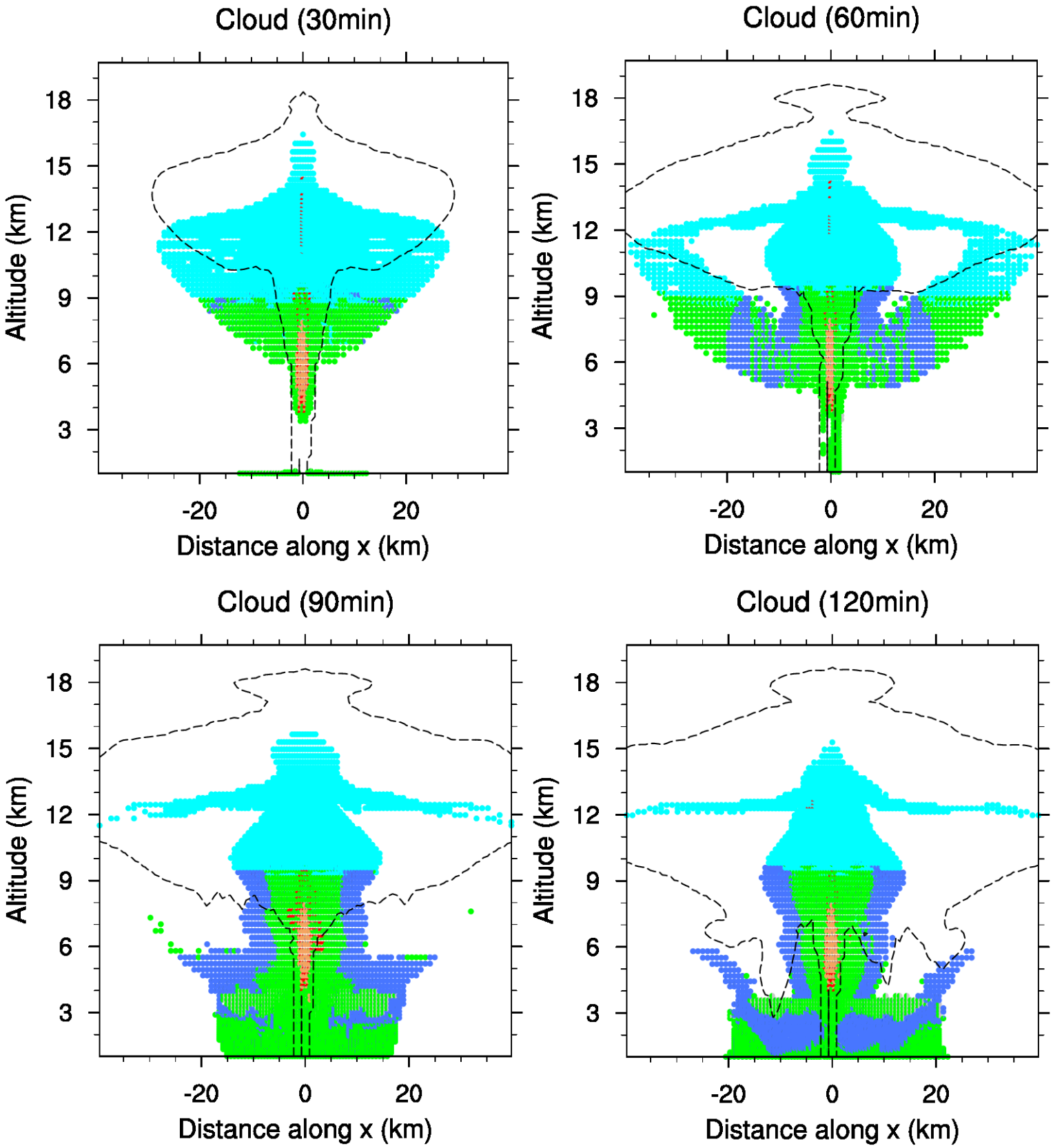
Cloud (30min)
Cloud (60min)
Cloud (90min)
Cloud (120min)
Altitude (km)
Distance along x (km)
18
15
12
9
6
3
-20
0
20

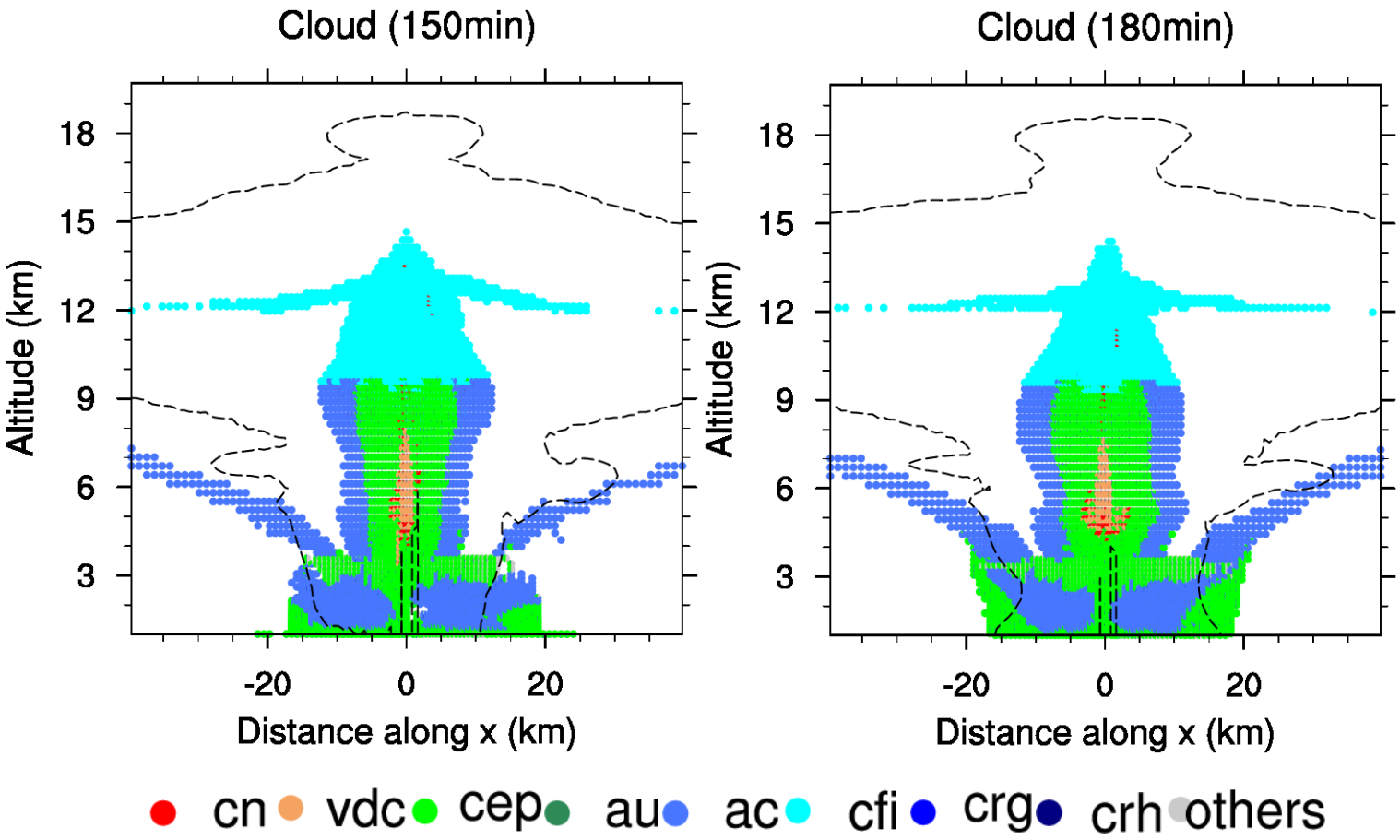

Figure 17. The pie charts summarize the vertical cross sections of the change rate of main microphysical processes contributing to cloud water content. Each pie chart shows the averaged contribution over the past 30 min. Colors within each pie chart reflect the percentage of processes in each grid. The black dashed line is the 0.1 μg kg^{-1} isoline of the interstitial aerosol, indicating the shape of smoke plume. The meaning of the acronyms is the same as in Figure 16. Warm colors denote the sources, while cold colors denote the sinks.

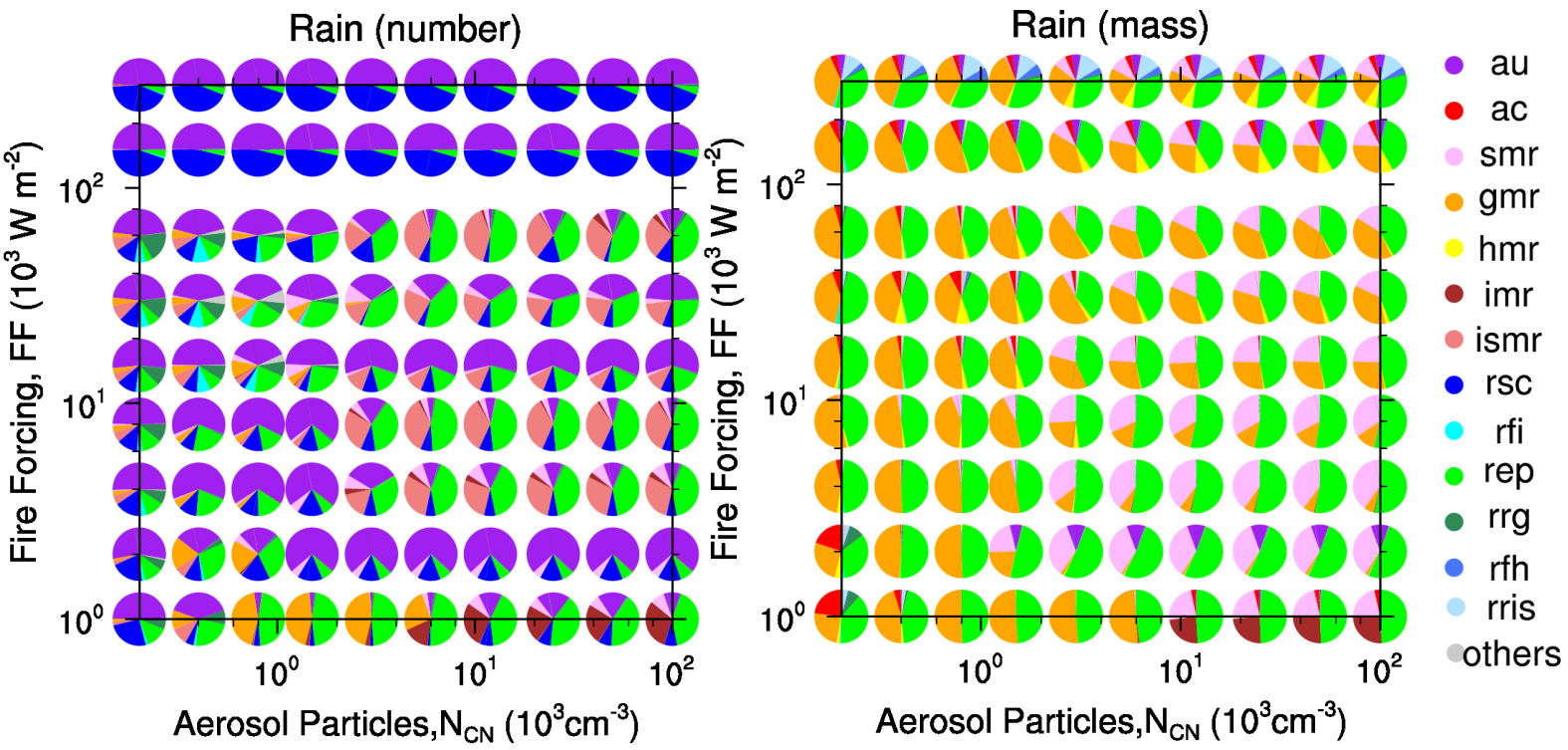

(a) (b)

Figure 18. Same as Figure 16 but for raindrops. The acronyms indicate au: autoconversion; ac: accretion; i/s/g/hmr: melting of ice/snow/graupel/hail to form raindrops; rsc: self-collection of raindrops; ismr: melting of ice and snow to form raindrops; rfi/h: freezing of raindrops to form ice crystals/hail; rep: raindrop evaporation; rrg: riming of raindrops to form graupel; rris: riming of raindrops to form ice and snow.

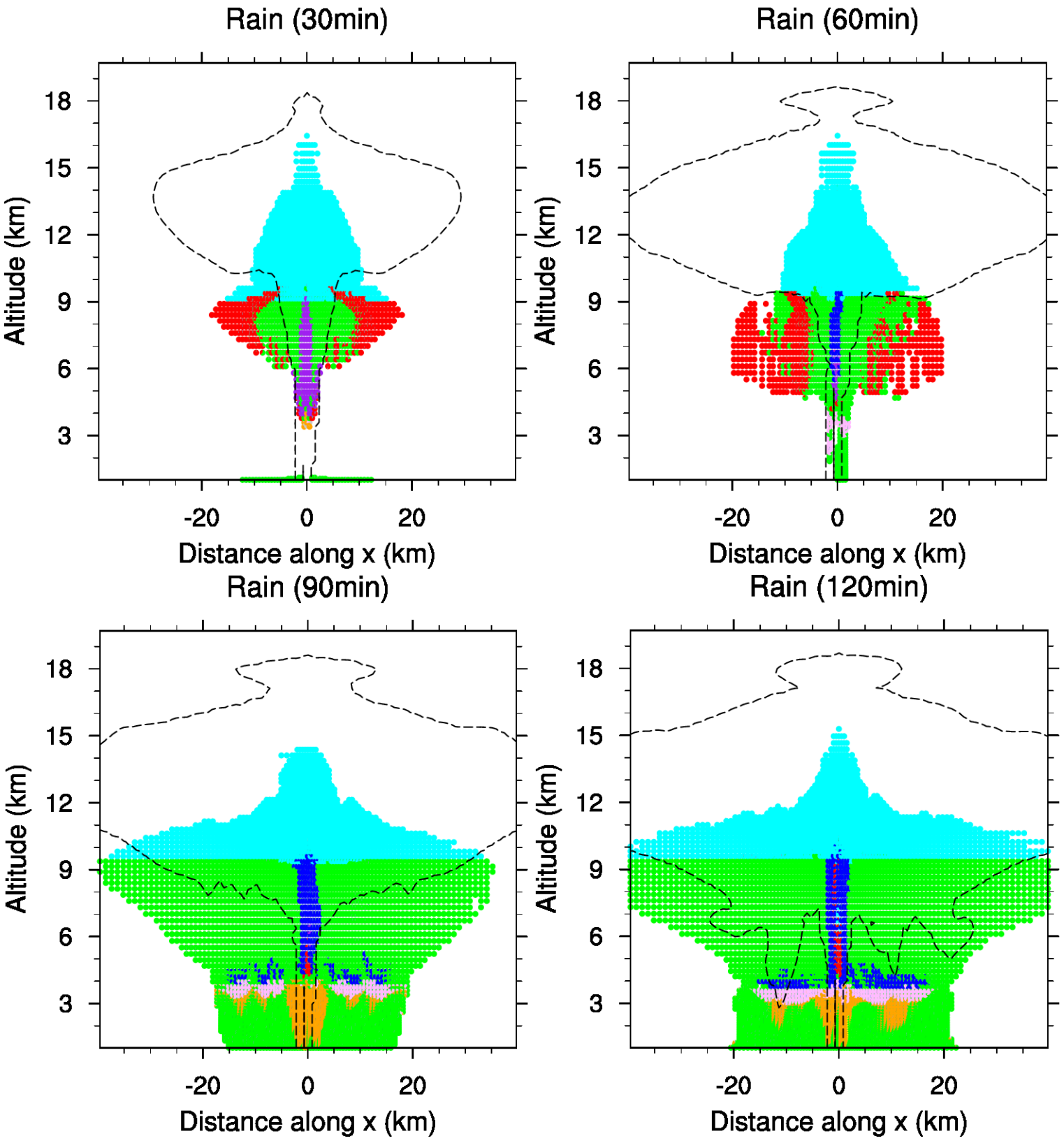
Rain (30min)
Rain (60min)
Rain (90min)
Rain (120min)
Altitude (km)
Distance along x (km)
18
15
12
9
6
3
-20
0
20

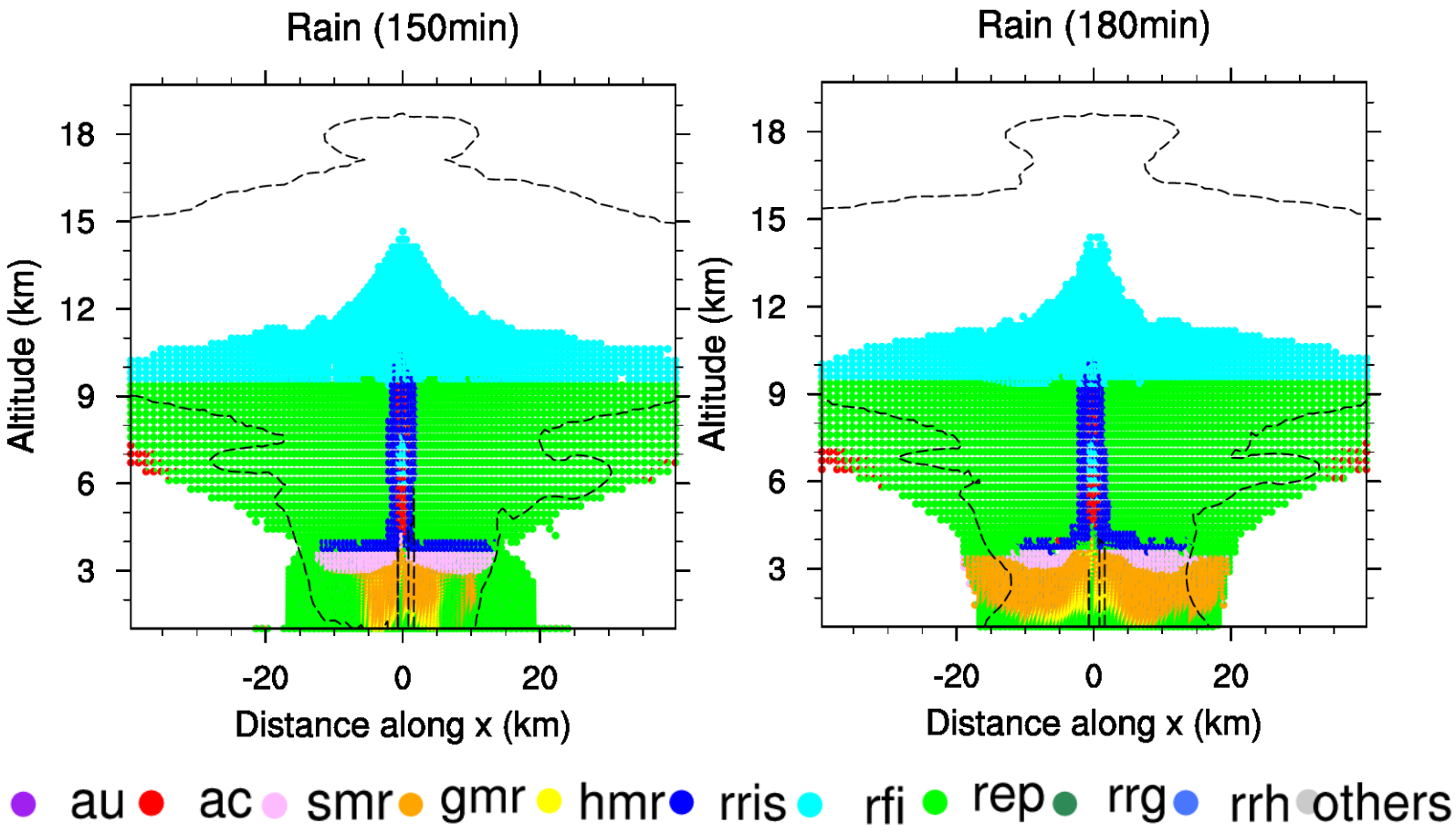

Figure 19. Same as Figure 17, but for raindrops.

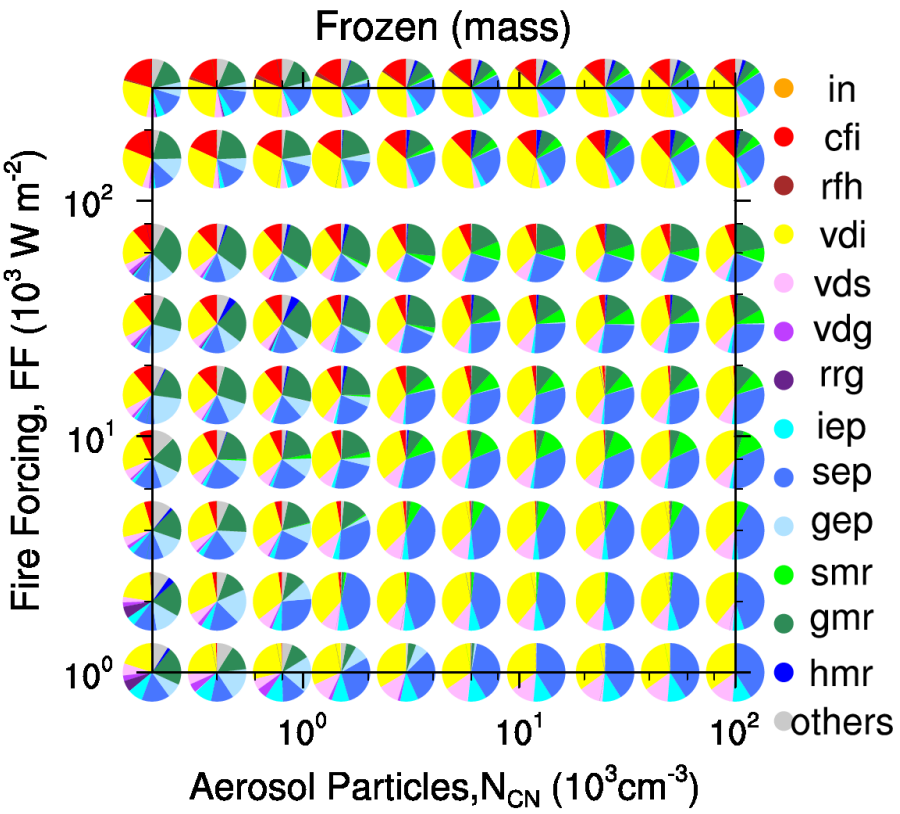

Figure 20. Same as Figure 16 but for the total frozen water content. The acronyms indicate in: ice nucleation; cfi: freezing of cloud droplets to form ice crystals, including homogeneous and heterogeneous nucleation; rfh: freezing of raindrops to form hail; vdi/s/g: condensational growth of ice crystals/snow/graupel by water vapor; rrg: riming of raindrops to form graupel; i/s/gep: evaporation of ice/snow/graupel; s/g/hmr: melting of snow/graupel/hail to form raindrops.

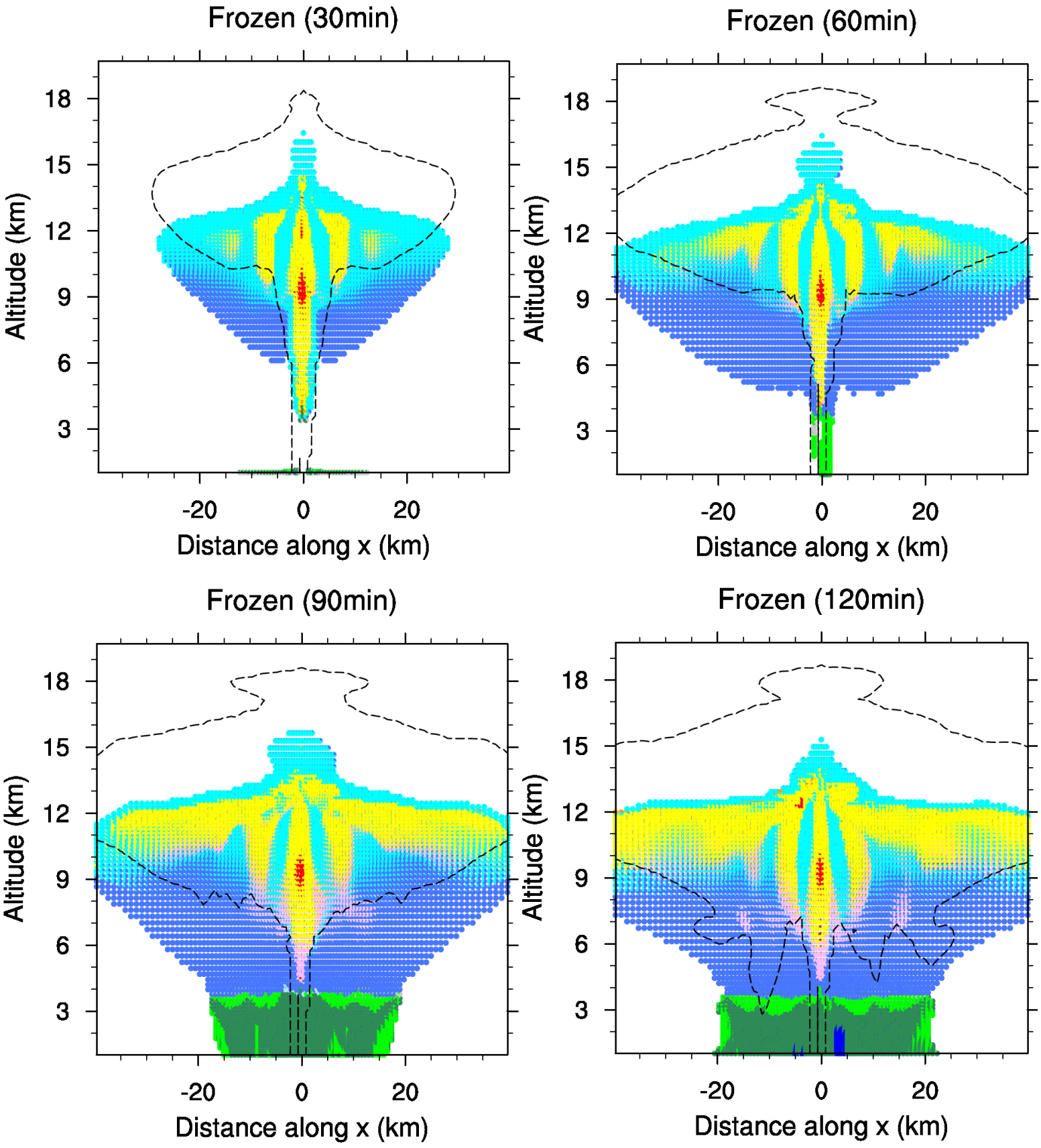
Frozen (30min)
Frozen (60min)
Frozen (90min)
Frozen (120min)
Altitude (km)
Distance along x (km)
18
15
12
9
6
3
-20
0
20

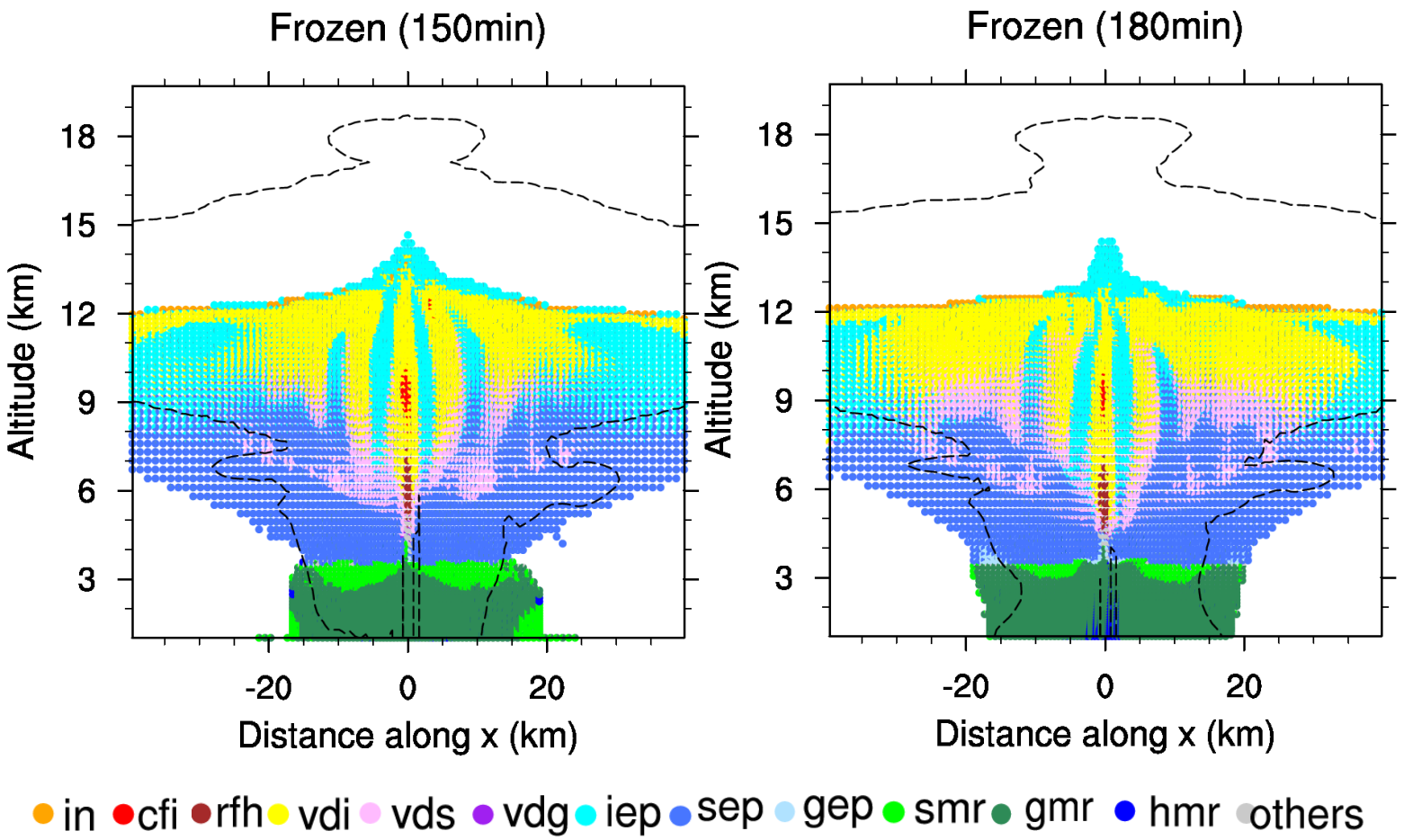

Figure 21. Same as Figure 17 but for frozen particles.

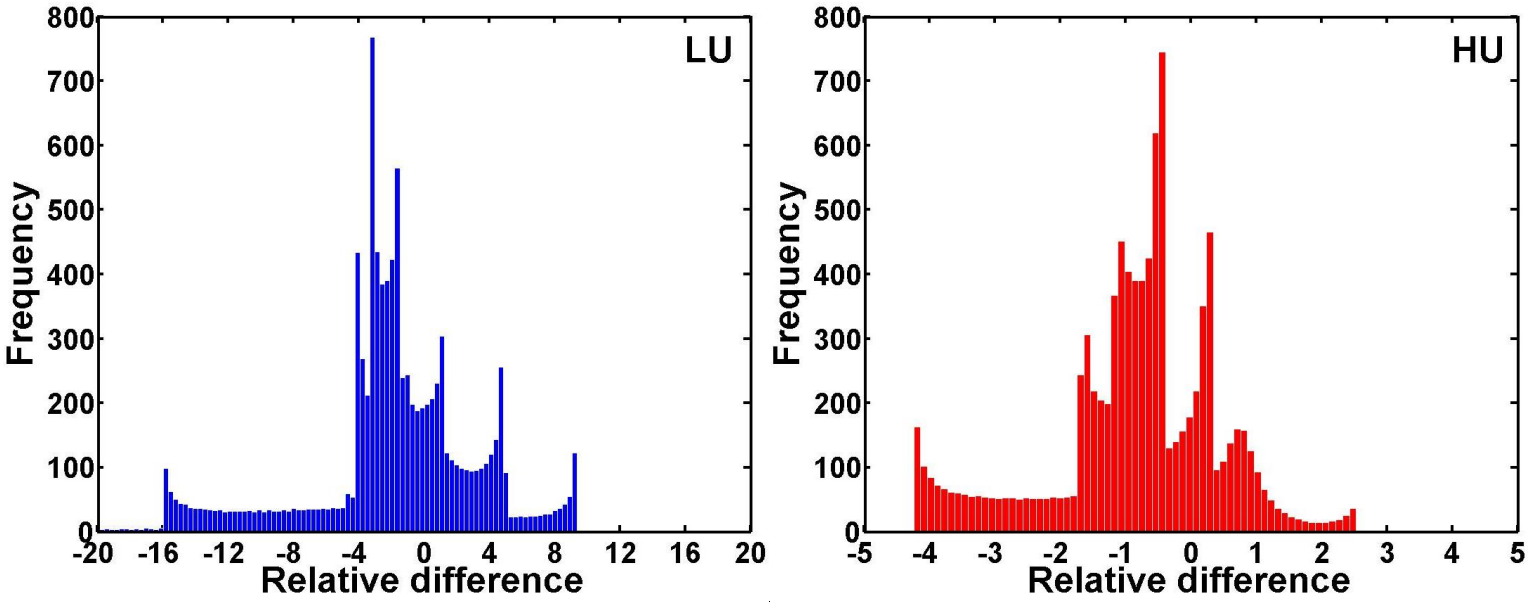

Figure 22. Histograms of the relative difference between $\frac{\Delta Y}{\Delta N_{CN}}$ and $\frac{dY}{dN_{CN}}$ under LU and HU conditions, where *Y* here denotes precipitation rate. $\frac{\Delta Y}{\Delta N_{CN}} = \frac{Y(2N_{CN}) - Y(N_{CN})}{2N_{CN} - N_{CN}}$, and $\frac{dY}{dN_{CN}}$ is the derivative of the precipitation rate along the variable N_{CN}.

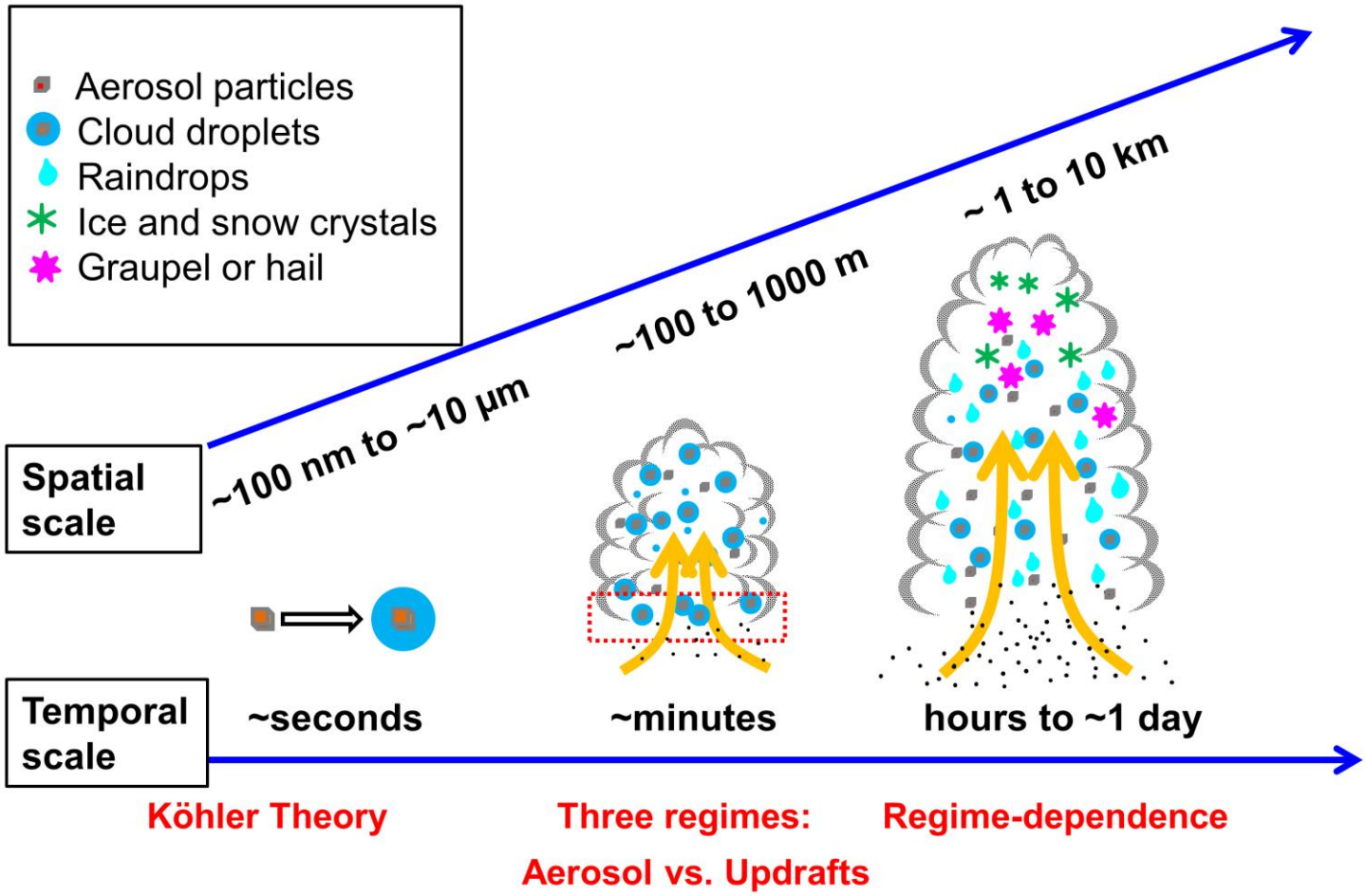

Figure 23. Overview of the research approaches on multi-scale cloud initialization and development.